

2013-09-23

Photovoltaic Array and Shading Loss Simulation for the Optimization of Solar Tracking PV Farms

Anderson, Kenneth Alexander

Anderson, K. A. (2013). Photovoltaic Array and Shading Loss Simulation for the Optimization of Solar Tracking PV Farms (Master's thesis, University of Calgary, Calgary, Canada). Retrieved from <https://prism.ucalgary.ca>. doi:10.11575/PRISM/27341

<http://hdl.handle.net/11023/1004>

Downloaded from PRISM Repository, University of Calgary

UNIVERSITY OF CALGARY

Photovoltaic Array and Shading Loss Simulation for the
Optimization of Solar Tracking PV Farms

by

Kenneth Alexander Anderson

A THESIS

SUBMITTED TO THE FACULTY OF GRADUATE STUDIES
IN PARTIAL FULFILMENT OF THE REQUIREMENTS FOR THE
DEGREE OF MASTER OF SCIENCE

DEPARTMENT OF ELECTRICAL AND COMPUTER ENGINEERING
CALGARY, ALBERTA

SEPTEMBER, 2013

© Kenneth Alexander Anderson 2013

Abstract

Solar photovoltaic tracking systems differ from fixed-tilt systems in that they track the position of the sun and in the process, partially shade one another over a range of solar angles. The resulting power loss calculations are non-linear and computationally intensive, so broad approximations are often applied in PV simulation tools. However, if one is to optimize the design of a solar PV tracking system, such as the arrangement and interconnection of PV cells and modules on a tracker, and the spacing between trackers and tracker rows, shading losses must be well understood and accurately accounted for. This thesis aims to design and implement a PV simulation model in MATLAB which predicts annual energy production using site-specific weather parameters while accurately accounting for shading losses at a PV-cell level. The model is then used to optimize the spacing of a hypothetical tracking system.

Acknowledgements

I would like to thank the following people for their support:

My primary supervisor, Dr. Edwin Nowicki for his infinite kindness, patience and encouragement.

My co-supervisor, Dr. David Wood, for his wisdom and whose support came at a time of great need.

To Elita, for the four years of sacrifices that made this possible.

Table of Contents

Approval Page.....	i
Abstract.....	ii
Acknowledgements.....	iii
Dedication.....	iv
Table of Contents.....	v
List of Tables.....	viii
List of Figures and Illustrations.....	ix
List of Symbols, Abbreviations and Nomenclature.....	xi
 CHAPTER ONE: INTRODUCTION.....	 1
1.1 General Introduction.....	1
1.2 Tracking Photovoltaic Systems.....	1
1.3 Shading Losses.....	2
1.4 Motivation.....	3
1.5 Scope of Project.....	5
1.6 Contributions.....	6
1.7 Outline of the Dissertation.....	8
 CHAPTER TWO: LITERATURE REVIEW.....	 10
2.1 Model of a Photovoltaic Cell.....	10
2.2 Shading of PV Cells.....	10
2.3 Shading Losses in a Dual-Axis Tracking System.....	11
2.3.1 Worst Case Shading Loss.....	11
2.3.2 Best Case Shading Loss (Proportional Loss).....	12
2.3.3 Mixed Case Shading Loss.....	12
2.3.4 Electrically Modeled Shading Loss.....	12
2.4 Weather Data.....	13
2.5 Spacing Optimization.....	14
 CHAPTER THREE: CONSIDERATIONS IN PHOTOVOLTAIC SYSTEM DESIGN AND SIMULATION.....	 16
3.1 Installed Cost.....	16
3.2 Lifetime Maintenance Cost.....	19
3.3 Energy Generating Potential.....	20
3.3.1 Design Decisions Affecting Energy Generating Potential.....	20
3.3.2 Output Power Prediction: Loss Factors.....	29
3.4 The Optimal System and the Value of a Software Simulation Tool.....	33
3.4.1 Other Benefits of a Simulator.....	36
3.4.2 Existing Simulators.....	37
3.4.3 Development Platforms for a Simulator.....	40
 CHAPTER FOUR: THE PV SYSTEM SIMULATION MODEL.....	 42
4.1 Introduction.....	42
4.2 Development of a PV System Simulator: A Phased Approach.....	42
4.2.1 Phase I.....	43

4.2.2 Phase II	44
4.2.3 Phase III.....	45
4.3 Chosen Development Environment	46
4.4 Description of PV Simulation model and Simulation Stages	46
4.4.1 Stage 1: Read Simulation Settings and PV Module Data.....	48
4.4.1.1 Worksheet 1: Simulation Settings.....	48
4.4.1.2 Worksheet 2: Physical Cell and Module Arrangement	53
4.4.1.3 Worksheet 3: PV Module Parameters.....	56
4.4.2 Stage 2: Read Weather Data	57
4.4.3 Stage 3: Calculate Sun Positions	58
4.4.4 Stage 4: Calculate Physical Shade Factors	61
4.4.4.1 <i>Shading Calculations for Dual-Axis Tracking</i>	62
4.4.4.2 Displaying Shade Factors	65
4.4.5 Stage 5: Calculate Baseline I-V Curves	68
4.4.5.1 The c-Si Single-Diode Model	69
4.4.5.2 Determining R_s and R_{sh}	71
4.4.5.3 PV Module Sub-Division.....	73
4.4.6 Start of Main Loop	75
4.4.7 Stage 6: Adjust Sub-Module I-V Curves for Conditions	76
4.4.8 Stage 7: Determine Module, String and Array I-V Curves	78
4.4.9 Stage 8: Determine MPPs within Inverter Limits	81
4.5 PV Simulator Results.....	82
4.6 Model Verification.....	82
4.7 Discussion.....	85
4.8 Chapter Summary	87
CHAPTER FIVE: TESTING AND RESULTS.....	89
5.1 Hypothetical PV System Under Test.....	89
5.2 Large Variation in Spacing	91
5.3 Small Variation in Spacing	94
5.4 Optimization of Spacing for Cost of Energy	98
5.5 Comparison with Other Shading Loss Approximation Methods.....	100
5.6 Effect of Day-Intervals	102
5.7 Code Execution Time Profile	104
CHAPTER SIX: DISCUSSION	107
6.1 Assumptions and Approximations.....	107
6.1.1 Albedo	107
6.1.2 Sky Diffuse Model	108
6.1.3 System Losses	108
6.1.4 Edge Trackers	109
6.1.5 Tracker Layout	110
6.1.6 Time Interval	110
6.1.7 PV Cell Model.....	110
6.1.8 Reverse-Bias Characteristics of a PV Cell	111
6.1.9 PV Cell Operating Temperature	111
6.2 Other Optimization Opportunities for the Proposed Simulation Model.....	112

6.3 Other Optimization Methods	113
CHAPTER SEVEN: CONCLUSIONS AND FUTURE WORK.....	114
7.1 Summary of Work	114
7.2 Summary of Results and Contributions	115
7.3 Recommendations for Future Work	118
REFERENCES	119
APPENDIX A: SAM MODEL VERIFICATION - TEST SETUP AND RESULTS.....	124
APPENDIX B: PV MODULE PARAMETERS	131

List of Tables

Table 3-1 – Characterization of PV System Costs.....	19
Table 4-1 - Weather File Data	58
Table 4-2 - Simulator Settings for Model Validation	83
Table 5-1 - PV System Setup for Testing	89

List of Figures and Illustrations

Figure 1.1 – A Shadow is Cast from One Tracker onto Another	2
Figure 3.1 - Diagram of a Typical PV Module.....	24
Figure 3.2 - Typical PV Cell I-V and P-V Curves.....	27
Figure 4.1 - PV Simulator Flowchart.....	47
Figure 4.2 - Tracker and Row Spacing of PV Farm	49
Figure 4.3 - Tracker Shading Radius	51
Figure 4.4 – Worksheet 1: Simulation Settings	52
Figure 4.5 – Worksheet 2: Module Cell Layout	54
Figure 4.6 – Worksheet 2: Layout on Tracker.....	55
Figure 4.7 - Worksheet 3: PV Module Parameters	57
Figure 4.8 – Sun Azimuth and Elevation Plot	60
Figure 4.9 - Sun Azimuth and Elevation Plot with Approximation	61
Figure 4.10 - 3-D Visualization of Tracker Shading (Blue is non-shaded; Red is fully shaded; and colours in between are partially shaded cells)	66
Figure 4.11 - Rendering of PV Farm Under Shaded Conditions.....	68
Figure 4.12 - c-Si PV Cell Single-Diode Model.....	69
Figure 4.13 - Simulink Tool for Determining R_s and R_{sh}	73
Figure 4.14 - Baseline Sub-Module I-V Curves	75
Figure 4.15 - Main Simulation Output Screen.....	78
Figure 4.16 - Example of Un-Shaded PV-Cell, Sub-Module, Module, String and Array I-V Curves	81
Figure 5.1 - Cell and Bypass Diode Layout on PV Module for Testing. The module is comprised of three sub-modules connected in series, each shown in a different colour. Each sub-module consists of 16 series-connected PV cells with a bypass diode in anti-parallel at its output terminals (not depicted).	90
Figure 5.2 - PV Module Layout on Tracker for Testing. Each PV module is shaded a different colour, and each PV cell (48 per module) contains the module-number	

of its parent module. 11 modules are in portrait orientation, and one is rotated 90 degrees, in landscape orientation (module number four).....	91
Figure 5.3 – Annual Tracker Output vs. Large Variations (1m) in Tracker and Row Spacing.....	93
Figure 5.4 - Annual Tracker Output vs. Large Variations (1m) in Tracker and Row Spacing (Contours). Contours correspond to a change of 30.27 Wh/yr/tracker.	94
Figure 5.5 - Annual Tracker Output vs. Small Variations (0.1m) in Tracker and Row Spacing.....	95
Figure 5.6 – Annual Tracker Output vs. Small Variations (0.1m) in Tracker and Row Spacing with Regression Plane	96
Figure 5.7 – Annual Tracker Output vs. Small Variations (0.1m) in Tracker and Row Spacing: Excursion of Data from Regression Plane	97
Figure 5.8 - Annual Tracker Output vs. Small Variations (0.1m) in Tracker and Row Spacing: Excursion of Data from Regression Plane (Contours). Contours correspond to a change of 0.0353%.....	98
Figure 5.9 - Cost of Electricity (\$/kWh) as a Function of Tracker and Row Spacing....	100
Figure 5.10 - Cost of Electricity (\$/kWh) as a Function of Tracker and Row Spacing (Contour).....	100
Figure 5.11 – Comparison of Simulation Model Shading Loss Estimates with Other Approximation Methods	102
Figure 5.12 - Effect of Day-Intervals on Annual Energy Production.....	103
Figure 5.13 - Code Execution Time Profiles	106

List of Symbols, Abbreviations and Nomenclature

a-Si	Amorphous Silicon
AOI	Angle of Incidence
BoS	Balance of System
CdT	Cadmium Telluride
CEC	California Energy Commission
CIGS	Copper Indium Gallium Selenide
COE	Cost of Electricity
CPV	Concentrated Photovoltaic
c-Si	Crystalline Silicon
CSV	Comma Separated Values
CWEC	Canadian Weather for Energy Calculations
DNI	Direct Normal Irradiation
EPW	EnergyPlus Weather
E-W	East-West
GCR	Ground Coverage Ratio
GMT	Greenwich Mean Time
GUI	Graphical User Interface
IAM	Incident Angle Modifier
I-V	Current-Voltage
kW	Kilowatt
kWh	Kilowatt-hour
MPP	Maximum Power Point
MPPT	Maximum Power Point Tracking
MW	Megawatt
NRC	Natural Resources Canada
NREL	National Renewable Energy Laboratory
N-S	North-South
OPVC	Organic Photovoltaic Cell
PV	Photovoltaic

P-V	Power-Voltage
SAM	System Advisor Model
STC	Standard Test Conditions
TMY	Typical Meteorological Year

Chapter One: Introduction

1.1 General Introduction

As concerns grow over the effects of burning fossil fuels on our global climate, ever increasing efforts are being made to produce electrical energy from renewable sources. Perhaps no other renewable energy source offers more potential to power our civilization than that of the ceaseless and abundant irradiation arriving from the Sun. Photovoltaic (PV) technology is not a new discovery, but not until recently has it become cheap and efficient enough to begin to compete with non-renewable energy sources in some locations. Accelerating rates of advancement in photovoltaic materials and manufacturing techniques likely mean that grid parity with fossil fuel sources will be achieved for much of the world well within my lifetime. Paired with advancements in energy storage technologies, solar photovoltaic systems have the potential to provide most, if not all of our energy needs of the future with minimal environmental impact.

1.2 Tracking Photovoltaic Systems

Due to recent advancements in the technology, it is no surprise that the installed capacity of solar PV systems is growing exponentially in many places of the world. In the US alone, even in the face of decreasing government financial incentives, the total installed capacity of photovoltaic systems increased by more than 80% in 2011 [1]. Approximately 29% of utility-scale PV systems ($\geq 2\text{MW}_{\text{DC}}$) installed in the US in 2011 employed some form of solar tracking technology [1]. This compares with 19% of systems $\geq 1\text{MW}_{\text{DC}}$ installed in the US between 2008 and 2010 [2], which may suggest that tracking systems are gaining popularity for utility-scale PV projects

1.3 Shading Losses

Though tracking systems offer the obvious benefit of increased output from the same quantity of PV modules as compared to fixed-tilt systems, there is an inherent drawback aside from the added hardware costs: for certain positions of the sun and corresponding orientations of the trackers, shadows are cast by the trackers onto one another, blocking the sun from reaching portions of PV material resulting in system shading losses. An example of such shading is depicted in Figure 1.1.

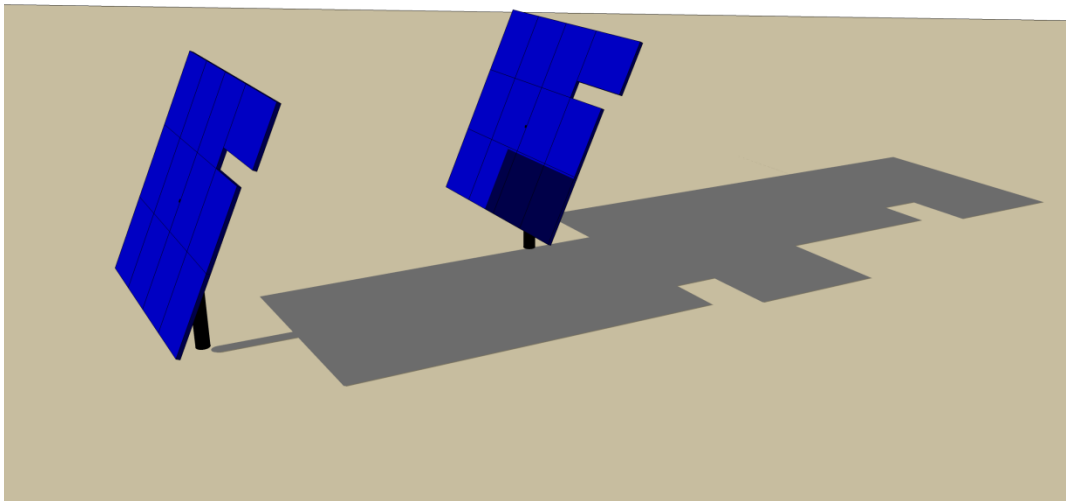


Figure 1.1 – A Shadow is Cast from One Tracker onto Another

Due to the electrical interconnection of cells and diodes in a PV module, and of PV modules in parallel and/or series combinations on a tracker, the power loss resulting from partially-shaded modules is almost always greater than the physical shading ratio may suggest. When considered together with the I - V characteristics of a PV cell and the maximum power point tracking (MPPT) voltage range of the inverter, the process of calculating the shading power loss of a PV tracker is

an involved one. For each new position of the sun, the shading patterns change, requiring the electrical shading loss calculations to be calculated once again.

The spacing between trackers in the N-S and E-W directions has a direct effect on the extent to which shading losses occur. More tightly spaced trackers shade each other more readily, and therefore experience higher shading losses. Widely spaced trackers experience less shading, but require more land area and wiring for the same annual energy production as a more tightly spaced system.

1.4 Motivation

A challenge arose during a professional project of mine, to determine the optimal row spacing for a ~1.3MW single-axis tracking PV system in Sacramento, California. The optimal spacing would be that which resulted in the PV system generating the lowest cost of electricity on an annual basis. The array was to be mounted over several parking lots, providing the added benefit of shading the cars beneath from the hot sun. The system, which was to power a new net-zero facility, was required to generate a specific amount of electricity per year and comprised of components priced by area, such as the raised steel mounting structure and wiring; by unit, such as the trackers; and by kW rating, such as the PV modules and inverters. The area-based costs increased with wider spacing between tracker rows as the system grew in physical area, but the kW-based costs decreased since lower shading losses meant that fewer PV modules would be required to reach the annual electrical energy generation target. Systems with more expensive PV modules favoured wider spacing which made better use of the expensive solar cells as shading losses dropped. Since system costs were well understood, the accuracy of the optimization would

rely on the accuracy of the predicted output of the PV system, which in turn would rely on the accuracy of the prediction of shading losses.

Numerous commercial and government sponsored, publically available PV software simulation tools were tested for predicting PV system energy production: PVSyst [3], SAM [4], HOMER [5], PV*SOL [6] and RETScreen [7]. Ultimately PVSyst was chosen as it was the most substantial and customizable tool found, and is highly regarded in the industry. After researching how shading losses are calculated in PVSyst and other simulation tools, it became apparent that only rough approximations were being applied, most likely in the interest of reducing simulation time, which was currently on the order of seconds. Though in PVSyst, physical shadows were being accurately modeled, their effects on the PV system output were not being modeled as they pertain to the electrical interconnection of cells, diodes, modules and inverters in the PV system. Instead, approximations were made which would reduce a PV string's (a group of series-connected modules) output by pre-set factor if any part of that string were shaded (PVSyst recommends setting this to 60% to 80% of the string's non-shaded output). Other tools rely on the user to enter shading losses manually, and still others do not address shading in tracking systems at all. No tools were found which accurately addressed shading losses in tracking PV systems. It was therefore felt that the optimization of tracker spacing for the project would suffer as a result. My thesis topic was therefore chosen based on the need for a PV simulation tool which can accurately model shading losses in a tracking PV system and use this to optimize tracker spacing. If even incremental improvements in system optimization result, the enormous cost of utility-scale projects could make a new, more accurate simulation model worthwhile.

1.5 Scope of Project

The goal of this project is to develop a simulation model of a dual-axis tracking PV system, which is to include an accurate calculation of shading losses. The model will predict the annual energy production of a sample dual-axis tracking PV system, and will be used to optimize the N-S and E-W spacing between trackers in order to minimize the cost of electricity produced. The goal is not to account for all system losses in order to achieve a high degree of absolute accuracy, but rather to demonstrate the effect that shading losses have on the optimal spacing of trackers. As such, emphasis is on the energy production *differences* between systems with varied tracker spacing (all other things being equal).

To achieve this goal, the following items fall within the scope of the project:

1. Perform a search of the literature in order to determine the latest state of the art for the mathematical modeling of PV cells, the calculation of shading losses for PV cells, and the modeling of dual-axis tracking systems and the shading thereof.
2. In a suitable programming language, implement a model of a PV cell and derive an I - V curve from the model based on cell parameters, ambient temperature and irradiation.
3. Implement the calculation of the sun's azimuth and elevation for any time and date of the year.
4. Implement the ability to import weather data and latitude for a particular site into the simulation model.
5. Construct a user interface for the simulation model which will allow the PV tracker and simulation settings to be defined by the user.
6. Derive a method for calculating shading patterns cast onto trackers from neighbouring trackers based on the dimensions and arrangement of PV modules mounted to the

trackers, the spacing between in the trackers in the N-S and E-W directions, and the position of the sun. Plot the shading patterns in real-time on a 3D visualization graph representation of a tracker, in order to provide a check to the user.

7. Devise a method for determining the module I - V curves from the individual cell I - V curves, the shading patterns they are subject to, and the placement of bypass diodes within the modules. Then, determine the string and tracker I - V curves based on the module I - V curves and the interconnection scheme of modules on the tracker.
8. Apply the inverter MPPT range to the appropriate I - V curve and determine the maximum power point of the module (in the case of micro-inverters) or tracker (in the case of a string or central inverter).
9. Implement a loop around the relevant portion of the model in order to run through an annual simulation period based on hourly time steps. Add additional nested loops to test a range of parameters sequentially.

1.6 Contributions

The thesis contributions include:

1. A review of published work on the analysis and calculation of dual-axis shading losses, and the testing of existing commercial and public (government-funded) PV simulation tools. This research revealed that very little work had been done on analysing shading losses accurately (electrically, down to a PV-cell level) for dual-axis tracking systems over an annual period. Instead, basic approximations are universally applied in existing simulators of tracking PV systems.
2. A model developed in MATLAB Simulink which derives through iteration, the equivalent series resistance (R_s) and shunt resistance (R_{sh}) of a solar cell based on known

parameters provided from the manufacturer's data sheet (I_{sc} , V_{oc} , I_{mp} and V_{mp}) and an assumption for diode ideality (n). These parameters are required for the single-diode model of a PV cell.

3. A user interface built in Microsoft Excel which allows the user to input many different design and simulation parameters for a tracking PV array.
4. A PV simulation model developed in MATLAB which reads settings from the user-interface and weather data from a standardized EPW file, calculates solar angles and the positions of physical shadows cast by trackers onto one another for each solar angle, determines the shading ratio of every PV cell on a tracker array for every sun angle, calculates the I - V and P - V curves of each sub-module, module, string and array using the single-diode model of a PV cell and based on the weather conditions for each hour of the year, and finally determines the power generated by various inverter schemes by applying inverter maximum power point (MPP) limits to the P - V curve data over an annual period.
5. A simulation model for dual-axis PV tracking systems which provides the relationship between shading losses and any number of different system design variables, however in this thesis, only the relationship between shading losses and tracker spacing is studied.
6. The results of a simulation of a hypothetical PV system which was run through the simulation model, which revealed a non-linear, complex relationship between tracker spacing and shading losses.
7. The results when hypothetical system component costs are combined with the predicted annual energy outputs of the system over a range of spacing, with the goal of

determining the optimal spacing of trackers and trackers rows (in this case, optimal spacing meaning the spacing which results in the lowest cost of electricity generated).

8. A roadmap for future model development, including suggestions for additional features to be added in future versions of the simulation model. The roadmap details feature sets to be added to reach successive phases of the project. This project represents phase I of a proposed three-phase roadmap.

1.7 Outline of the Dissertation

The thesis is structured as follows:

Chapter Two: Literature Review - A review of the latest published work on the modeling of PV cells and PV systems, with a focus on the treatment of shading losses.

Chapter Three: Considerations in Solar Farm Design and Simulation - A more thorough look at the scope of designing a PV system simulation model. This chapter describes the relevant design parameters of a tracking PV system which will need to be modeled. A closer look is given to several common commercial PV simulators to highlight the strengths and weaknesses of each. Finally, the merits of potential development platforms are weighed.

Chapter Four: The PV System Simulation Model - A flowchart of the simulation model is presented with detailed descriptions of each stage in the simulation. The user interface is presented with descriptions of each design parameter. The PV cell model is described, as are the methods of determining the solar elevation and azimuth, hourly weather parameters, and shading patterns cast onto trackers. Screenshots of the real-time visualization outputs of the simulation model are provided, showing calculated shading patterns on the tracker and

calculated module, string, and tracker I - V and P - V curves. Finally, the model is verified against a commercial PV simulation tool.

Chapter Five: Testing and Results - A sample PV system is defined and run through the simulation model for a one-year period with varying tracker spacing in the N-S and E-W directions. Surface plots of the results show the non-linear, complex relationship between tracker spacing and shading losses. The difference between the results and the best-fit linear regression plane highlights the nature of the relationship. Sample system component costs are chosen and applied to the results in order to determine the optimal spacing of the trackers based on the lowest cost of electricity generated. Next, the simulation model shading loss predictions are compared to those of common rough approximation methods. Finally, an analysis is performed on the execution time of each portion of the simulation model in order to show which steps are most computationally intensive and which offer the most room for improvement.

Chapter Six: Discussion - A review of the simulation model assumptions and approximations is presented.

Chapter Seven: Conclusions and Future Work - The simulation model and sample PV system test results are summarized, and recommendations are given for future work.

Chapter Two: Literature Review

2.1 Model of a Photovoltaic Cell

At the core of any PV system simulation model is the model on an individual PV cell; a system of equations which describes the relationship between the current and voltage (the I - V curve) generated by a PV cell. A search of the literature was performed to find such models; particularly those which lend themselves well to implementation in a computer program. Though numerous models exist, the single-diode model stood out as the most common, and of adequate accuracy when compared to more complex models, such as the two-diode model [8]. One interpretation of the single-diode model, which consists of a system of five equations in five unknowns, is described and validated in [9] and forms the basis for the PV cell model used in this thesis.

2.2 Shading of PV Cells

The result of shading a single PV-cell is that direct incident irradiation is reduced by the fraction of the cell which is shaded, and the photocurrent generated by the cell is reduced proportionally. When the shaded cell is in a circuit with bypass diodes and other PV cells in series and parallel combinations, the behaviour of the overall circuit becomes less clear. A search of the literature was performed to review methods of analyzing the effects of partially shaded PV cells in a network of PV cells and bypass diodes. [10] and [11] demonstrate the dramatic effect that the placement of bypass diodes and arrangement of series-parallel combinations of PV cells play in determining the I - V curve of an array of cells. In [12], a MATLAB model was created to model the effects of partial shading on a PV array, but with limited flexibility and designed for static shadows.

2.3 Shading Losses in a Dual-Axis Tracking System

Next, a search of the literature was performed to determine the extent to which self-shading losses have been characterized in dual-axis PV tracking systems, and whether these losses have been applied to the optimization of tracker design or placement of trackers in a solar PV farm. Though there were an abundance of papers found on various aspects of PV shading, the most popular application of this research was focused on inverter MPPT techniques for shaded arrays. Only a small number of papers attempted to characterize self-shading losses in dual-axis tracking PV systems, and only a small subset of these applied the losses to the optimization of tracker spacing. Twelve papers were found which were most relevant to this topic. Each of the twelve papers estimated tracker self-shading losses, but there were several different methods utilized, and each method employed different levels of detail and approximation in the calculations. Most made significant simplifications of the problem in order to avoid addressing the computationally intensive simulation of the electrical interconnection of cells, diodes and modules on a tracker. The accuracy of these approximation methods, which are listed below, is analysed in 5.5.

2.3.1 Worst Case Shading Loss

In [13], [14] and [15], the approximation is made that if any portion of a tracker is shaded, then the output of that tracker is assumed to be zero. This represents the worst-case scenario for the estimation of shading loss and necessarily over-estimates the resulting power loss. This is, however the simplest method to implement.

2.3.2 Best Case Shading Loss (Proportional Loss)

In [16], [17], [18], [19], [20] and [21], the approximation is made that electrical shading losses are directly proportional to the fraction of the tracker shaded. For example, if a shadow covers one quarter of a tracker, then it is assumed that the tracker's output drops by one quarter. This is a simple and fast approximation to implement, but represents a best-case scenario which almost always guarantees an under-estimation of shading losses. This is because the shading loss experienced by one PV module usually affects nearby modules due to their electrical inter-connection and the fact that they usually share an inverter.

2.3.3 Mixed Case Shading Loss

In [22], both the worst-case and best-case shading losses are calculated, with an average result used for the estimated shading loss. Of note, PVSyst allows the user to select the best-case, the worst-case, or some pre-defined fraction of the worst-case for the overall estimation of shading loss. Shading losses are very system- and location-specific however and there is no way of knowing where within the minimum and maximum bounds the actual shading loss lies without actually modeling and simulating the tracker electrically down to a sub-module level.

2.3.4 Electrically Modeled Shading Loss

One paper, [23], does describe the modeling of the trackers electrically in order to accurately determine shading losses, but is the research of manufacturer SolFocus Inc., and only simulates concentrating photovoltaic (CPV) modules (which are composed of multi-junction cells at the focus of a lens or reflector, thereby only converting direct normal irradiation, and each with their own bypass diode) mounted in a fixed 4x7 rectangular configuration. The concept of sub-

modules (groups of cells protected by a single bypass diode) as found in non-concentrating PV, is not addressed in this paper. Furthermore, being privately funded research, the details of the model and methods used are not publically available.

2.4 Weather Data

The use of a complete annual cycle of actual representative weather data for the geographical site of the PV tracking farm is crucial for the accurate prediction of shading losses and energy production. Not only do direct normal irradiation (DNI) and diffuse irradiation dictate the current generated by PV cells, but cell temperature affects the output voltage of PV cells. Cell temperature can be estimated based on ambient air temperature and the magnitude of DNI incident on the cell. If a greater level of detail is desired, wind speed and mounting method can also be factored in, but this is of limited use in a simulation which focuses on the differences between the output of PV trackers based on changes in tracker spacing, module arrangement, etc. For many of the papers cited which focus on self-shading in dual-axis tracking systems, it is difficult to determine if weather data is used. For those papers which estimated shading losses and annual energy production formulaically without simulating discrete time steps over a representative annual period, it would not be possible to factor in a complete weather dataset accurately, therefore requiring some form of statistical averaging or other approximation. [14], [17], [20], and [24] make no mention of the use of weather data. [21] uses the Bird model to approximate average direct normal irradiation (DNI) based on the site latitude and air properties, but uses no other weather information. [16] uses irradiation data only, making no mention of using ambient temperatures to help determine PV cell temperatures. [13] calculates irradiation based on geographical location, and approximates cell temperatures based solely on the

irradiation incident on the PV cells. In [18], a formula is used to estimate hourly DNI from daily and monthly averages, which does not factor in typical daily weather patterns. In [19] and [22], monthly averages for irradiation and temperature are used. In [23], Typical Meteorological Year (TMY) irradiation and temperature weather data is used in a simulation model. [15] mentions briefly that actual irradiation and temperature data are used in a simulation model, but does not give any details.

2.5 Spacing Optimization

Of the twelve most relevant papers found, three ([17], [20] and [24]) focused exclusively on the estimation of shading losses in a dual-axis tracking system, and did not move on to use this data for the optimization of any aspect of the PV system design. [15] performed various sensitivity analyses for shading in tracking PV systems against parameters such as tracking method, ground coverage ratio (GCR), aspect ratio of tracker spacing and maximum tracker rotation angle.

Though the charts may be useful from a design perspective in a general sense, they will only provide rough insights into how various design aspect may affect shading losses. [23] used a simulation model to test four different electrical interconnection schemes of CPV modules on a tracker (with the same physical arrangement) in order to determine which produces the most power annually, where differences in shading losses account for the differences in annual output. [13] used estimated shading losses for a single-axis PV system to optimize single-axis tracker row spacing, but did not consider a dual-axis tracking system. The six remaining papers [14], [16], [18], [19], [21] and [22]) did apply shading loss calculations to the optimization of tracker placement to some degree in a dual-axis tracking system. [16] varied dual-axis tracker spacing based on a rectilinear arrangement of trackers with equal north-south and east-west spacing. The

purpose was to study the effects of trackers on the edge of a field of CPV trackers on total system output, and is therefore of limited relevance to research which assumes an infinitely large field of PV trackers. For simplicity, [22] assumes dual-axis trackers to have a square arrangement of PV modules, and that trackers are arranged in a rectilinear fashion with east-west spacing equal to north-south spacing. This results in a single optimization parameter, ground coverage ratio (GCR), but this simplification severely limits the scope of the results. [18] and [19] optimize tracker spacing only for a rectangular pattern of trackers, with [18] also optimizing for inverter type (based on a CPV system). [21] assumes a hexagonal arrangement of trackers, but also uses the GCR parameter which does not allow the E-W and N-S spacing to be changed independently. Instead of optimizing spacing for cost of electricity, the aim was to determine the optimal aspect ratio of PV modules mounted to the tracker for different GCRs. [14] optimized the placement of trackers using an evolution-based algorithm, based not only on neighbour-tracker shading but also on shading from nearby fixed objects, such as buildings.

Chapter Three: Considerations in Photovoltaic System Design and Simulation

A common goal in PV system design is to minimize the average cost of electricity (COE) over the lifetime of the system, measured in \$/kWh. In other words, the PV system must generate the most electricity per dollar of installed cost plus lifetime maintenance costs (which are relatively low for PV systems as compared with other energy sources). In order to minimize the \$/kWh metric, it is important for the designer to understand both halves of the equation: system costs and energy generating potential.

3.1 Installed Cost

The installed cost of a PV system is quite a bit easier to estimate than its electrical output potential, and can be roughly broken down into the following categories. Note that this list is not necessarily complete for all projects, and is based primarily on the author's experience and reflections, though references are given where appropriate.

1. *PV Modules* – PV modules usually constitute the largest single cost in a PV system. In non-concentrating systems, a module consists of a multitude of solar cells electrically connected in series (48, 60 or 80 series-connected cells are common). A typical module incorporates a high-transmittance, low-iron tempered glass outer layer, and is held together with a weatherproof aluminum frame. Additional layers of various materials are applied to the back of the PV cells to provide protection from the elements. A junction box attached to the back of the module houses bypass diodes and wiring interconnections. The total cost for the PV module portion of the overall PV system cost is approximately proportional to the combined peak output power of the system under standard test

conditions (STC): 1000W/m^2 of irradiation, at a cell temperature of 25°C . PV module cost can therefore be considered a $\$/\text{kWp}$ (kilowatt-peak) cost.

2. *Trackers/Mounts* – In tracking PV systems, PV modules are affixed to sun-tracking mounts which offer increased daily energy production compared to fixed-tilt systems. Trackers continually adjust their orientation (often using motors) so as to minimize the angle of incidence (AOI) of incoming solar irradiation with respect to the perpendicular of the surface of the PV modules, according to the changing position of the sun over the course of each day. There exist many different sizes and types of tracking systems which will be discussed later in this chapter. Whether the system is tracking or fixed-tilt, it must be able to withstand wind and snow loads according to the local building code. Since the quantity of trackers and/or mounting hardware required scales according to the number of modules in the system (not to be confused with the total power rating of the modules in the system), tracker cost is considered a $\$/\text{module}$ cost. For example, a 1MW system using low-efficiency PV modules would require more trackers than a 1MW system using high-efficiency PV modules.
3. *Land* – This is the area upon which the PV system is installed. In commercial-scale installations, this cost may be zero if an existing rooftop or parking area is to be used, but generally for utility-scale PV systems, land must be purchased or leased for the project. Land represents a $\$/\text{m}^2$ cost.
4. *Structural* – In the case of installations over parking areas (which provide the ancillary benefit of providing shade to parked vehicles), structural costs can be significant for elevating the trackers and/or PV modules off the ground. The structure must be strong enough to withstand extreme wind loads to ensure the safety of the public. Usually

dominated by the price of steel, this cost scales according to area and therefore represents a $\$/\text{m}^2$ cost.

5. *Inverters* – Inverters convert the DC power generated by PV cells into highly regulated AC power that can be consumed locally and/or fed into the electrical grid. The required inverter power rating is proportional to the power rating of the PV modules they are connected to. For example, it is common to have an inverter network rated at 80% to 90% of the peak power rating of the PV array (for reasons which will not be discussed in this chapter). Inverters therefore represent a $\$/\text{kWp}$ cost.
6. *Labour* – The labour cost associated with the installation and commissioning of PV systems generally scales according to the number of modules in the system, resulting in a $\$/\text{module}$ cost.
7. *Balance of System (BoS)* – BoS costs includes all remaining components such as wiring, junction boxes, transformers and power monitoring equipment. Often dominated by the wiring component, this category can generally be considered a $\$/\text{module}$ cost, since each PV module requires wiring from its junction box to another module, inverter and/or array. In reality, wiring cost would also have a $\$/\text{m}^2$ component, which is neglected in this analysis. The wiring cost is also affected by the operating voltage of the system. A lower voltage system will experience higher resistive losses than a higher voltage system assuming the same gauge of wiring is used. To achieve the same resistive losses, the lower voltage system would require a more expensive, heavier gauge wire than the higher voltage system. This difference becomes apparent when comparing micro-inverter-based systems (using one inverter per PV module) operating at 240VAC, to centralized inverter-based systems operating at 600VDC.

The various PV system costs are categorized in Table 3-1. As the table shows, each project cost scales in one of three ways: according to the peak rated power of the system, the number of PV modules in the system, or the area required for the installation. The fact that the various system costs scale differently from one another adds complexity to the task of optimizing the system to produce the lowest cost electricity.

Table 3-1 – Characterization of PV System Costs

	\$/kWp	\$/module	\$/m ²
PV Modules	✓		
Trackers/Mounts		✓	
Land			✓
Structural			✓
Inverters	✓		
Labour		✓	
Balance of System		✓	

3.2 Lifetime Maintenance Cost

Maintenance costs for PV systems are quite small compared to the installed cost, and also considerably lower than most other energy sources. Costs may include periodic cleaning of the PV modules, and replacement of faulty equipment (though much of the equipment is often under warranty for a 25-year operating life).

3.3 Energy Generating Potential

Accurately predicting the energy generating potential of a PV system is a complex but necessary step in the process of designing a cost efficient PV system. These predictions, whether derived from rough hand calculations or supplied by computer simulations, provide a basis for comparison between the multitude of components available to choose from, and the multitude of ways in which these components can be combined and configured.

3.3.1 Design Decisions Affecting Energy Generating Potential

With so many variables in the design of a PV system, there are a huge number of possible designs, each one having a different annual output for the specific installation site. These design variables include:

1. *Tracking Hardware* – Options include fixed-tilt or tracking. Tracking systems include single-axis and dual-axis trackers. Single-axis tracking systems include E-W-horizontal-axis, N-S-horizontal-axis, N-S-tilted-axis, and azimuthal-axis (vertical axis). Dual-axis tracking systems include tip-tilt and azimuth-altitude. Different tracking systems have different costs and offer different energy harvesting improvements over a fixed-tilt system, depending on their placement, and the latitude and annual weather profile of the installation site.
2. *Tracker Placement* –
 - a. *Spacing* - The spacing between trackers in a single row, spacing between rows of trackers, orientation of the rows, and offset between trackers in alternating rows are all variables in the design of a tracking PV system. Placing trackers very close to one another increases the total energy generated per unit area, but at increased

cost because PV modules on tightly-packed trackers experience increased shading losses due to neighbouring trackers. Placing trackers very far apart will generate the most energy per tracker due to decreased shading losses, but the additional required space increases the $\$/\text{m}^2$ costs. The optimal spacing lies somewhere between the extremes, and depends on many factors including the various costs and cost characterizations, the physical shading characteristics of the trackers, the type of tracking used, the electrical properties of the PV modules, the wiring scheme of the modules and inverters in the array, and more.

- b. *Offset* – The most common layout for a network of PV trackers can be visualized by first imagining a row of equally spaced trackers in the E-W direction, where the distance between two adjacent trackers is x . Next, duplicate this row many times to the North and South of the original row, with equal spacing, y , between each row. Finally, shift every second row to the East by $x/2$. This forms a hexagonal pattern (each tracker has six neighbours, which form a hexagon), or honeycomb lattice with a tracker at each vertex. As common as this layout is, it is not likely the most efficient one in many geographic locations. For example, in a location which regularly sees more sun in the morning than in the afternoon due to local weather patterns, it would likely be of net benefit to shift the rows slightly differently to minimize shading losses in the morning at the expense of additional shading losses in the afternoon.
3. *Tracking Control Methodology* – A simple tracking system would make continuous adjustments in an attempt to orient the PV modules perpendicular to incident solar irradiation as it tracks the sun across the sky, under the premise that this would generate

the most energy over the course of the day. In a tracking PV system where trackers shade their neighbours during certain times of the day however, non-linear shading losses (i.e. power loss is not proportional to the area of shading) occur which can be significant, requiring a more advanced tracking technique to maximize daily net output. A method currently in use, referred to as ‘back-tracking’ ensures that trackers never shade one another and within this constraint, orients the PV modules as close to perpendicular to the sun’s rays as possible at all times. The tracker layout dictates the range of orientations (azimuth/tilt angles) which prevent any tracker-to-tracker shading. This method is called back-tracking because once the sun reaches a position at which the trackers begin to shade one-another, they actually begin to tilt away from the sun to prevent shading from occurring.

4. *PV Module* – The selection of the PV module is one of the major factors affecting the performance of the PV system. Some of the variations between PV modules include:
 - c. *Technology* - There are many different photovoltaic technologies available including traditional mono- and poly-crystalline silicon (c-Si), numerous thin-film technologies including amorphous silicon (a-Si), cadmium telluride (CdTe), copper indium gallium selenide (CIGS), and various types of organic PV cells (OPVC). Each technology produces different inherent cell voltages and behaves differently under changing light and temperature conditions. Furthermore, shading losses are subject to vastly differing mechanisms, such that the same mathematical shading model cannot be applied to all PV technologies.
 - d. *Efficiency* – Each technology exhibits different typical efficiencies. Even within a single particular technology, polycrystalline silicon for example, there is a wide

range of operating efficiencies available. Not only do different manufacturers use different processes, but due to statistical manufacturing variations, cells from a single production line will exhibit a distribution of cell efficiencies. These cells are sorted into efficiency ‘bins’ (e.g. 13-14%, 14-15%, 15-16%, etc.) and the PV modules they are built from are priced accordingly, with higher efficiency modules coming at a price premium.

- e. *Cell Grouping* – The PV cells within a module are divided up into groups, with a bypass diode connected in anti-parallel across each group. In a c-Si module, there is often a diode connected across a group of approximately 20 cells, which is designed to protect the cells in the event that a cell becomes shaded. In the worst-case scenario without diodes, when only a single cell becomes completely shaded and the rest are subject to high irradiation, the current in all cells is limited to near-zero due to the series connection with the shaded cell, and the voltage potential generated by the irradiated cells reverse-biases the shaded cell. Without bypass diodes, this would include all the remaining cells in the module, so in a 60-cell module this could easily be 35 volts, which is much higher than the c-Si cell reverse breakdown voltage of $\sim 13\text{V}$. This causes a ‘hot-spot’, damaging the cell as it over-heats. By adding bypass diodes, the diode protecting the cell-group with the shaded cell automatically begins to conduct, providing the other cell groups a bypass current path and limiting the reverse-biasing voltage across the shaded cell to a safe level. Not only does this protect cells from damage, but it also serves to limit power loss during shading conditions. Almost exclusively, cell groups in c-Si modules are arranged lengthwise along the module, presumably to

simplify wiring as all cell groups begin and end on the same side of the module as shown in Figure 3.1. The downside however is that if a shadow is cast across the bottom (or, top) row of cells in the module, all cell groups are affected and the power output of the module can drop to near-zero. This is especially important in linear arrays of fixed-tilt modules where the shadow of one row reaches the bottom of the next row. At least one manufacturer has designed PV modules in which the bottom rows of cells form a single cell group to mitigate these losses. One can imagine many possible arrangements of cells into groups, but the difficulty lies in understanding which arrangement is optimal for a specific system.

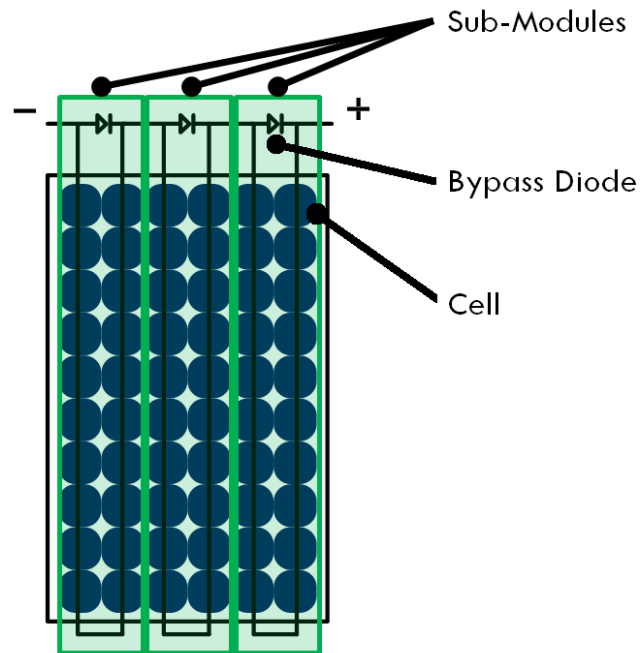


Figure 3.1 - Diagram of a Typical PV Module

5. *PV Module Placement on the Tracker* – There are any number of ways to arrange PV modules on a tracker. The simplest perhaps is a rectangular arrangement, but this is not an option if the tracker is using a single inverter which requires an odd number of the PV modules chosen. A quick review of photos of various tracking PV systems from around the world reveals that there is no consistent manner in which modules are arranged on trackers. Some adopt an ovular arrangement, others a rectangular arrangement with empty spaces at the corners or in the centre, and still others are rectangular with additional modules added around the edges. Some mount the PV modules in landscape orientation, others in portrait orientation and still others in mixed orientations. The arrangement of PV modules on a tracker has a direct effect on the shadows cast from one tracker onto another, meaning a direct effect on the shading losses of the system. Due to the placement of bypass diodes across cell groups within the PV modules and the series or series-parallel interconnection of modules on the tracker, the quantification of shading losses is difficult to impossible to accurately predict without simulating the system over the course of a year with accurate weather data for the site.
6. *PV Module Connection Scheme and Placement* – A PV module consisting of a string of series-connected PV cells will exhibit a particular I - V relationship under certain temperature and irradiation conditions. Figure 3.2 shows the I - V and P - V curves for a typical PV cell. Since the voltage generated by a single PV module is lower than the minimum input voltage of most inverters (micro-inverters are the exception, which are discussed later), multiple PV modules must be connected in series to achieve the required voltage. It is also common to connect multiple such strings in parallel to increase the current in order to match the inverter's current rating. Such a series-parallel grouping of

PV modules is referred to as a PV array. Due to the electrical interconnection, modules in a series-string are forced to operate at the same current, and strings in parallel are forced to operate at the same voltage. This means that even though the inverter may be operating the array at an optimal voltage and current representing the maximum power point (MPP) for the collective group of modules under certain conditions, it is still a compromise because each individual PV module will not be operating at its unique MPP. Furthermore, since losses affecting a single PV module (such as shading) will affect the output power of all the PV modules in its parent array, it follows that the physical arrangement of PV modules and/or arrays on a solar tracker is another factor affecting power generation potential.

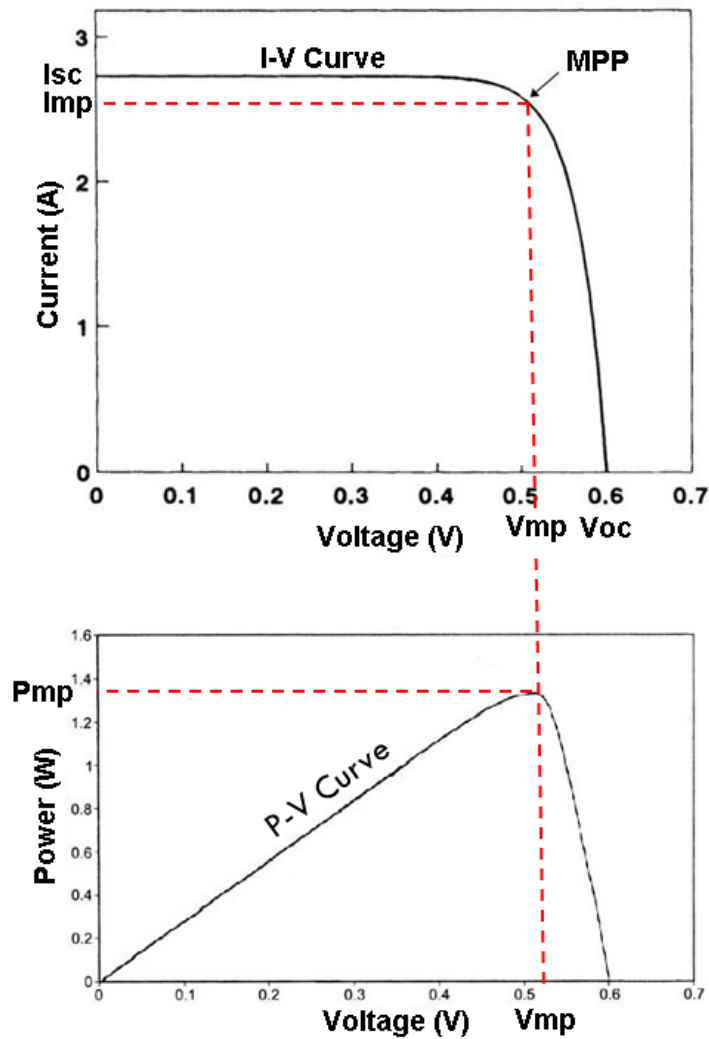


Figure 3.2 - Typical PV Cell I-V and P-V Curves

7. *Inverter Scheme* – An inverter converts the DC power supplied by the PV modules or arrays into AC power to be used on-site or exported to the electrical grid. Just as there is great variety among PV modules, there is also great variety among inverter designs. A micro-inverter (generally 200 to 300W) is designed to be connected to a single PV module, eliminating the need to connect multiple modules together to form arrays. For example, a micro-inverter may convert 35VDC to split-phase 240VAC. Advantages

include the fact that module shading losses are isolated to the individual PV module, but disadvantages include a slightly lower conversion efficiency and a higher total inverter cost. Also, due to the limited MPP input voltage range, there are some shading situations where the micro-inverter will harvest less power from the shaded module than a larger multi-module inverter would. String inverters and central inverters have much higher input voltages, requiring multiple modules to be connected in series (for example, 10-13 in series) to achieve the required input voltage. Series strings are connected in parallel to increase the current as per the central inverter's current rating. The advantages of large central inverters include higher efficiency, lower cost (per kW) and reduced resistive heating losses due to the higher operating voltage as compared to micro-inverters. The main disadvantage however, is that losses caused by a single module (such as due to shading) may be magnified across the entire array.

8. *Power Optimizers* – A relatively new technique being used for electrical power conversion is to use DC-DC converters for each PV module, referred to as 'power optimizers', and a centralized inverter. Doing so allows for greater flexibility in setting the operating voltage and current of each module in an array. Efficiency improvements may result from operating individual modules at their unique MPPs while still allowing the connection of a series-parallel configuration to a highly efficient central inverter. This technology effectively combines the benefits of micro-inverters with the benefits of central inverters, but with additional conversion power loss and increased cost.

3.3.2 Output Power Prediction: Loss Factors

In order to arrive at the optimal solution (that which generates the lowest cost electricity) for a particular PV project, the power generating potential of various design permutations must be predicted based on the characteristics of the available components and the weather profile of the installation site. Key to understanding the output potential of a PV system is to understand the various loss mechanisms at play in the system:

1. *Module and String Mismatch* - Since no two PV modules are identical (manufacturers often test the rated power of PV modules and sort them into 5W incremented bins, each priced accordingly), each has a unique I - V curve (at STC) describing its range of possible operating points, along which is a point called the MPP representing the voltage and current at which the respective module will output the most power (see Figure 3.2). This I - V curve and corresponding MPP shifts with changing irradiation and temperature. When a string of modules are electrically connected in series, they must operate at the same current. Since there is usually no single current that will intersect the MPPs of all the modules in the string, the inverter must choose the best compromise for the string as a whole. The module mismatch power loss is defined as the difference between the maximum power generating potential of a group of modules operating at their individual MPPs, and the maximum power generating potential of the same group of modules connected in a series string. A similar loss mechanism occurs when multiple module-strings are connected in parallel to form an array. Since each string must operate at the same voltage in such a configuration, this voltage will not be optimal for each string and instead will be the best compromise for the group of strings. The power loss arising from the compromise is called the string mismatch loss. In each case, the goal of the inverter

controller is to find the MPP of the connected module, string or array by continually make adjustments to the operating voltage and current to track this point as it moves under changing conditions. To partially mitigate these losses, installers may decide to sort the modules by their maximum power current (I_{mp}) and group modules with similar I_{mp} together into strings. Strings can also be grouped together according to their maximum power voltage (V_{mp}) in larger systems with multiple central inverters.

2. *Soiling* – Any material deposited on the PV module glass which interferes with the incoming radiation will adversely affect the power generating potential of the module. Most often taking the form of dust and snow, the magnitude of soiling losses depends heavily on the climate of the installation site. For example, desert climates that experience long stretches without rain tend to accumulate more dust in the absence of rain to wash the dust from the modules. Similarly, climates with heavy snowfall and long time-spans without winter warm spells experience more soiling losses due to accumulated snow that does not melt for long stretches of time. These losses also depend on the mounting angle of the modules, as a steeper pitch will shed dust and snow more readily than a shallow one. Other sources of soiling are very site-specific and can include fallen leaves from nearby trees and bird droppings. It is difficult to model and predict soiling losses, so approximations are often used based on the properties of the local climate, and may amount to about 1-5% of annual output [25].
3. *Aging* – The output of any PV module will drop gradually over the course of its lifetime once the initial break-in period has elapsed. Manufacturers often provide a lifetime performance warranty on modules, with the industry standard of guaranteeing that modules will output at least 90% of their rated power after ten years, and at least 80% of

their rated power after 25 years. This corresponds to a maximum degradation of approximately 1% per year.

4. *Non-uniform Aging* – Manufacturing deviations and differences in soiling, shading or irradiation mean that some modules will degrade more quickly than others. Diverging module performance means diverging maximum power points for each module in an array. If the modules are connected in series or series/parallel combinations to a string or central inverter, these diverging MPPs often result in a magnification of the power loss, over and above what would result if each module's MPP were tracked individually such as with micro-inverters.
5. *Wiring Loss (Resistive Heating)* – A portion of the electrical energy flowing through the PV system's interconnecting conductors is converted into heat due to resistive losses, which are dependent on wire diameter, total wiring length, and the current flowing through each conductor. A higher system voltage is advantageous as it results in a lower current for the same power transmitted, which results in lower resistive losses. Higher voltage systems may also use less expensive, smaller diameter wire.
6. *Temperature* – Each PV technology is affected differently by changes in temperature, however it is universally true that higher temperatures result in decreased power production potential, and vice-versa. In c-Si PV, the coefficient K_i , which represents the percent change in current with respect to the change of temperature (in %/°C), is negative, meaning that increasing temperatures result in decreased cell current. The coefficient K_v is the equivalent relationship for cell voltage with respect to temperature, and is positive for c-Si cells (meaning a higher temperature results in a higher cell voltage), though with considerably less magnitude than K_i . The net result of the combined

effect of K_i and K_v , is that power decreases with increasing temperature. Thin film technologies are traditionally more resilient to higher operating temperatures than c-Si. Along with the ambient air temperature and magnitude of incident solar irradiation, wind speed and type of installation play role in the operating temperature of the PV modules. Elevated, well-ventilated systems operate cooler than those with PV modules mounted in sealed enclosures or in close proximity to a hot roof.

7. *Shading* – As different PV technologies are affected differently by changing temperatures, the same is also true for module shading. Differences in the physics of the material comprising the solar cells and the internal electrical interconnection between cells (say, between c-Si and thin-film technologies) mean that an entirely different set of formulae exist for modelling shading on different PV technologies.

To simplify the treatment of shading in a PV simulator, it is often divided into two separate categories: near-field shading and horizon shading. The former includes shading from nearby structures or neighbouring PV modules and requires some form of 3D modeling to determine the position, size and shape of shadows cast by these objects. The latter includes distant features such as mountain ranges, which are much easier to factor in since they provide complete shade for a well-defined range of solar azimuth and elevation.

8. *Incident Angle Modifier (IAM) Loss* – Most of the solar irradiation incident on a PV module is transmitted through the protective glass onto the solar cells, but some is lost due to refractions and reflections at the glass-air and glass- solar cell boundaries, and due to absorption by the glass itself. These losses are minimized when the solar rays are perpendicular to the PV module (IAM of 1), and increase as the angle of incidence (AOI)

increases (IAM approaches 0 as the angle of the sun's rays approach 90° from the normal of the PV module surface). Manufacturers have taken steps to minimize these losses, including the use of low-iron, high-transmittance glass and using stippling on the surface of the glass to trap light. A table of IAM as a function of the AOI of incoming irradiation for the glass used in the modeled PV module allows for the quantification of this loss factor in the simulation model.

9. *Inverter Losses* – Conversion losses are inherent with any inverter. These losses are not directly proportional to the power converted however, and inverter manufacturers therefore provide efficiency vs. power curves for their products. Inverter efficiency is commonly low at low power, peaks at a mid-range power and slowly drops off up to the rated power. Manufacturers also often provide a single efficiency number representing a weighted efficiency based on a typical daily load profile as determined by the California Energy Commission (CEC efficiency) or equivalent European body (Euro efficiency), to provide rough estimation of what can be expected when the PV array is sized optimally for the inverter in a typical installation.

3.4 The Optimal System and the Value of a Software Simulation Tool

As shown above, there are many variables in the design of a PV system, which together provide a difficult optimization challenge for any designer trying to determine the most cost effective system for a particular site (lowest \$/kWh). Some of the questions the designer may have to consider include: Are more expensive high-efficiency PV modules worth the extra cost? What type of tracking should be used, if any? If using trackers, how should trackers and tracker-rows be spaced? In what arrangement should modules be placed on the trackers? What is the best

compromise between tracker-to-tracker shading losses and array compactness? What series/parallel configuration should be used for the modules? What inverter topology (micro-inverters, string inverters, central inverters, with or without power optimizers) would yield the most energy per unit cost? How much energy will the system produce annually considering all the different loss mechanisms?

Each project has a unique set of inputs and therefore each has a unique optimal solution. For example, each geographic site has a unique weather dataset for hourly temperatures (affecting PV performance), precipitation (affecting soiling loss) and solar irradiation (both direct-normal and diffuse). Furthermore, each project has a unique set of products from which to choose based on local availability, and at whatever costs that can be agreed upon with each supplier at the desired quantity. Some projects may require the purchase of land, or the construction of an elevated parking shade structure, each of which adds a cost-per-area element to the equation, while others may be using a free available space such as a roof.

Due to the complexity of the optimization problem, a designer that simply relies on rough calculations and intuition will not likely arrive at a solution that is very close to optimal. Even if a best guess is a system that generates 95% of the energy that the optimal system could generate at the same cost, this can equate to the loss of a significant amount of money over the operational life of the system (25 years or more). For this reason, a PV system simulation tool can be invaluable to a system designer. In theory, a simulation tool could predict the optimal system given these inputs:

1. Costs of available components (PV modules, inverters, trackers, mounts, etc.) and associated cost types (\$/kW, \$/unit and \$/area)

2. Technical specifications for available components (which would allow for the determination of I - V curves for PV modules, efficiency curves for inverters, restrictions for PV module arrangement on trackers, etc.)
3. Hourly weather data for the project site (irradiation, wind and temperature data for a statistically representative 12-month period)
4. Minimum project requirements for amount of annual energy harvested
5. Area of available installation space
6. Other design constraints

Considering the inputs, a simulator could simulate each possible permutation of system design hour-by-hour over the course of a year, comparing the costs and annual energy production of each design and ultimately arriving at the system producing the lowest cost of electricity.

Alternatively, a simulator could make some approximations and employ an optimization algorithm to more quickly arrive at a near-optimal solution, avoiding the necessity to test all permutations of the design. In order to predict the output of a single permutation of PV system design for any one particular hour of the year, the simulator would need to consider the weather conditions for that hour and apply them to the array design. Some of the calculations required at each time step would include:

1. The adjusted I - V curves of each module, string and array based on temperature, irradiation, and other factors.
2. The dimensions of the shadow cast by one tracker onto other trackers based on tracker position and orientation, and the position of the sun in the sky.

3. The adjustment of each module's I - V curve due to shading on portions of the module as determined by the shape of the shadow cast onto the module and the internal wiring of cells and bypass diodes in the module.
4. If applicable to the inverter scheme, the resultant I - V curves for each string according to the I - V curves of each module series-connected in each string.
5. If applicable to the inverter scheme, the resultant I - V curve of the array according to the I - V curves of the strings.
6. Determination of inverter operating point(s) on the I - V curve(s) of the PV modules, strings, or array according to the input voltage range and other specifications of the inverter(s).
7. Inclusion of other system losses.

3.4.1 Other Benefits of a Simulator

Beyond evaluating the performance of PV systems comprised of commercially available components, a simulator could also allow for the experimentation of new ideas and techniques in PV module and array design and control. For example, would a triangular PV module be beneficial under certain circumstances? How much could be gained by a system that could change its wiring scheme depending on current conditions? A simulator could also answer some procedural questions such as how much benefit can be achieved by sorting PV modules by their short circuit current, I_{sc} , compared to a random ordering before installation onto trackers, and at what interval does the benefits of cleaning the PV modules most greatly outweigh the cost?

3.4.2 Existing Simulators

There are several PV system simulators currently available; some developed commercially for which licenses may be purchased, and others developed or commissioned by government agencies which are available for free. Several of the more widely used PV simulators are listed below.

1. *RETScreen* – Developed by Natural Resources Canada (NRC), this tool is available free to the public. Being Microsoft Excel-based, it follows a spreadsheet format for user interface and is able to simulate many different renewable energy systems. It does not consider shading losses whatsoever and is therefore of limited use for simulating tracking PV systems. Furthermore, it does not allow for the automatic simulation of multiple permutations of a design and therefore offers no method for optimization. Instead, a single system is input by the user, and the results are given for that single system.
2. *System Advisor Model (SAM)* – Developed by the U.S. National Renewable Energy Laboratory (NREL), this simulator is available free to the public. It can simulate various renewable energy technologies, and uses the same mathematical engine found in TRNSYS, which is a powerful commercial parametric energy system simulator. Though the software does provide a rudimentary method for factoring in shading losses, it is cumbersome and relies on the user to determine the shading factors. The user may fill in a table values (each cell value constrained between 0 and 1) where each table entry represents an hour of the day and a month of the year. A value of 0 signifies complete shading of the array, a value of 1 indicates no shading losses, and anything between 0 and 1 indicates partial shading of the array. Another option is to input a table of shading factor values based on the sun's azimuth and altitude. There are some problems with this

approach. The first problem is that this approximation is only as accurate as the input data. There is no simple way for the designer to derive these values, and they would change if the spacing between trackers or arrangement of PV modules on trackers was changed. In fact, simply changing the PV module to a different model with slightly different dimensions would change the shadow size and therefore change these shading factors. Furthermore, shading power losses are incorrectly assumed to be proportional to the percentage of the array physically shaded. As was shown earlier in this chapter, the relationship between power loss and shadow size/position is much more complex due to the behavior and electrical interconnection of bypass diodes, PV cells and PV modules in an array.

Apart from the over-simplified treatment of shading losses, SAM does provide the user with a basic tool to aid in the optimizing of a design. The user may define ranges and increments for a large number of system variables, and the software will re-run the simulation for each permutation of the design. The user may then review the results and identify the best-performing combination of variable values. The disadvantage of this brute force method is that varying more than two or three variables at a time results in too many permutations and takes a very long time to simulate. This limitation is a problem because in a PV system simulation, many of the variables are interdependent and it is not enough to optimize one or two variables at a time – they must all be optimized simultaneously.

3. *PVSyst* – First developed at the University of Geneva, Switzerland, this software is now owned by PVSyst SA which sells the software commercially. PVSyst has a built-in three-dimensional (3D) modelling environment which allows the user to input basic 3D shapes

to represent buildings or other shadow-casting objects, and define two-dimensional (2D) ‘active’ planes which represent surfaces where PV modules are installed. A separate plane may be defined for each string of PV modules in the array and these planes can be configured to track the sun in a variety of ways including two-axis tracking. The software then calculates the overall shading factor (between 0 and 1) for the array for each sun azimuth and elevation in 20 and 10 degree increments respectively. There are numerous limitations to this method which limit the accuracy of the shading power loss predictions. Regardless of whether the user chooses the more accurate method of (a) defining PV strings separately, over (b) combining them all into one active polygon representing the array as a whole, the user is given the same choice regarding how shading power loss is calculated: they may choose to treat electrical shading loss as directly proportional to the physical shading of the active polygon(s), or to render active polygons as having a pre-defined power loss fraction regardless of how much of the polygon is shaded (as long as at least some portion of the polygon is shaded). For example, if this power loss factor is set to 100% then the entire PV string is considered to be completely shaded if any point of the shape experiences physical shading – even if this is the very tip of one corner. No matter which option is chosen, there is no consideration given to the array’s shading behavior due to the arrangement and electrical interconnection of inverters, bypass diodes, PV cells, modules and strings - beyond the ability to separate strings into independent shading surfaces. In actuality, strings sharing an inverter are not independent at all as they are all forced to operate at the same voltage. In addition to the shortcomings of the shading loss prediction engine of PVSyst, there is also no provision for the optimization of PV system variables.

4. *PV*SOL* – Developed by Valentin Software Inc., *PV*SOL* is designed for simulating roof-mounted fixed-tilt PV systems and does not simulate tracking systems. It does however include a 3D modelling environment and provides some consideration of electrical interconnectivity for fixed-tilt systems: it allows the user to group PV modules into strings and to assign these strings to inverters. It does not however consider the effect of bypass diodes on the shading behavior of PV modules, instead assuming that shading electrical power losses are proportional to the physical shading fraction of the module. An annual shading factor is calculated for each module based on the shadows cast in the 3D model (from trees, chimneys and other structures), and displayed on the screen in order to help the user decide which modules to group together into strings, however it is not apparent how best to group modules into strings based on their annual shading factor. There are also no system optimization tools included with *PV*SOL*.

3.4.3 Development Platforms for a Simulator

The following options were considered for the development environment of the proposed PV system simulator:

1. *C++* - The text-based programming language C++ offers a great deal of flexibility, as programming can be done at a very low level. Though this platform has the potential to offer the fastest program execution, the included mathematical and graphical functions are limited, meaning that significant time and effort would be required to write the necessary code.
2. *Simulink* - This is a GUI-based real-time simulation environment well suited to time-based circuits and systems. It is not well suited to iteration-based programming however,

and is less customizable than other options. Though it does include some built-in high-level math functions, many are missing and it would be quite difficult to construct them with the blocks available. Also, this platform would likely be the slowest in terms of program execution time of the options considered.

3. *MATLAB* - This development platform is text-based much like C++, but includes a significant number of built-in math and graphical functions. Though not as fast at executing code as C++, it does offer a straight forward development environment for the task.

Chapter Four: The PV System Simulation Model

4.1 Introduction

This chapter begins with the presentation of a proposed phased approach to the development of a full-featured PV system simulator for solar PV trackers, where each phase builds on the features of the previous phase. Due to limited development time, only those features described in Phase I were implemented for this project, which includes the core functionality of calculating shading losses in dual-axis tracking PV systems at a cell-level. The overall structure of the PV system simulation model, which was developed in MATLAB, will be presented as a flow chart with modularized tasks starting with data input, and leading to baseline reference calculations, the main program loop, and finally the simulation output which provides an estimate for the total electrical output of a dual-axis tracking PV system based on the selected inverter configuration(s). The formulae and methodology used in each stage of the simulation will be described in detail in separate sub-sections. Similarities and differences between this simulation model and others currently available will be discussed.

4.2 Development of a PV System Simulator: A Phased Approach

Due to the complexity of developing a full-featured PV system simulator, a phased approach to development offers several advantages. This approach allowed the author to attain intermediary goals and to test the functionality of each additional feature as the simulator evolves from one phase to the next. Though this project aims only to achieve those targets set out in Phase I below, subsequent phases are proposed for future work.

4.2.1 Phase I

This phase of the PV system simulator includes the following features:

1. *Weather Data* – The simulator reads and uses site-specific weather data files which include hourly data for temperature and irradiation (direct normal and diffuse) over a statistically representative 12-month period.
2. *Module and String Mismatch Losses* – The simulator includes the constraints that PV modules connected in series must conduct equal current, and strings of PV modules connected in parallel must operate at the same voltage. Electrical losses result from these constraints because individual PV modules may not be able to operate at their unique MPPs.
3. *User-Definable Layout Parameters* – The user is able to define (a) the grouping of PV cells into sub-modules within a PV module, where a sub-module is a group of series-connected cells in antiparallel with a bypass diode, (b) the arrangement and orientation of PV modules on a tracker, and (c) the spacing between trackers in a row and between adjacent rows of trackers in a homogeneous hexagonal PV farm layout.
4. *Inverter MPPT Voltage Limits* – The minimum and maximum inverter MPPT input voltages may be defined. If the MPP of the connected module or array at current conditions lies outside of this voltage range of the inverter, the closest allowable inverter MPPT input voltage is used, and a loss in output results from not operating at the MPPT of the PV module or string.
5. *Multiple Inverter Types* - The user is given the choice to simulate any, or all of the following inverter types: micro-inverters, string inverters, and central multi-string inverters.

6. *PV Module Data* - The user may enter PV module parameters for each individual module in the system, allowing for the incorporation any kind of statistical variation desired (or, actual module-by-module manufacturer data if available).
7. *Shading Losses* - Based on shadows cast by nearby trackers, the simulator will calculate shading losses down to the PV cell level for greatest accuracy, and propagate the electrical effects up to the sub-module, module, string and array levels. This is the core goal of the project.
8. *Approximation* - The user is given options to reduce the accuracy of various aspects of the simulation in order to reduce simulation time.
9. *Tracking* - Only dual axis tracking systems are simulated. Because PV modules in a dual axis tracking system are always oriented normal to incoming solar irradiation, shadow calculations are greatly simplified.

4.2.2 Phase II

This second phase of the PV system simulator would add the following features:

1. *Inverter efficiency curve* - The user may define a power vs. efficiency curve for inverters, which the simulator will use to attenuate power generated at each time step.
2. *Additional Losses*: The simulator will compute soiling, IAM, and wiring losses based on parameters input by the user.
3. *Backtracking* - Implement the backtracking feature, which is described in Chapter 3.
4. *Additional Tracking Types* - Addition of single-axis tracking systems.
5. *Basic Optimization* - A basic brute force optimization algorithm allows the user to select ranges and increments for some system variables, after which the simulator will simulate

each permutation of the system in order to determine the energy generated by each variant. Note that this form of optimization was implemented in code for this project, but was not added to the user interface.

6. *Tracker Farm Layout* - Instead of only a hexagonal layout (as is assumed in Phase I), the user may introduce a skew between rows. The skew may be increased to the point where the trackers are aligned in the N-S and E-W axes (rectangular layout).

4.2.3 Phase III

This third phase of the PV system simulator would add the following features:

1. *Component Variants* - The ability to define a range of different inverter and PV module models by entering all specifications required for simulation. The optimization algorithm would test the system with each desired combination of inverter and PV module in order to determine the best combination for the particular site.
2. *Component Costing* - Cost data is entered for each system component (\$/kW, \$/m² or \$/unit) which is used by the simulator to calculate a system's \$/kWh after the annual kWh production has been determined.
3. *Lifetime Degradation* - The simulator will calculate PV module aging effects in the form of an annual output degradation percentage when simulating a system over its projected lifespan. Furthermore, since each PV module is treated as a unique component with its own parameters defined separately, the effects of non-uniform PV module aging can be simulated for an entire array.
4. *Smart Optimization* - Moving beyond a simple brute-force method to system optimization, the simulator will employ a more intelligent optimization algorithm (such

as a genetic algorithm) to attempt to arrive close to the optimal solution, saving considerable simulation time.

As mentioned previously, the goal of this project is to attain only the functionalities listed in phase I above. The additional functions listed in phase II and III above are left for further work.

4.3 Chosen Development Environment

As discussed in Chapter 3, there are several development environments available within which a PV simulator may be developed. Early attempts were made with Simulink but major weaknesses were discovered with this tool including a lack of built-in functions and slow program execution. MATLAB, a command-line programming tool which boasts a multitude of useful built-in mathematical and graphical functions provided a much better development environment for creating a PV system simulator. For this reason, MATLAB was the chosen development environment.

4.4 Description of PV Simulation model and Simulation Stages

The program structure of the PV system simulation is as shown in the flowchart depicted in Figure 4.1. Each numbered block in the flowchart is discussed in detail below.

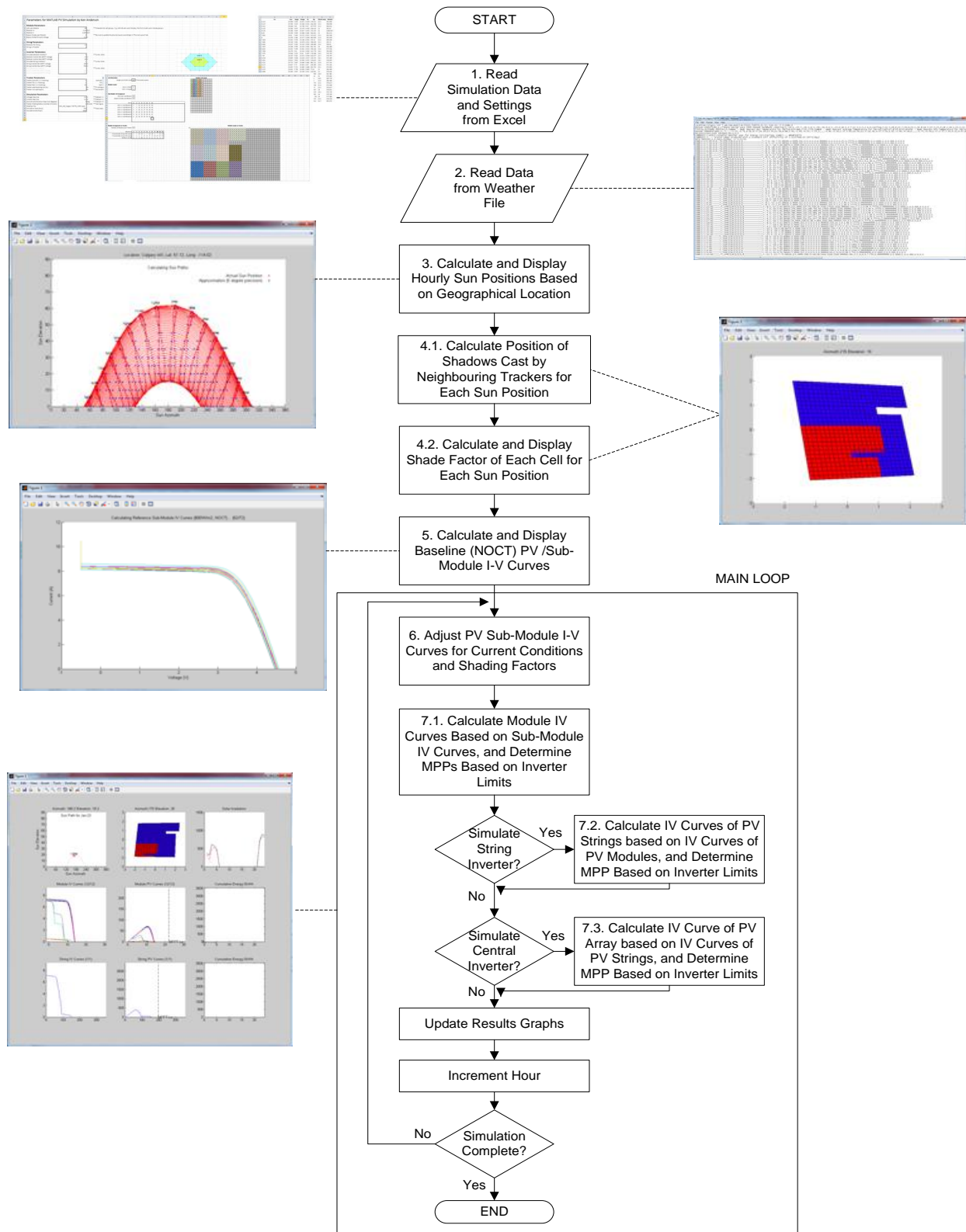


Figure 4.1 - PV Simulator Flowchart

4.4.1 Stage 1: Read Simulation Settings and PV Module Data

All simulation inputs are entered into a series of three Microsoft Excel worksheets. The first stage in the execution of the PV system simulator code is to import the data from the three worksheets and store them in arrays to be used later in the program. The first sheet includes user simulation settings, the second allows the user to define the physical arrangement of cells in the PV module and of PV modules on the tracker, and the third worksheet comprises a list of PV module parameters with one row for each PV module. Each worksheet is discussed in detail below.

4.4.1.1 Worksheet 1: Simulation Settings

From this worksheet, as shown in Figure 4.4, the user may define parameters in each of the following categories:

1. *Module Parameters* – The parameters defined here are applied generally to all PV modules in the simulation, and include: number of cells per module, module K_v ($\%/^{\circ}\text{C}$) and K_i ($\%/^{\circ}\text{C}$), number of diodes per module, and the bypass diode forward voltage.
2. *String Parameters* – The user can define the number of modules per string and number of strings in parallel.
3. *Inverter Parameters* – The user is given the choice to simulate any or all of the three inverter types: micro-inverters, string inverters and/or a central inverter. For those inverter types chosen, the user is required to enter the minimum and maximum MPPT input voltages.
4. *Tracker Parameters* – The details of the mounting and tracking configuration used in the PV system can be defined here. This is accomplished by setting three parameters:

azimuth, tilt and roll. Fixed angles can be applied to each, or a value of -1 can be entered for any parameter to signify that it is a free axis of rotation to be used for tracking the sun. A more detailed description of the notation used is included in the user input worksheet, however at this stage of development, only dual-axis tracking is implemented. Also defined here are the tracker-to-tracker spacing (referred to as tracker spacing) and row-to-row spacing (referred to as row spacing) which define the distribution of trackers on the PV farm. *Figure 4.2* shows how these measurements relate to the tracker layout.

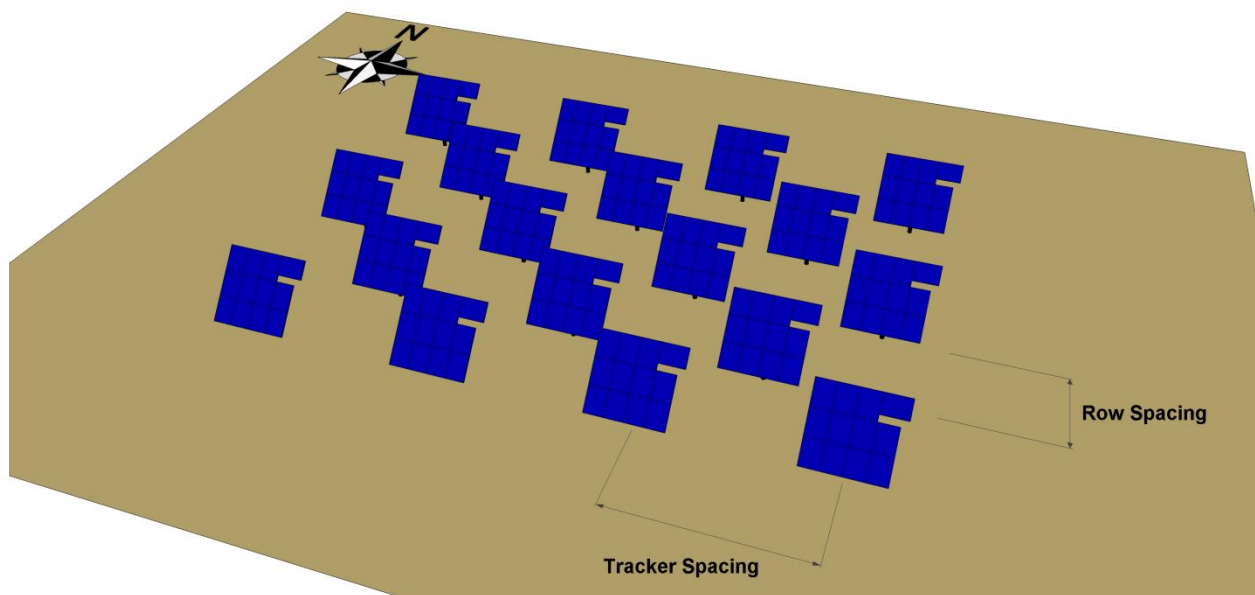


Figure 4.2 - Tracker and Row Spacing of PV Farm

5. *Simulation Parameters* – This category includes various general simulation settings.

Firstly, the user may define the voltage and current step sizes in order to set the level of accuracy acceptable in the simulation. Larger numbers increase the speed of the simulation but decrease accuracy, and vice versa. Voltage and current stepping is used in

the generation and manipulation of I-V curves in the simulation. Another, similar setting is the angle step size which is used to approximate sun azimuth and elevation angles for each hour of the year at a given geographical location. As expected, a larger number reduces the number of initial shading calculations to be performed which speeds up the simulation. A parameter called ‘tracker shading radius’ allows the user to define how many ‘levels’ of neighbouring trackers the simulator should consider when calculating shading losses for a hexagonal layout. As shown in *Figure 4.3*, Level 1 includes only the immediate six closest neighbours which form a hexagon (green trackers) around the simulated tracker (blue tracker in the centre). Level two includes the six trackers of level 1 and also the 12 next closest trackers (yellow trackers) which form a larger hexagon around the level 1 hexagon. The further a shading object is from the tracker being simulated, the lower the sun must be for shading to occur, and the less of an impact it will have on total shading losses. Therefore, a setting of level 1 will only omit some of the shading losses which occur at very low sun elevations, but will significantly speed up the simulation. Note that from the perspective of the simulated tracker, based on a hexagonal layout (as is assumed in this project) six of the twelve ‘level 2’ trackers lie directly behind ‘level 1’ trackers and can therefore be ignored for shading purposes. Therefore a setting of level 2 will consider shadows cast by a total of twelve nearby trackers – six from level 1 and six from level 2.

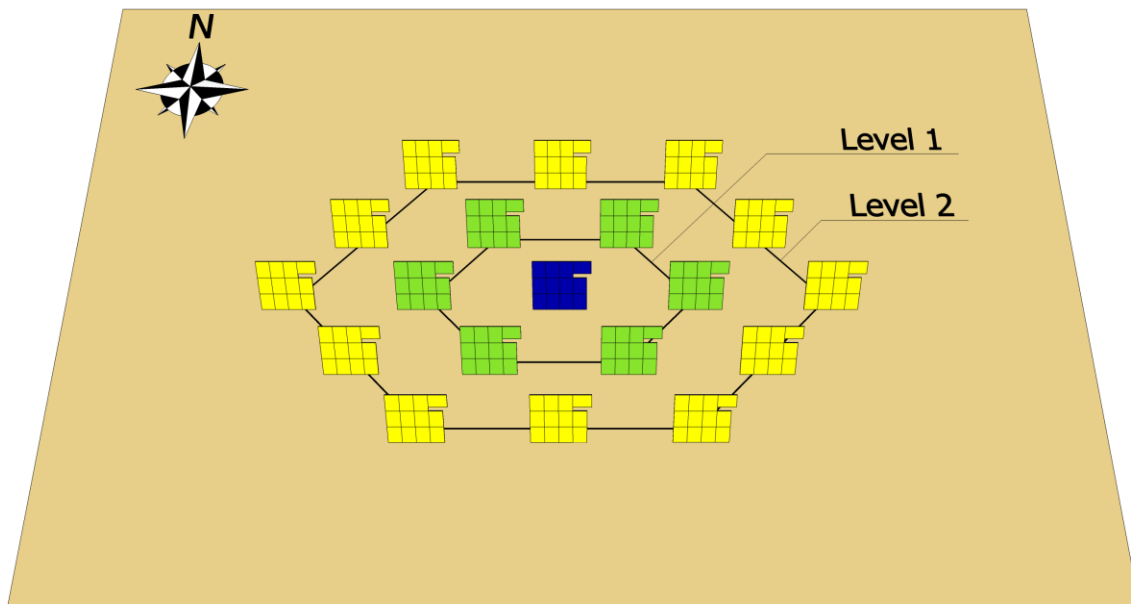


Figure 4.3 - Tracker Shading Radius

6. *Other Settings* - The final settings comprise the folder and filename of the weather file, the day interval (e.g. set to 10 to simulate every 10th day of the year), and the simulation starting and ending hours (between 1 and 8760 – the total number of hours in a year).

Parameters for MATLAB PV Simulation by Ken Ande

Module Paramaters		
Cells per Module	48	
Module KV	-0.34 %/C	
Module KI	0.065 %/C	
Bypass Diodes per Module	6	
Bypass Diode Forward Voltage	-0.5 V	
String Paramaters		
Modules Per String	12	
Strings in Parallel	1	
Inverter Paramaters		
Simulate Module Inverters?	1	
Module Inverter Min MPPT Voltage	22 V	
Module Inverter Max MPPT Voltage	40 V	
Simulate String Inverters?	1	
String Inverter Min MPPT Voltage	195 V	
String Inverter Max MPPT Voltage	550 V	
Simulate Array Inverter?	0	
Array Inverter Min MPPT Voltage	240 V	
Array Inverter Max MPPT Voltage	550 V	
Tracker Parameters		
Tracker Azimuth (-1 = tracking)	-1	
Tracker Tilt (-1 = tracking)	-1	
Tracker Roll (-1 = tracking)	90	
Tracker spacing along row (m)	7 m	
Tracker row spacing (m)	5 m	
Simulation Parameters		
Voltage Step Size	0.1 V	
Current Step Size	0.1 A	
Azimuth and Elevation Step Size (degrees)	2 deg	
Tracker Shading Radius (number of levels)	1 # levels	
Weather File	CAN_AB_Calgary.718770_CWEC.epw	
Simulation Day Decimation	10	
Simulation Start (hour)	510	
Simulation End (hour)	6000	

Figure 4.4 – Worksheet 1: Simulation Settings

4.4.1.2 Worksheet 2: Physical Cell and Module Arrangement

1. *Cell Dimensions* – The user enters the length the solar cell, in millimeters. Solar cells are assumed to be square, which is common for c-Si cells.
2. *Module Cell Layout* – The user enters the number of cells along the length and width of the PV module. A depiction of what the module would look like is shown to the user by shading spreadsheet cells in the worksheet, with each cell numbered.
3. *Sub-Module Cell Assignment* – In this section, information on the number of sub-modules (i.e. the number of bypass diodes) in the PV module and the number of cells per sub-module are automatically taken from the first worksheet. The cell numbers belonging to each sub-module are entered by the user, and the PV module depiction is automatically updated (using a combination of formulae and conditional formatting rules) to show the PV module with each sub-module (each having its own anti-parallel bypass diode) coloured uniquely. This gives the user complete control over both the physical and internal electrical configuration of the PV module. An example is shown in *Figure 4.5*. In this example, there are six sub-module groups, each with eight cells arranged as vertical strips with the PV module in the portrait orientation.

	A	B	C	D	E	F	G	H	I	J	K	L	M	N	O	P	Q	R	S	T	U	V	W	X	Y	Z	AA	AB	AC	AD	AE	AF
1	Cell Dimensions																															
2	Length and Width (mm)	165	***Assumed square																													
3																																
4	Module Layout																															
5	Cells in Width	6																														
6	Cells in Height	8																														
7																																
8	Sub-Module Cell Assignment																															
9	Cells per Sub-Module	8																														
10	Bypass Diodes per Module	6																														
11																																
12	Cell #	1	2	3	4	5	6	7	8																							
13	Cells in Sub-Module 1	1	7	13	19	25	31	37	43																							
14	Cells in Sub-Module 2	2	8	14	20	26	32	38	44																							
15	Cells in Sub-Module 3	3	9	15	21	27	33	39	45																							
16	Cells in Sub-Module 4	4	10	16	22	28	34	40	46																							
17	Cells in Sub-Module 5	5	11	17	23	29	35	41	47																							
18	Cells in Sub-Module 6	6	12	18	24	30	36	42	48																							
19																																
20																																

Figure 4.5 – Worksheet 2: Module Cell Layout

4. *Module Arrangement on Tracker* – In this section (at the bottom of worksheet 2, below cell assignment), the number of modules per tracker is calculated by multiplying the number of PV modules per string by the number of strings in parallel, as defined in the first worksheet. By definition, this means that each tracker in the PV farm is its own unique array. Therefore, it is assumed that each array and the string(s) that comprise them do not span multiple trackers (so, trackers cannot share an inverter). The user enters the location and orientation (landscape or portrait) of each PV module on the tracker, and with the help of spreadsheet cell formulae and conditional formatting rules, the worksheet automatically shows the tracker with PV modules numbered and coloured uniquely. An example of one possible layout is shown in *Figure 4.6*, where there are 12 PV modules on the tracker, each coloured differently. One of the modules is rotated 90 degrees, in landscape orientation while the remainder are in portrait orientation. This sample layout

is used throughout the project because it is non-symmetrical in both axes and provides a better test of the simulation model.

Module Arrangement on Tracker																																									
Number of Modules per Tracker		12																																							
Module #		1	2	3	4	5	6	7	8	9	10	11	12																												
X-Coordinate of top-left corner		1	7	13	19	1	7	13	19	1	7	13	19																												
Y-Coordinate of top-left corner		1	1	1	1	9	9	9	9	17	17	17	17																												
Rotation (0, 90)		0	0	0	90	0	0	0	0	0	0	0	0																												

Figure 4.6 – Worksheet 2: Layout on Tracker

4.4.1.3 Worksheet 3: PV Module Parameters

This worksheet, shown in Figure 4.7, comprises a list of PV module data with each row representing a unique individual PV module with the following data columns:

1. I_{sc} – The PV module short-circuit current.
2. V_{oc} – The PV module open-circuit voltage.
3. I_{mpp} – The PV module operating current at its MPP on the I - V curve.
4. V_{mpp} – The PV module operating voltage at its MPP on the I - V curve.
5. R_s – The equivalent series resistance of the PV module (see 4.4.5 for a more detailed explanation).
6. R_{sh} – The equivalent parallel resistance of the PV module (see 4.4.5 for a more detailed explanation).
7. $NomTemp$ – The temperature of the PV module at which the above measurements were made.
8. $NomIrr$ – The level of irradiation incident on the PV module while the above measurements were made.

	A	B	C	D	E	F	G	H	I
1	Isc	Voc	ImpP	Vmpp	Rs	Rsh	NomTemp	NomIrr	
2	8.213	29.484	7.659	23.871	0.259	186	23.3	992.009	
3	8.137	29.388	7.619	23.268	0.531	156.364	23.3	996.008	
4	8.312	29.644	7.81	23.758	0.47	197.579	23.2	986.811	
5	8.115	29.286	7.697	23.279	0.478	238.619	23	987.61	
6	8.125	29.288	7.647	23.427	0.473	271.153	23	1000.007	
7	8.09	29.255	7.599	23.448	0.481	366.662	23	981.612	
8	7.982	29.02	7.423	23.171	0.512	112.622	23.1	993.209	
9	8	29.259	7.496	23.377	0.494	483.984	22.9	991.609	
10	7.964	29.303	7.578	23.148	0.502	371.31	22.6	995.209	
11	7.886	29.138	7.421	23.074	0.513	208.939	22.3	991.21	
12	8.006	29.197	7.433	23.232	0.505	108.468	23.6	990.81	
13	7.997	29.298	7.555	23.229	0.502	431.761	24	996.408	
14	8.015	29.101	7.478	22.821	0.519	258.166	23.6	977.156	
15	7.994	29.275	7.51	23.322	0.509	313.774	24.3	992.809	
16	7.975	29.098	7.523	23.01	0.497	176.948	24.3	976.787	
17	7.99	29.147	7.561	23.072	0.504	510.077	23.7	976.787	
18	8.324	29.805	7.844	23.628	0.527	130.372	24.2	973.365	
19	8.361	29.812	7.853	23.956	0.472	224.602	24.1	974.093	
20	8.221	29.713	7.807	23.845	0.481	481.121	23.8	977.291	
21	8.127	29.417	7.72	23.432	0.47	135.305	23.5	971.181	
22	8.121	29.407	7.722	23.405	0.488	432.732	23.1	972.582	
23	8.227	29.601	7.738	23.665	0.465	77.62	23	969.443	

Figure 4.7 - Worksheet 3: PV Module Parameters

4.4.2 Stage 2: Read Weather Data

The accuracy of a PV system simulation is limited by, among other factors, the accuracy of the weather data used. Specific to each geographical location, a suitable weather file includes hourly temperature and irradiation data for each hour of a one-year period. Since weather at any particular location changes from year to year with a great deal of unpredictable variation, a problem exists for what data to use in a PV simulation which is meant to predict future electricity production. To address the need for representative weather data sets for the simulation of energy systems in various locations around the USA, the National Renewable Energy Laboratory (NREL) created the Typical Meteorological Year (TMY) data sets which contain hourly solar irradiation, temperature and other meteorological data for a one-year period that typifies the climate based on data sampled over much longer time frame (for example, 15 years) [26]. In Canada, the National Research Council of Canada, in collaboration with Environment Canada

and Numerical Logistics created the Canadian Weather for Energy Calculations (CWEC) data sets using methods similar to those used in the creation of the TMY data sets [27]. The raw data is stored in an EPW file, which is in comma-separated value (CSV) format and has 36 data fields for each hour of a one-year period, and eight header rows which include site data such as latitude, longitude and time zone [28]. Since only a sub-set of this data is required for the PV system simulation model, only the data shown in Table 4-1 is extracted from the file and stored in data arrays to be used later.

Table 4-1 - Weather File Data

Location in EPW File	Data
Header Row 1, Item 2	Site Name
Header Row 1, Item 7	Latitude
Header Row 1, Item 8	Longitude
Header Row 1, Item 9	GMT Offset
Data Column 1	Dry Bulb Temperature
Data Column 9	Direct Normal Irradiation
Data Column 10	Diffuse Horizontal Irradiation
Data Column 16	Wind Speed*

* For future use in estimating a more accurate PV module temperature

4.4.3 Stage 3: Calculate Sun Positions

Based on the latitude, longitude and GMT offset of the simulation site, the azimuth and elevation of the sun can be calculated for every hour of the year using known methods [29]. First, the site declination, D , is calculated using equation (4.1), where 23.45 represents the Earth's tilt from its orbital plane around the sun, 360 represents the number of degrees in a full orbit and 365.24 represents the number of days in a year.

$$D = 23.45\sin(B) \quad (4.1)$$

where,

$$B = \left(\frac{360}{365.24} \right) (N + 284)$$

and,

$$N = \text{Day number starting from January 1st}$$

Next, an empirical approximation of the ‘equation of time’ shown in (4.2) is used to account for the Earth’s elliptical orbit around the sun and tilted axis of rotation, correcting for the offset between sun’s true position and its mean position based on a circular orbit and vertical axis of rotation. The correction factor, E , represents the number of minutes that day N is longer (positive) or shorter (negative) than 24 hours.

$$E = 9.87 \sin(2B) - 7.53 \cos(B) - 1.5 \sin(B) \quad (4.2)$$

The standard-time-to-solar-time correction factor (in minutes) is then calculated based on the site’s longitude and time zone, where the number 15 represents the number of degrees per time zone and the number four represents the number of minutes which elapse per degree of the Earth’s rotation about its axis.

$$STCF = 4(\text{Longitude} - (15 * W)) \quad (4.3)$$

where,

$$W = \text{Number of time zones West of GMT}$$

The solar time can then be calculated from standard time and the correction factors.

$$\text{Solar Time} = \text{Standard Time} + STCF + E \quad (4.4)$$

From this, the hour angle (ω) can be calculated. The hour angle represents how many degrees the sun is away from solar noon, which is when the sun is directly overhead.

$$\omega = (Solar\ Time - 12hrs) * 15degrees \quad (4.5)$$

Finally, the sun's azimuth and elevation can be calculated from its hour angle (ω), the site's latitude and declination (D).

$$Elevation = \arcsin\{[\sin(D) * \sin(Lat)] + [\cos(D) * \cos(Lat) * \cos(\omega)]\} \quad (4.6)$$

$$Azimuth = \arccos\left[\frac{\sin(Elevation) * \sin(Lat) - \sin(\omega)}{\cos(Elevation) * \cos(Lat)}\right] \quad (4.7)$$

where,

$Lat = Site\ latitude$

As the sun's elevation and azimuth are calculated for each hour of the year at the site coordinates given in the weather file, they are plotted as shown in Figure 4.8.

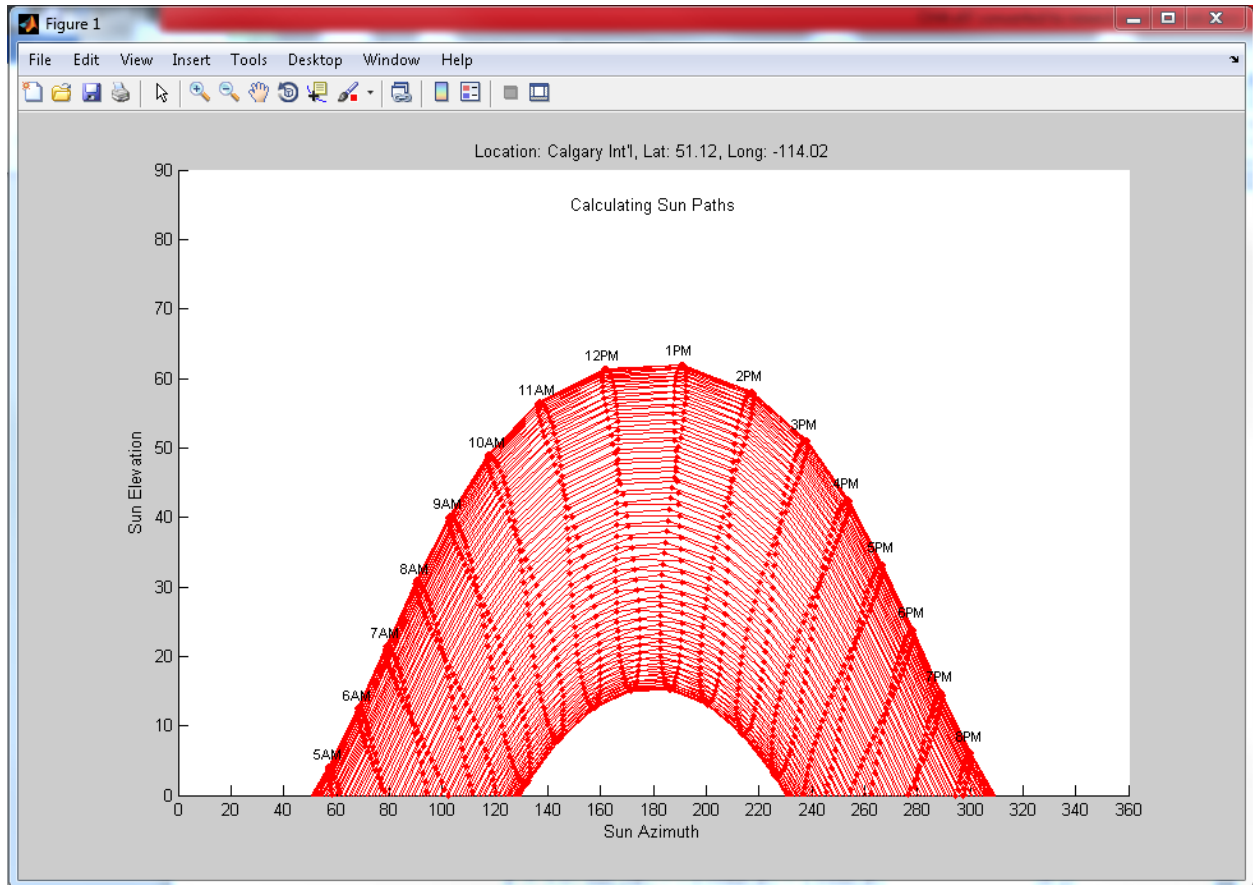


Figure 4.8 – Sun Azimuth and Elevation Plot

The final step is to apply the angle approximation as defined by the user in the parameter ‘angle step size’. For example, if five degrees is chosen as the angle step size, each hourly sun azimuth and elevation will be rounded to the nearest five degrees. The new approximated values are shown as blue dots in Figure 4.9. This reduces the number of possible sun positions (from ~4400 to ~400 in this example) which reduces the number of shading scenarios, thereby speeding up the shadow calculation.

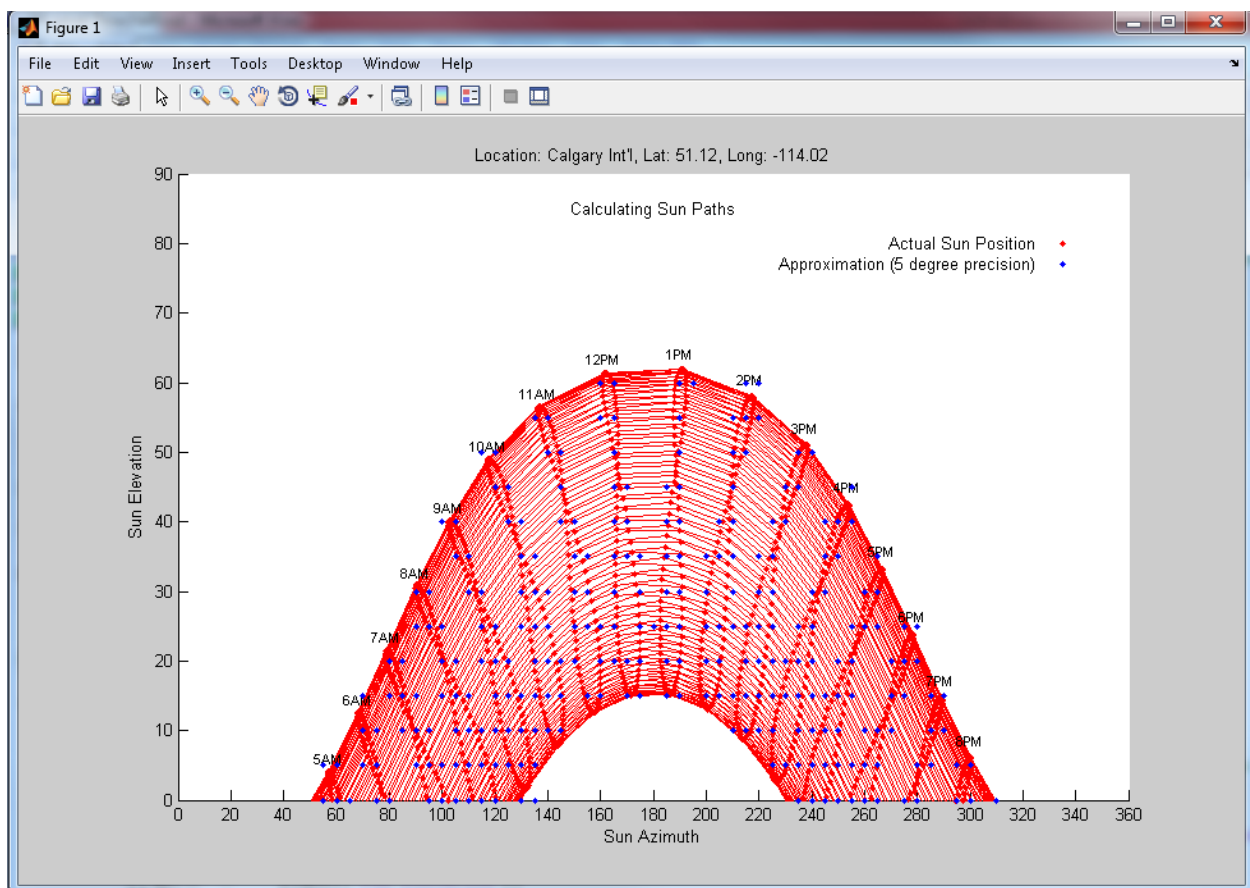


Figure 4.9 - Sun Azimuth and Elevation Plot with Approximation

4.4.4 Stage 4: Calculate Physical Shade Factors

Central to the PV system simulator is the calculation of electrical power loss due to the shading of solar PV cells. In order to perform these calculations later in the simulation, the location of the

physical shadows cast by the trackers must first be determined. Since the array is assumed to be a regular repeating pattern of trackers, only the shading pattern cast upon a single tracker by its immediate neighbours must be found. This shading pattern is calculated for every possible above-horizon sun position as determined by Stage 3. If a sun-position approximation has been defined, such as shown by the blue dots in the example of Figure 4.9, then only these sun positions are used for the calculation of shading patterns. As the positions of the shadows cast by neighbouring trackers are determined for each valid solar azimuth and elevation, the physical shading ratio of each PV cell on the tracker is recorded for later use in the simulation.

4.4.4.1 *Shading Calculations for Dual-Axis Tracking*

As mentioned in section 4.1, only dual-axis tracking is simulated for phase I of the PV system simulator. The reason for this is that shading calculations are greatly simplified in this case. In a dual-axis tracking system, assuming that no backtracking is implemented, PV modules are always oriented directly towards the sun. This means that the shadows they cast onto other nearby dual-axis trackers (which are also facing directly towards the sun) are always the same shape and size as the PV modules that are casting the shadows (since the Sun can be assumed to be a point source of radiation at an infinite distance from the Earth). The only property of the shadow left to calculate is its location with respect to the shaded tracker, which depends on the position of the sun and the spacing between the trackers in the N-S and E-W directions. The position of this shadow must be determined for each neighbouring tracker, and for each valid sun position throughout the year.

To tackle this problem, several nested loops are employed to step through each potential shading event imposed upon a sample tracker by its neighbours. The outer-most loop steps

through each valid sun position (azimuth-elevation pair) for which shadow positions must be calculated. Nested within this loop, is a loop which steps through each of the neighbouring trackers (six or twelve, depending on tracker shading radius chosen - level 1 or level 2 as depicted in Figure 4.3) which may cast a shadow on the tracker being analyzed (the central tracker). For each shading tracker, the distance and direction angle from the central tracker is calculated based on its relative position in the array, and the tracker-to-tracker and tracker row spacing using simple geometry. Based on the sun position, the shading tracker position relative to the central tracker, and the geometry of the PV modules on the shading tracker, the outermost extents of the shadow cast onto the PV plane of the central tracker is calculated using geometry in two axes. A set of further-nested inner loops step through each PV cell of each PV module on the central tracker, and quickly determines if it lies within the extents of the shadow. For those which lie outside the shadow, a shading factor of zero is saved in the shading array for that PV cell. For those cells which are determined to lie within the extents of the shadow, further calculations are required to determine how much of the cell is shaded. This is achieved in the inner-most nested loop, which steps through each module of the shading tracker to determine the position of its shadow with respect to the cell in question. This is a simple calculation because the PV module shadow position relative to the shading PV module is the same as was already calculated for the shadow position of the tracker relative to the shading tracker. Since PV modules are rectangular, this involves simply shifting the four vertices representing the four corners of the module (taking into account the position of the PV module on the tracker and the PV module orientation – portrait or landscape). From the co-ordinates of the four vertices of the PV module shadow in the plane of the PV cell, and the coordinates of the four corners of the PV cell, the proportion of the cell shaded can easily be determined. With a 2-D axis system aligned

with the edges of the PV cell, shading factors are calculated separately in the X and Y axes, and multiplied to arrive at the total shading factor of that particular PV cell due to the shadow cast by the PV module in question. This is repeated for all PV modules on the shading tracker, with the calculated shading factors summed to arrive at the final shading factor for the cell (under the reasonable assumption that PV modules do not overlap). This process is repeated for every PV cell of every PV module on the sample tracker. Though this involves many nested loops and therefore many repeated instructions, the calculations performed are very simple and do not require significant processing time. The final shading factors of each PV cell at each valid sun position are stored in a large multi-dimensional array for use later in the simulation. The shading factors of each PV sub-module are then calculated as being equal that of the most shaded cell of each respective sub-module at each valid sun position. For example, if a sub-module consists of 12 series-connected PV cells protected by a single bypass diode, and at a sun elevation of 45 degrees and azimuth of 180 degrees, one cell in the sub-module is 80% shaded and the remaining 11 cells are not shaded at all, then a shading factor of 0.8 is applied to the entire sub-module for this sun position because all 12 cells are limited in current to that of the most-shaded cell (current and irradiation are proportional in a PV cell). Later, when the simulation reaches the hourly energy generation stage, it will begin calculations at the sub-module-level and work up to the PV module, PV string, and finally PV array level by performing the necessary series/parallel connection calculations. Calculations can start at the sub-module level because the PV cell-level shading data will have already been incorporated at the sub-module-level.

4.4.4.2 Displaying Shade Factors

In order to provide a visual check of the shading calculation results, a visualization of the tracker and PV cell shading factors was developed. The visualization shows a 3-D representation of the tracker, with PV modules subdivided into cells. Each cell is coloured according to its shading factor for the particular sun position with blue representing no shading, red representing complete shading, and a spectrum of colours in between representing partial shading. The 3-D visualization is updated in real-time as the tracker orientation changes according to the changing sun position. A single frame from this moving visualization is shown in Figure 4.10. In this figure, the blue-coloured cells are un-shaded, the red-coloured cells are completely shaded, and those with shades of colour between red and blue are partially shaded (the redder the colour, the more shade that PV cell is subjected to).

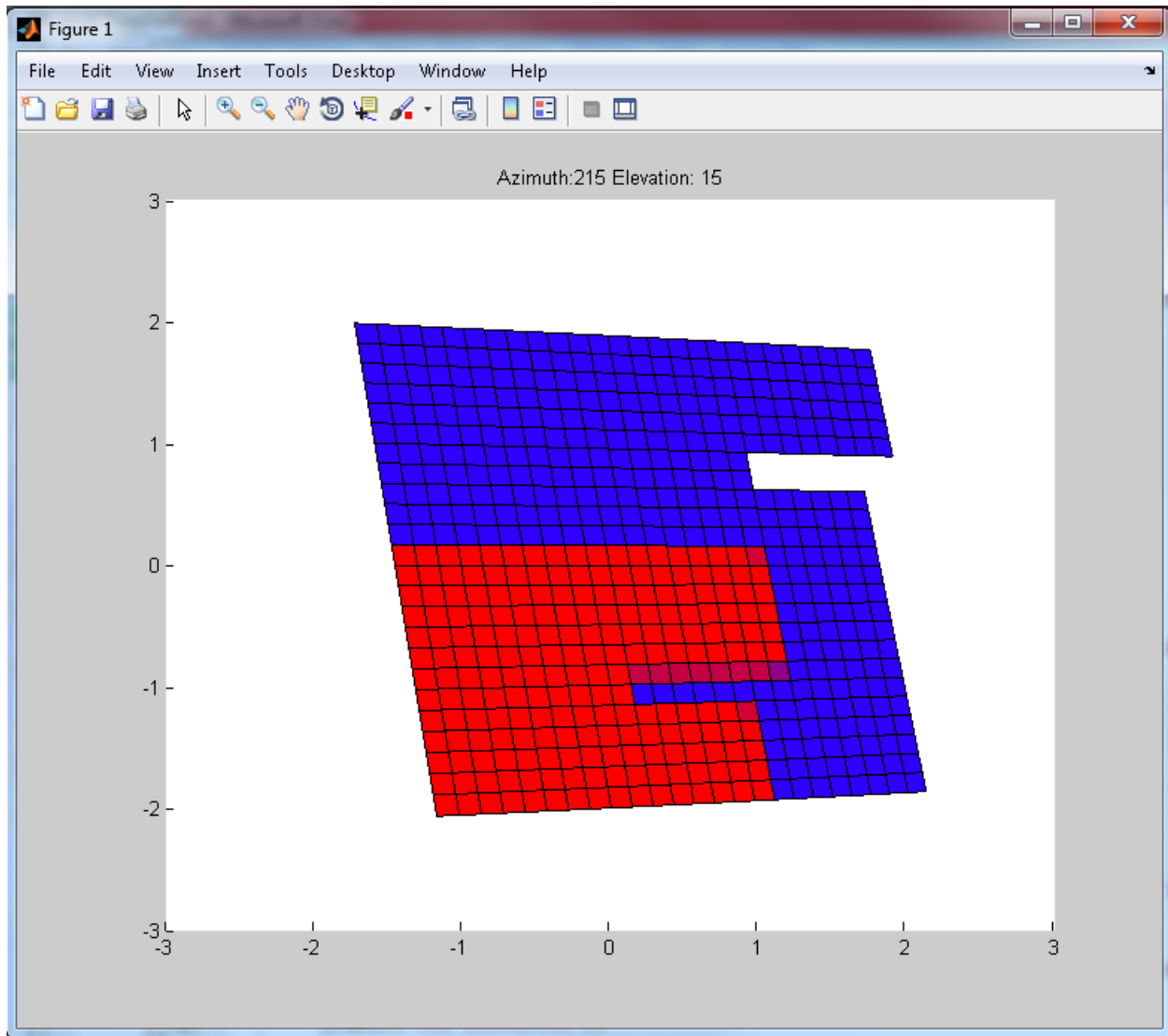


Figure 4.10 - 3-D Visualization of Tracker Shading (Blue is non-shaded; Red is fully shaded; and colours in between are partially shaded cells)

Though the 3D visualization is accomplished with relatively few lines of code, it requires a fair amount of calculation and processing time within the built-in MATLAB graphical functions.

Each of the four vertices of each PV cell must be transformed in the spherical co-ordinate system which is based on r (radius), θ (elevation/polar angle) and ϕ (azimuthal angle), by an azimuthal rotation and an elevational rotation, and then converted to Cartesian co-ordinates which is based

on X , Y and Z axes so that they may be displayed as a MATLAB graph. Though MATLAB does have some built-in functions which perform the transformation between spherical and Cartesian co-ordinate systems, they were not easily compatible with the specific conventions used in the simulation. Therefore, the translations and conversions were derived from first principles and combined into a single transformation matrix consisting of trigonometric expressions as shown in (4.10).

$$T_{\theta} = \begin{bmatrix} 1 & 0 & 0 \\ 0 & \cos \theta & \sin \theta \\ 0 & -\sin \theta & \cos \theta \end{bmatrix} \quad (4.8)$$

where,

$$\theta = \text{Elevation Angle}$$

$$T_{\varphi} = \begin{bmatrix} \cos \varphi & 0 & \sin \varphi \\ 0 & 1 & 0 \\ -\sin \varphi & 0 & \cos \varphi \end{bmatrix} \quad (4.9)$$

where,

$$\varphi = \text{Azimuth Angle}$$

$$\begin{bmatrix} X' \\ Y' \\ Z' \end{bmatrix} = T_{\theta} T_{\varphi} \begin{bmatrix} X \\ Y \\ Z \end{bmatrix} = \begin{bmatrix} X \cos \varphi - Y \sin \theta \sin \varphi + Z \cos \theta \sin \varphi \\ Y \cos \theta + Z \sin \theta \\ -X \sin \varphi - Y \sin \theta \cos \varphi + Z \cos \theta \cos \varphi \end{bmatrix} \quad (4.10)$$

Finally, the X and Y co-ordinates of each vertex are scaled slightly from the origin according to its Z co-ordinate (depth into the screen) in order to provide a visual perspective effect. In order to speed up the calculations, the trigonometric functions \sin , \cos and \tan were pre-calculated for each valid angle according to the angle step size defined in the user input data sheet (5 degrees by default), and stored in lookup arrays.

A rendering created in Google SketchUp of a small PV farm under shaded conditions is shown in Figure 4.11.

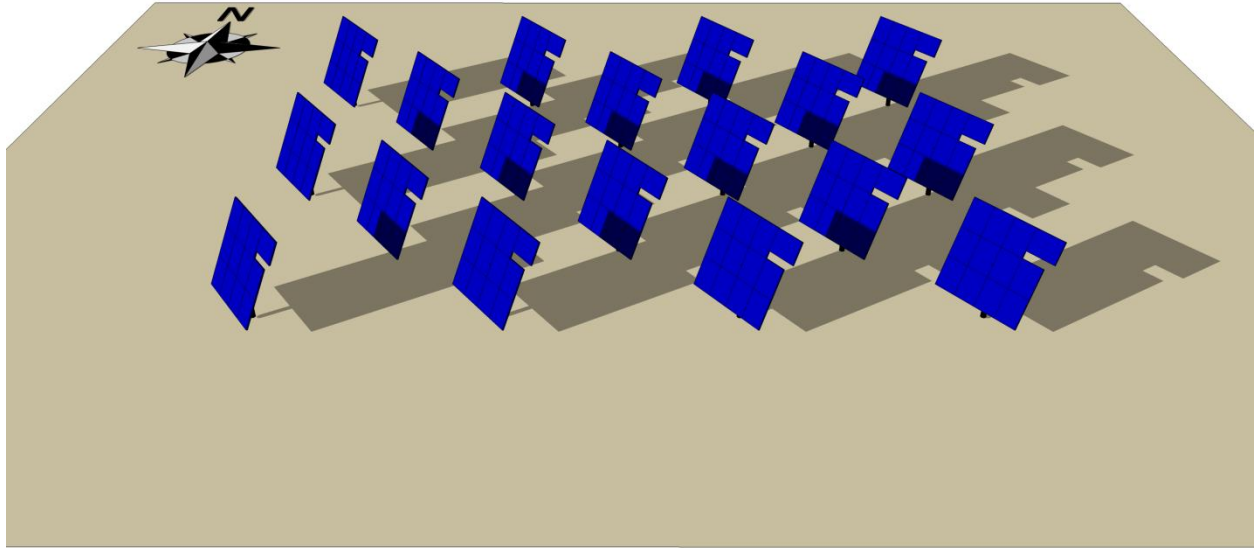


Figure 4.11 - Rendering of PV Farm Under Shaded Conditions

4.4.5 Stage 5: Calculate Baseline I-V Curves

As mentioned in 4.1, for phase I functionality, only crystalline silicon (c-Si) PV technology is considered due to the relative simplicity of the single-cell model and the straight-forward application of shading loss. Another popular choice for PV arrays is amorphous silicon (a-Si) PV technology (a thin-film technology), however the mathematical model for the I - V characteristics of a group of a-Si cells takes the form of an implicit function that cannot be solved analytically [30], and requires the use of an iterative procedure to generate a module I - V curve. Furthermore, once the baseline curve is calculated, it cannot be easily scaled according to changing conditions. Finally, the relationship between cell shading and energy output for a-Si modules is much more

complicated than that for c-Si modules. Of note, a-Si modules are more shade-tolerant than c-Si modules, suffering from lower losses under the same shading patterns (a single completely-shaded cell will only decrease the output power of an a-Si PV module by less than 10% [30], whereas in a typical c-Si PV module, this figure would be closer to 25% or 33%).

4.4.5.1 The c-Si Single-Diode Model

A c-Si PV cell can be approximated as the electrical circuit shown in Figure 4.12 using the single-diode model [9].

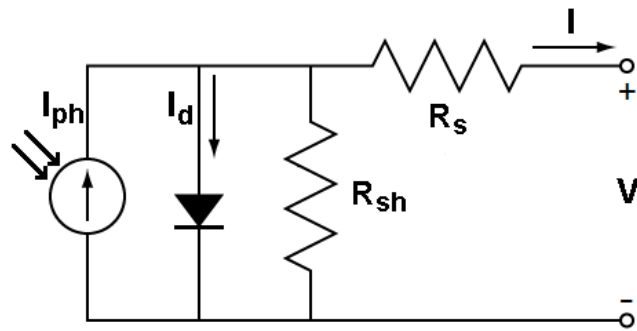


Figure 4.12 - c-Si PV Cell Single-Diode Model

Though more accurate models exist, such as the two-diode model [31], the single-diode model provides a good compromise between accuracy and complexity (calculation time) [8], and as such it is commonly used in commercial PV simulation software, such as PVSyst. The formula which describes the relationship between voltage and current in this circuit can be used to generate PV cell and module I - V curves, and is shown in (4.11).

$$I = I_{ph} - I_d - \frac{V + IR_s}{R_{sh}} \quad (4.11)$$

where,

$$I_{ph} = \frac{G}{G_{nom}} \left[K_I (T - T_{nom}) + I_{SC} \left(\frac{R_s + R_{sh}}{R_{sh}} \right) \right] \quad (4.12)$$

and,

$$I_d = I_0 \left[e^{\frac{q(V + IR_s)}{nkT}} - 1 \right] \quad (4.13)$$

where,

$$I_0 = \frac{K_I (T - T_{nom}) + I_{SC} \left(\frac{R_s + R_{sh}}{R_{sh}} \right)}{e^{\frac{q[K_V (T - T_{nom}) + V_{OC}]}{nkT}} - 1} \quad (4.14)$$

In (4.12), I_{ph} represents the current generated by the photo cell, which is directly proportional to the incident radiation, G and corrected for the temperature dependence of current using the junction temperature, T , and the coefficient K_I (A/°K). The short-circuit current, I_{SC} is a baseline measurement performed by the manufacturer as the cell or module leaves the production line.

The cell or module is subjected to a specific spectrum (as determined by an air mass (AM) index of 1.5. Note that an AM of 1 would indicate that the sun is directly overhead) and intensity of irradiation ($G_{nom} \approx 1000 \text{ W/m}^2$) and held at a specific temperature ($T_{nom} \approx 25^\circ\text{C}$) while its outputs are shorted and output current measured. These conditions are referred to STC. (4.13) is the Shockley diode equation, where I_0 is the reverse saturation, or leakage current of the diode, q is the charge of an electron, k is Boltzmann's constant and n is the diode ideality constant which is typically in the range of 1-2. In (4.14), the open-circuit voltage, V_{OC} , is another parameter measured by the manufacturer before shipping. With the cell or module at T_{nom} and subjected to G_{nom} , the output leads are left open and the output voltage is measured. K_V is the temperature dependence of the cell open-circuit output voltage and is usually negative so that a colder cell will generate a higher output voltage (conversely, the K_I coefficient, the temperature dependence

of the cell short-circuit current, is typically positive). For each model of PV module, typical K_I , K_V , I_{SC} and V_{OC} values (measured under STC) are provided by the manufacturer in the product datasheet.

4.4.5.2 Determining R_s and R_{sh}

The only variables in the equations (4.11) to (4.14) which are not typically provided by PV module manufacturers are diode ideality, n , and the series and shunt equivalent resistances, R_s and R_{sh} . These variables must be known in order to generate accurate I - V curves for PV cells and modules. In cases where they are not given, a method must be used to derive them.

With a reasonable assumption for diode ideality, n , it is possible to use an iterative method to determine R_s and R_{sh} based on additional specifications provided in the product datasheet [9]. Along with V_{OC} and I_{SC} , which represent points where the I - V curve intercepts the X (voltage) and Y (current) axes respectively, manufacturers also often provide the voltage and current at the maximum power point (MPP) - the point on the I - V curve at which the PV module produces maximum power. These parameters are referred to as V_{mp} and I_{mp} , respectively, and result in power P_{mp} when multiplied. For a given n , only one combination of R_s and R_{sh} results in an I - V curve which intercepts the MPP, V_{OC} and I_{SC} , and iteration is used to find it. Starting with a very low initial value of R_s , a corresponding value of R_{sh} can be calculated using (4.15), where N_c is the number of cells in the PV module.

$$R_{sh} = \frac{V_{mp} + I_{mp}R_s}{I_{ph} - I_0 \left[e^{\frac{q(V_{mp} + I_{mp}R_s)}{nKT N_c}} - 1 \right] - I_{mp}} \quad (4.15)$$

This pair of values, R_s and R_{sh} , can then be substituted into (4.11) to generate an I - V curve and the MPP of this curve can be found and compared with the manufacturer-provided MPP for the module. The next iteration involves incrementing R_s , and repeating the above calculations. The process is repeated until an R_s and R_{sh} pair is found which satisfies the system of equations, resulting in an I - V curve and MPP that is similar to that quoted by the manufacturer. Since this need only be performed once per PV module model, the algorithm efficiency is not critical. Since this process is not central to the PV simulator itself, a stand-alone tool was developed as a part of this project in MATLAB Simulink to derive R_s and R_{sh} . Figure 4.13 shows the interface for this tool. The manufacturer-supplied PV module parameters (and assumption for diode ideality, n) are entered into the variables along the left side of the screen, and the program is run. During execution, the central plot shows the error in maximum power decreasing until the correct values of R_s and R_{sh} are found, at which point the I - V and P - V curves are shown in the top-right and middle-right plots respectively. These should bare a close resemblance to the I - V and P - V curves shown on the PV module datasheet.

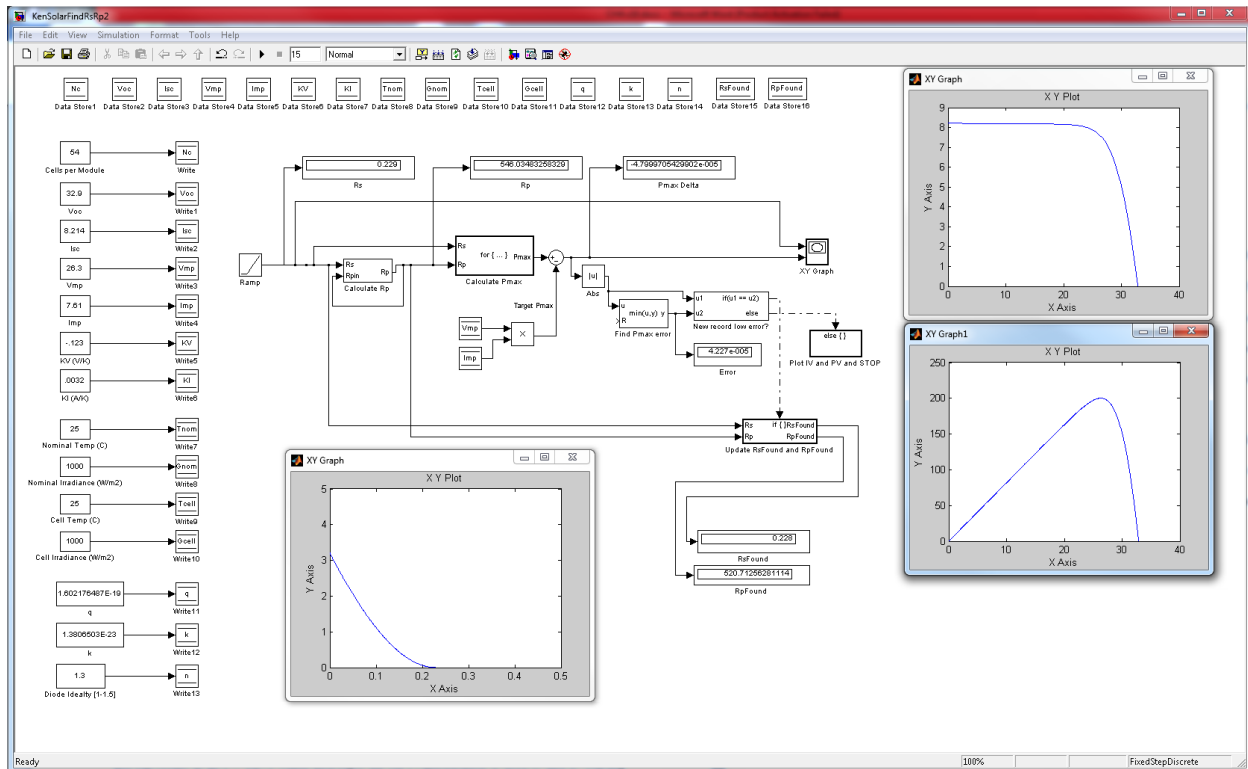


Figure 4.13 - Simulink Tool for Determining R_s and R_{sh}

The values for R_s and R_{sh} found can then be entered manually into the PV System Simulator in the PV Module Data tab of the data entry spreadsheet, along with all of the other PV module parameters.

4.4.5.3 PV Module Sub-Division

Each group of series-connected cells which is protected by a single anti-parallel diode in a PV module is constrained to operate at a common operating current. If the protection diode is conducting, then this group of cells is bypassed and their current is assumed to be zero. If the cell-group is not bypassed, then their non-zero current must equal that of the other non-bypassed, series-connected cell-groups in the PV module. A typical PV module may have three or four such bypass diodes and associated cell-groups connected in series. Each group of cells protected

by a diode forms a so-called sub-module, which operates as a single entity, either conducting current in a non-bypassed state or conducting no current in a bypassed state. As mentioned previously, when individual cells in the sub-module experience differing shading factors, the worst-shaded cell in the group dictates the current of the entire sub-module. Therefore, as long as shading is calculated on a per-cell basis, and applied appropriately to sub-modules, sub-modules may be treated as the smallest independent PV elements in the simulation model. This means that I - V curves need not be calculated for each individual cell, but rather only for each sub-module, which greatly reduces the number of calculations required (typical sub-modules comprise up to twenty cells). PV module data is imported from the data entry spreadsheet and used to create elements representing its constituent sub-modules. For example, if a PV module has three bypass diodes, then three sub-modules will be created for each module, each with one third of the open-circuit voltage of the module, the same short-circuit current as the module, etc. The sub-module I - V baseline curves are then calculated, displayed (see Figure 4.14), and stored in arrays for later use. Since (4.11) is an implicit equation (the variable I cannot be isolated), the MATLAB function *fzero* is used to solve for sub-module voltage, V , while the sub-module current, I is swept through the full expected range of operating current. At, and below the cell current of 0A, the diode is considered to be conducting and the output voltage of the sub-module is equal to the bypass diode forward voltage as defined in the parameters data sheet (-0.5V is used in the example). In this case, the power dissipated in the bypass diode is equal to the product of diode forward voltage and the bypassed current, which is the current demanded by the load and flowing through neighbouring conducting series-connected cell groups.

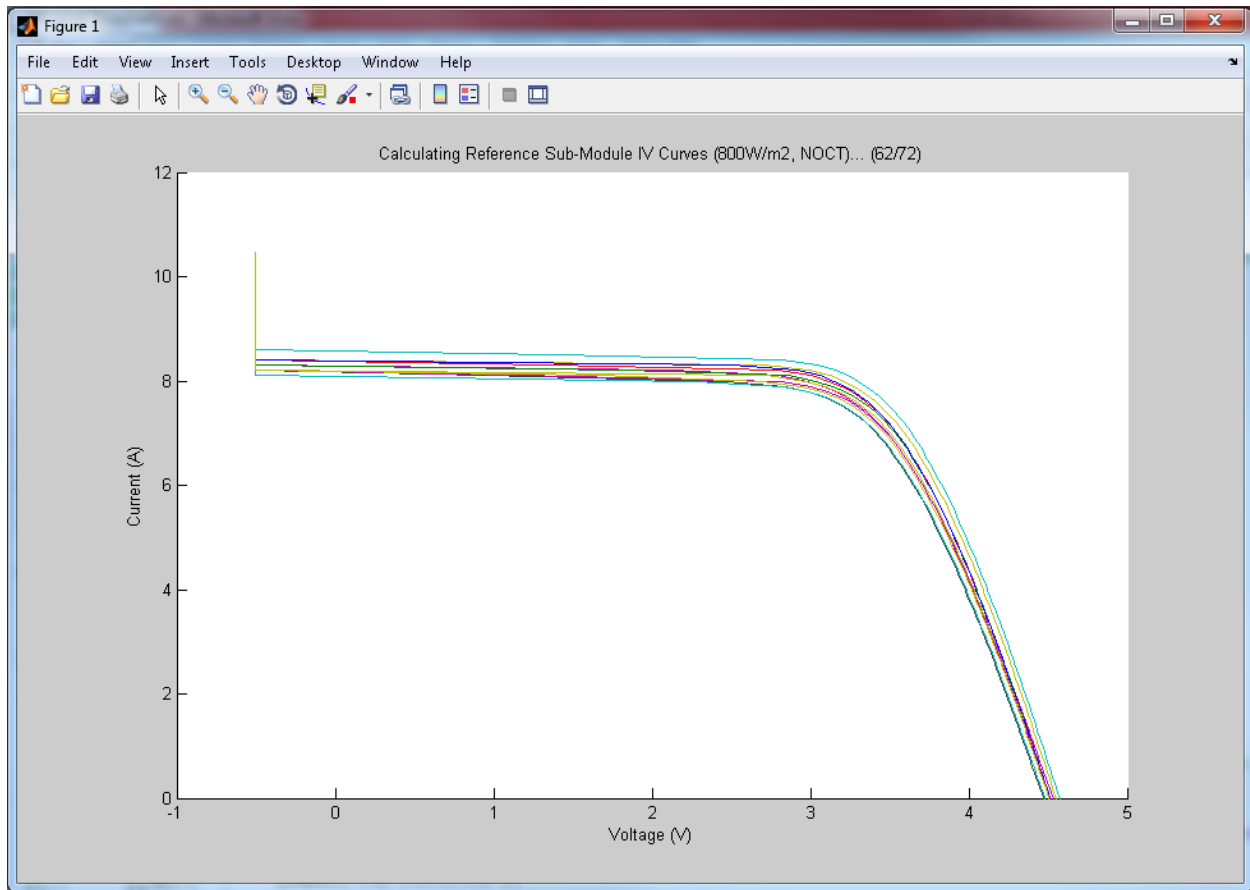


Figure 4.14 - Baseline Sub-Module I-V Curves

4.4.6 Start of Main Loop

The tasks performed by the PV simulator up until this point have been for the purpose of populating data arrays in preparation for execution of the main program loop. From this point forward, the simulation code is repeated and the time marker (hour number) is incremented after each iteration, until the defined end-state is reached. For example, the user may want to simulate an entire year and therefore enter a starting hour of 1, and an ending hour of 8760.

4.4.7 Stage 6: Adjust Sub-Module I-V Curves for Conditions

Based on the simulation hour, the pre-calculated solar azimuth and elevation are retrieved from the solar position data array. If the sun is below the horizon then the time step is skipped, otherwise calculations proceed. The position of the sun, represented by a small red circle is updated in the top-left plot of Figure 4.15, shown on a dotted blue line representing the solar path for that day. The shading pattern and position of the tracker based on this sun position is retrieved from the pre-calculated shading array and shown in the top-centre plot of the same figure (axes are in metres). The solar direct normal (red dashed line) and diffuse irradiation (blue dotted line) levels are then retrieved from the weather data array based on the hour index and updated in the top-right plot of the same figure (the x-axis is the hour of the day, and y-axis is irradiation in W/m^2). The solid black line represents total irradiation, which is the sum of direct and diffuse irradiation.

The baseline sub-module *I-V* curves which had been calculated and stored previously, were based on arbitrary values of irradiation, 800 W/m^2 and temperature, 45°C (which are closer to typical conditions than STC), and need to be adjusted to reflect current conditions. First, the direct-normal portion of solar irradiation is scaled for each sub-module according its shading factor at the current hour index. For example if a sub-module is 10% shaded, then the direct-normal portion of irradiation incident upon this sub-module is reduced by 10%. The diffuse portion of irradiation, which is assumed to radiate from all points in the sky equally, is largely unaffected by shading and so is not attenuated by shading in this simulation model. Direct-normal and diffuse components of irradiation for each sub-module are then added to give total irradiation, which is used to scale the current (*I*) axis of each sub-module's *I-V* curve. This

causes the I - V curve to shift up or down depending on whether there is more or less total irradiation than was used to calculate the baseline I - V curve.

Next, each sub-module I - V curve is adjusted based on the estimated cell operating temperatures and the linear temperature coefficients of I_{sc} and V_{oc} , K_i and K_v . The cell operating temperatures are estimated for each time step based on the outdoor ambient dry bulb temperature and irradiance using the basic empirical formula shown in (4.16) [32] (though more accurate models for PV cell temperature exist [33]). Note that the value for cell irradiance will have already been adjusted according to the cell shading factor, meaning that a shaded cell will have a significantly lower operating temperature, resulting in a higher cell voltage. An approximation is made that all the cells within a sub-module operate at the same temperature, represented by the most shaded cell.

$$T_{cell} = T_{ambient} + \frac{(T_{ref} - 20) * Irradiance}{Irradiance_{ref}} \quad (4.16)$$

Note that the calculations used to adjust the pre-calculated baseline sub-module I - V curves for hourly temperature and irradiation are far simpler and faster to execute than those required to completely re-construct I - V curves from (4.11). Therefore, this method offers significant execution time savings over the more straight-forward method of calculating new I - V curves at each time step.

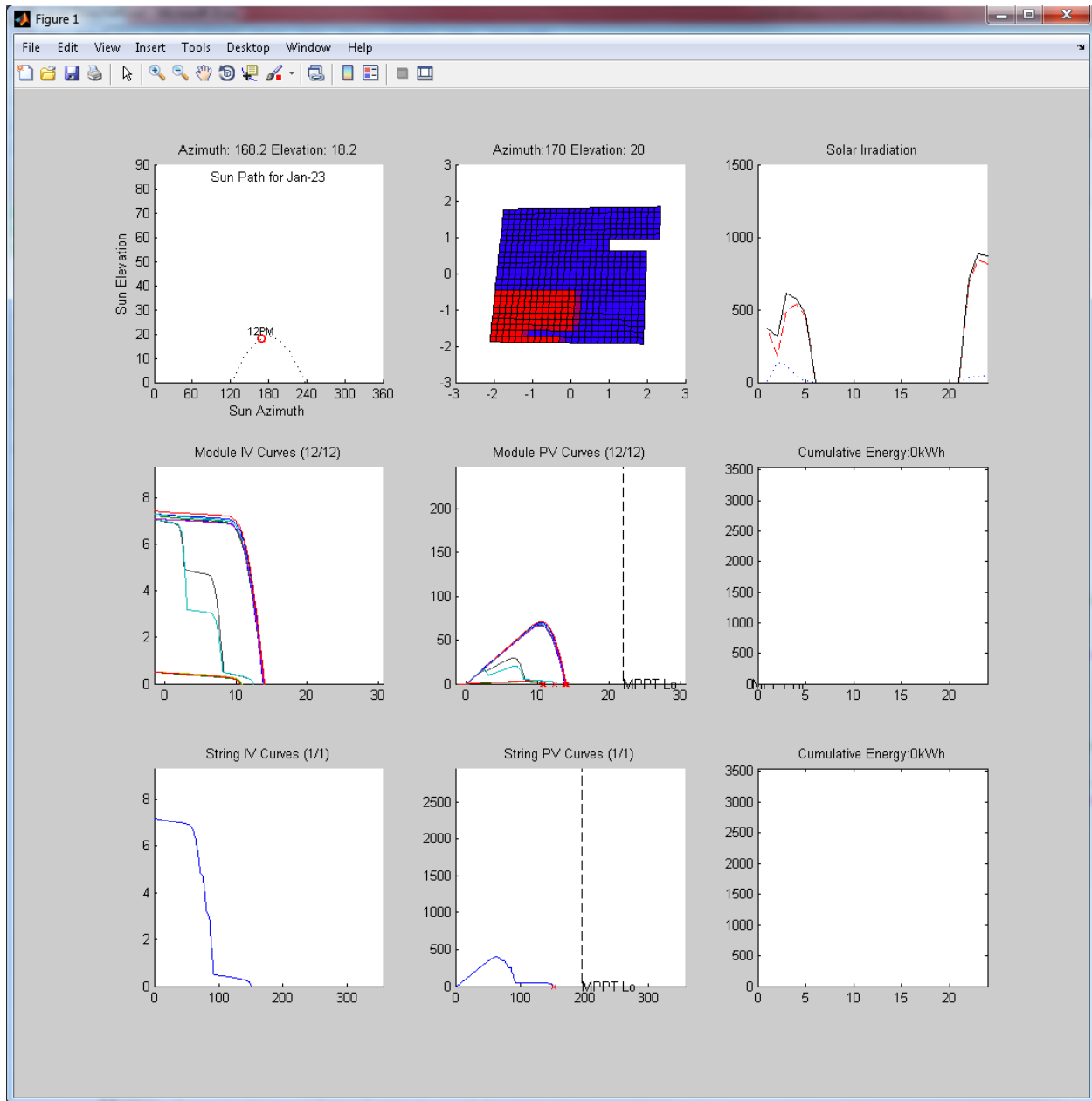


Figure 4.15 - Main Simulation Output Screen

4.4.8 Stage 7: Determine Module, String and Array I-V Curves

After each sub-module I - V curve has been adjusted from the baseline curves to those reflecting current weather conditions for the particular hour of the simulation, they are used to construct I - V curves for larger PV elements in the system, starting with PV modules. A PV module is a group

of series-connected sub-modules which must all operate at the same current, and whose voltages sum at the output of the PV module. Since each sub-module I - V curve has been scaled based on its particular illumination, the group of sub-modules no longer has data points which line up along specific current increments (e.g. 0.1A, 0.2A, 0.3A, etc.). As a result, in order to generate new PV module I - V curves with the original current increments, linear interpolation is used to determine each sub-module's voltage at these pre-set current increments. The sub-module voltages are added at each current to construct the PV module I - V curves. These curves are then plotted in the centre-left position of Figure 4.15. Note that some of the PV module I - V curves show a stepping down of voltage (X -axis) as the current (Y -axis) increases, which is due to the fact that one or more of its sub-modules are partially shaded. These partially shaded sub-modules are unable to supply as much current as the un-shaded sub-modules in the module, and when the maximum current of the partially-shaded sub-module is surpassed, the anti-parallel bypass diode conducts. Instead of the cells of the partially-shaded sub-module contributing a large positive voltage to the module, the bypass diode contributes a small negative voltage.

The module P - V curves are then generated from the I - V curves by multiplying the current (Y -axis) of each data point by its corresponding voltage. The module P - V curves are then drawn on the centre plot of Figure 4.15. Note that the peaks of these curves represent the MPPs of the PV modules in the system under the current weather and shading conditions, which is updated at each time step.

If the user has chosen to simulate PV string inverters, then the PV module I - V curves are used to generate PV string I - V curves. A PV string is a group of PV modules connected in series to a single inverter. Since the PV module I - V curves have already been generated (from interpolation of the individually scaled sub-module I - V curves) using the base increments in

current (e.g. 0.1A, 0.2A, 0.3A, etc.), it is a simple exercise to add the voltages of the PV modules in the string at each current to generate the string I - V curves. Once complete, the PV string I - V curves are drawn in the bottom-left plot of Figure 4.15. The same procedure which was used to generate PV module P - V curves from module I - V curves is used to generate PV string P - V curves from string I - V curves, which are then drawn in the bottom-centre plot of Figure 4.15.

Finally, if the user has chosen to simulate a PV array inverter, then the PV string I - V curves are used to generate the array I - V curve. A PV array is a group of PV strings connected in parallel, so that each string operates at the same overall voltage, but each may contribute its own current such that the sum of string currents is the array output. Due to this relationship, the array I - V curve data is structured in set increments in voltage (not current as with sub-module, module and string I - V curve data). The conversion is accomplished by performing a linear interpolation of the data points of the string I - V curves. In this format, string currents may be added at each possible incremental voltage in order to arrive at the complete array I - V curve. The array P - V curve is then generated from the array I - V curve using the same method which is used with PV modules and strings. The array I - V and P - V curves are not plotted due to graphing space constraints.

An example of how I - V curves are constructed from the cell-level up to the sub-module-, module-, string- and array-levels, is shown in Figure 4.16 (no shading effects shown). The purple curve represents the I - V curve of a single PV-cell, which intersects the current axis at approximately 8A (I_{SC}), and the voltage axis at approximately 0.6V (V_{OC}). In this example, 20 cells in series form a sub-module, whose I - V curve is shown in red. Three sub-modules in series form a module, whose I - V curve is shown in yellow. If we assume that 13 modules in series form

a string, then the string I-V curve would be as shown in blue. Finally, if we assume that an array consists of four parallel strings, the resulting array I-V curve would be as shown in green.

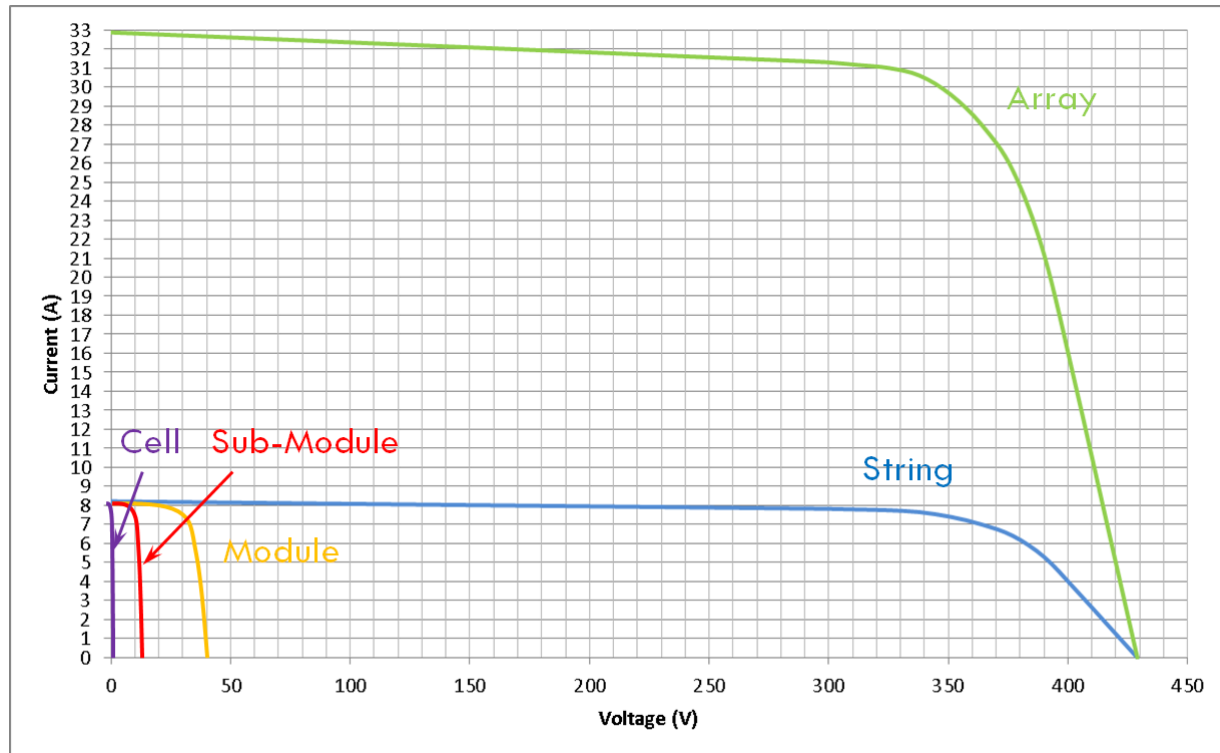


Figure 4.16 - Example of Un-Shaded PV-Cell, Sub-Module, Module, String and Array I-V Curves

4.4.9 Stage 8: Determine MPPs within Inverter Limits

Once the PV module, string and/or array P - V curves have been calculated, the next step is to select the highest point of each curve which lies within the MPPT voltage range of the relevant inverter (micro-inverters for PV-modules, string inverters for PV strings, or a central inverter for a PV array). This point on each P - V curve is marked with a red 'x', and the MPPT limit(s) of the inverters are marked on the P - V plots with vertical dashed lines indicating 'MPPT Lo' and 'MPPT Hi' (each only visible if within the axis extremes). In the example of Figure 4.15, the MPPT Lo limits are visible in the centre and bottom-centre plots, and are higher than all the

module and string P - V curves. As a result, the red 'x's are at the far right of each P - V curve, and these inverters are therefore unable to extract any power from these modules or strings. This example shows clearly that the layout of PV modules was not matched well to the inverters chosen.

In the case of micro-inverters, the total power output of the tracker array is the sum of MPPs for each PV module within the MPPT range of the micro-inverters. In the same manner, the total output of the array when strings are defined is the sum of the MPP outputs of each individual string based on the MPPT range of the string inverters. For an array using a central inverter, the total output power is the MPP output of the array within the MPPT range of the central inverter.

4.5 PV Simulator Results

Hourly sums of total array energy generated by each inverter type are plotted to the right of each respective P - V plot: in the centre-right plot of Figure 4.15 is the hourly energy generated by all micro-inverters combined, and in the bottom right is the hourly energy generated by all the string inverters combined. The cumulative total energy generated in each case is indicated above each of these two plots, in the plot title. The energy generated by a central inverter is not plotted due to space constraints, but is instead displayed as text. These results may be recorded and other simulations run for comparison purposes.

4.6 Model Verification

In order to test the accuracy of the model in predicting annual energy produced from a single tracker, simulation results were compared against those from System Advisor Model (SAM) of

the US Department of Energy. PV system and simulation parameters were setup to be as close as possible between the two simulation models. Since SAM is unable to calculate the shading losses of a 2-axis tracking system, shading effects were disabled in the PV system simulation model developed for this project. A summary of the simulation settings for both simulators is shown in Table 4-2.

Table 4-2 - Simulator Settings for Model Validation

Item No.	Item	Settings
1	Weather Data	The same EPW weather file for Calgary, AB, Canada was used in each simulator.
2	PV Module	The same PV module data was used for each module in each simulator (Canadian Solar CS6A-180P: $I_{sc} = 8.2\text{A}$, $V_{oc} = 29.4\text{V}$, $I_{mp} = 7.62\text{A}$, $V_{mp} = 23.6\text{V}$, $R_s = 0.282\Omega$, $R_{sh} = 165.38\Omega$, $NomTemp = 25^\circ\text{C}$, $NomIrr = 1000\text{ W/m}^2$, $K_V = -0.3565\text{ \%/}^\circ\text{C}$, $K_I = 0.045\text{ \%/}^\circ\text{C}$). A ‘Module Model’ loss of 1.65% is used for both simulators, as dictated by SAM (subtracted manually in the case of the proposed simulator model).

Item No.	Item	Settings
3	Inverter	A micro-inverter scheme was used for both simulators (Enphase M190-72-240-S12 240V). No MPPT voltage limitations were imposed. An annual inverter loss of 4.35% was found in SAM, and subtracted manually from the results of the proposed simulation model.
4	Array Configuration	For both simulators, the PV array consisted of 12 PV modules connected to independent micro-inverters.
5	Tracking	Both simulators set to dual-axis tracking
6	Simulation Parameters	<p>For each simulator:</p> <ul style="list-style-type: none"> a) Ground reflectance ignored b) No AC wiring loss c) No transformer loss d) Isotropic radiation model e) No soiling loss f) No module mismatch g) No diode/connections loss h) No DC wiring loss i) No tracking error j) No nameplate de-rating k) 100% annual system availability

Based on the above settings, SAM predicted an annual output of 4,655kWh from the single tracker, whereas the PV System Simulator developed here predicted an annual output of 4,269kWh, a difference of 9.0%. It is difficult to say what differences in the simulation methods result in the discrepancy in predicted annual output since there is limited access to the inner workings of SAM (or any other PV simulator for that matter). Nevertheless, the absolute accuracy of the simulator seems sufficiently high to validate the true purpose of the simulator, which is to compare the *difference* in annual energy output of variants of the same basic design (for example, how does the annual energy output of the system change when the tracker spacing is increased by 0.12m?). Even without a high degree of absolute accuracy, elements of the system design can still be effectively optimized. The complete setup and output of the SAM simulation is included in APPENDIX A.

4.7 Discussion

Though there are many other PV simulation tools currently available in the market, there are many features which are not available in any of these tools which are available in this tool:

1. *Shading Losses* – The proposed PV simulation model accurately calculates electrical shading losses at the cell, sub-module, module, string and array levels for two-axis tracking systems. One tool, PV*SOL, is able to calculate annual PV module shading as a percentage of total module area due to nearby obstacles such as trees and chimneys, but cannot accurately translate this into an electrical loss factor, as the tool does not have any information on the internal wiring of the PV module. Furthermore, PV*SOL does not simulate tracking systems. PVSyst performs a crude calculation of shading loss in

tracking systems at a string-level with very rough approximations applied, and no consideration of electrical interaction within the strings. If a string experiences any shading, a pre-set shading loss factor is applied for that time-step (for example, 60% to 80% is recommended by the software creator) and multiplied by the physical shading ratio to arrive at the electrical loss ratio.

2. *Internal wiring of PV modules* – The proposed model allows the user to define the grouping of cells into sub-modules, and the physical location of each cell in the module, thereby allowing the user to experiment with different PV module designs. For example, instead of cell-groups arranged in rows or columns, they may be defined to be located in the corners of the PV module. No other known PV system simulator has this feature.
3. *PV Module Parameters* – Through the user-interface, the PV simulator allows the user to uniquely define the parameters of each individual PV module in the array. Other simulators rely on statistical means and sometimes standard deviations (in the case of PVSyst) to define all of the PV modules in the system based on the datasheet parameters. The ability to define these parameters for each individual module becomes especially useful if the manufacturer has provided module-by-module data to the user, or if the user would like to experiment with unique distributions of module parameters to see the effect on the system output.
4. *Calculation accuracy* - Unlike other tools, this tool allows the user to set the level of accuracy in the calculations according to how long they are willing to wait for the simulation to complete. Accuracy may be defined for solar elevation and azimuth angles, step sizes for current and voltage in I - V and P - V curves, and to a limited extent, the number of neighbouring trackers to be considered as potential shading obstructions.

Of the features that are common between this tool and others, it is difficult to tell in most cases the level of ambiguity between the methods of implementation due to the fact that source code is not publically available for other simulators. Still, some similarities in process can be observed. For example, the tool developed for this project employs a similar method to PVSyst in that shading losses are calculated first and stored based on sun position, and later applied on a time basis to determine annual losses. Furthermore, it is known from the documentation that PVSyst also uses the single-diode model of the PV cell, and it is likely that most if not all of the other PV simulators do as well. Beyond these examples, it is difficult to identify any further similarities between this tool and the others currently available. For example, it is not known how the other tools deal with the often unknown PV module parameters of R_s and R_{sh} . These parameters often appear in the PV module databases included with the tools (if the user is lucky enough to find their desired PV module in the database), but it not apparent how they were derived. This tool provides a method for determining these parameters based on data commonly found on PV module datasheets.

4.8 Chapter Summary

This chapter has presented a proposed phased approach to the development of a full-featured PV system simulator where each phase builds on the features of the previous phase. Due to limited development time, a goal was set to implement those features described in Phase I only, which includes the core functionality of calculating shading losses in dual-axis tracking PV systems at a cell-level. The overall structure of the simulation model was presented as a flow chart with modularized tasks starting with data input, and leading to preparatory calculations, the main

program loop, and finally the simulation output which provides an estimate for total electrical output based on the selected inverter configuration(s). The equations and methodology used in each stage of the simulation were described in detail in separate sub-sections. Similarities and differences between this tool and others currently available were discussed.

Chapter Five: Testing and Results

5.1 Hypothetical PV System Under Test

For the testing of the proposed PV system simulation model, a hypothetical PV system was entered into the data input spread sheets, as summarized in Table 5-1.

Parameter	Setting
Location and Weather	Calgary, AB Canada (51.12°N, 114.02°W). EPW weather file.
Tracker	Dual-axis tracking.
PV Module	48 PV cells and 3 bypass diodes arranged as shown in Figure 5.1 (different colours represent different sub-modules – each with their own bypass diode). Realistic variation of parameters across PV modules (I_{sc} , V_{oc} , I_{mpp} , V_{mpp} , R_s , R_{sh}). Actual module parameters used can be found in APPENDIX B. $K_V = -0.34\%/^{\circ}\text{C}$, $K_I = 0.065\%/^{\circ}\text{C}$.
PV Layout	12 series-connected PV modules arranged as shown in Figure 5.2 (different colours represent different PV modules).
Inverter	Single string inverter per tracker. 195V-500V MPPT range.
Precision	0.1V, 0.1A, 2 degrees, level-1 tracker shading.
Day Interval	10-day interval (simulate every 10 th day of the year).

Table 5-1 - PV System Setup for Testing

Module Layout on Tracker																																												
y\X	1	2	3	4	5	6	7	8	9	10	11	12	13	14	15	16	17	18	19	20	21	22	23	24	25	26	27	28	29	30	31	32	33	34	35	36	37	38	39	40	41	42		
1	1	1	1	1	1	1	2	2	2	2	2	2	3	3	3	3	3	3	4	4	4	4	4	4	4	4																		
2	1	1	1	1	1	1	2	2	2	2	2	2	3	3	3	3	3	3	4	4	4	4	4	4	4	4																		
3	1	1	1	1	1	1	2	2	2	2	2	2	3	3	3	3	3	3	4	4	4	4	4	4	4	4																		
4	1	1	1	1	1	1	2	2	2	2	2	2	3	3	3	3	3	3	4	4	4	4	4	4	4	4																		
5	1	1	1	1	1	1	2	2	2	2	2	2	3	3	3	3	3	3	4	4	4	4	4	4	4	4																		
6	1	1	1	1	1	1	2	2	2	2	2	2	3	3	3	3	3	3	4	4	4	4	4	4	4	4																		
7	1	1	1	1	1	1	2	2	2	2	2	2	3	3	3	3	3	3																										
8	1	1	1	1	1	1	2	2	2	2	2	2	3	3	3	3	3	3																										
9	5	5	5	5	5	5	6	6	6	6	6	6	7	7	7	7	7	7	8	8	8	8	8	8	8	8																		
10	5	5	5	5	5	5	6	6	6	6	6	6	7	7	7	7	7	7	8	8	8	8	8	8	8	8																		
11	5	5	5	5	5	5	6	6	6	6	6	6	7	7	7	7	7	7	8	8	8	8	8	8	8	8																		
12	5	5	5	5	5	5	6	6	6	6	6	6	7	7	7	7	7	7	8	8	8	8	8	8	8	8																		
13	5	5	5	5	5	5	6	6	6	6	6	6	7	7	7	7	7	7	8	8	8	8	8	8	8	8																		
14	5	5	5	5	5	5	6	6	6	6	6	6	7	7	7	7	7	7	8	8	8	8	8	8	8	8																		
15	5	5	5	5	5	5	6	6	6	6	6	6	7	7	7	7	7	7	8	8	8	8	8	8	8	8																		
16	5	5	5	5	5	5	6	6	6	6	6	6	7	7	7	7	7	7	8	8	8	8	8	8	8	8																		
17	9	9	9	9	9	9	10	10	10	10	10	10	11	11	11	11	11	11	12	12	12	12	12	12	12	12																		
18	9	9	9	9	9	9	10	10	10	10	10	10	11	11	11	11	11	11	12	12	12	12	12	12	12	12																		
19	9	9	9	9	9	9	10	10	10	10	10	10	11	11	11	11	11	11	12	12	12	12	12	12	12	12																		
20	9	9	9	9	9	9	10	10	10	10	10	10	11	11	11	11	11	11	12	12	12	12	12	12	12	12																		
21	9	9	9	9	9	9	10	10	10	10	10	10	11	11	11	11	11	11	12	12	12	12	12	12	12	12																		
22	9	9	9	9	9	9	10	10	10	10	10	10	11	11	11	11	11	11	12	12	12	12	12	12	12	12																		
23	9	9	9	9	9	9	10	10	10	10	10	10	11	11	11	11	11	11	12	12	12	12	12	12	12	12																		
24	9	9	9	9	9	9	10	10	10	10	10	10	11	11	11	11	11	11	12	12	12	12	12	12	12	12																		
25																																												
26																																												
27																																												
28																																												
29																																												
30																																												
31																																												
32																																												
33																																												

Figure 5.2 - PV Module Layout on Tracker for Testing. Each PV module is shaded a different colour, and each PV cell (48 per module) contains the module-number of its parent module. 11 modules are in portrait orientation, and one is rotated 90 degrees, in landscape orientation (module number four).

5.2 Large Variation in Spacing

The first test performed was to run a year-long simulation of a single tracker under the influence of shading from neighboring trackers (a PV farm of any size can be extrapolated from the output of a single tracker, neglecting edge-effects of the trackers around the periphery) with variations in tracker-to-tracker spacing along a single row (referred to as tracker spacing, or E-W spacing)

and variations in row-to-row spacing (referred to as row spacing, or N-S spacing). Spacing in each direction was varied from 5m to 15m in increments of 1m, for a total number of 121 test cases. The results are shown as a 3D surface plot in Figure 5.3, from which the following observations can be made:

1. The tracker will have a higher annual energy output (coloured red) when the distribution of trackers is sparse (large spacing), due to lower shading losses.
2. The flattening out of the top of the surface indicates that there are diminishing returns from increasing the spacing between the trackers and rows.
3. The annual energy output is more sensitive to row spacing than tracker spacing, since a decrease in row spacing is met with a more dramatic drop in annual energy output than an equivalent drop in tracker spacing.

It is also notable that the surface plot is not perfectly smooth but rather exhibits various bumps and dips which can be attributed to the non-linear properties of shading losses and the existence of discrete elements (PV cells) in the model. This phenomenon is more apparent in the contour plot of Figure 5.4, which depicts the same data.

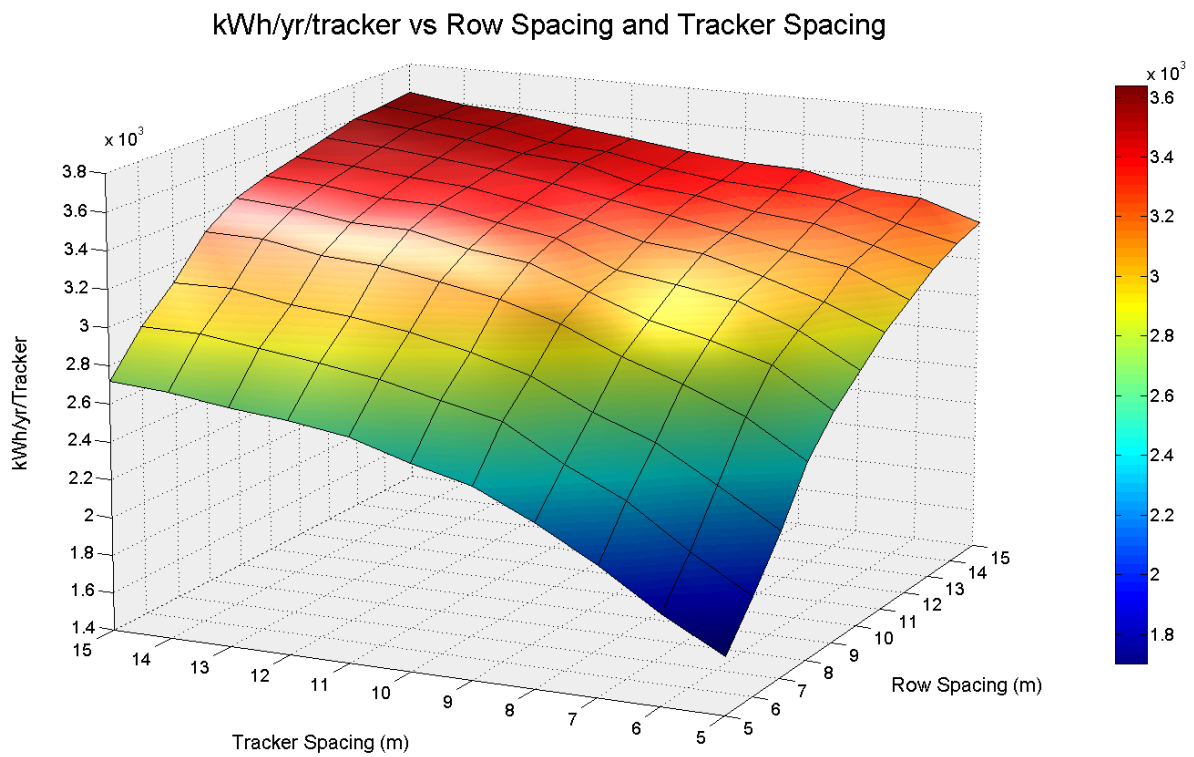


Figure 5.3 – Annual Tracker Output vs. Large Variations (1m) in Tracker and Row Spacing

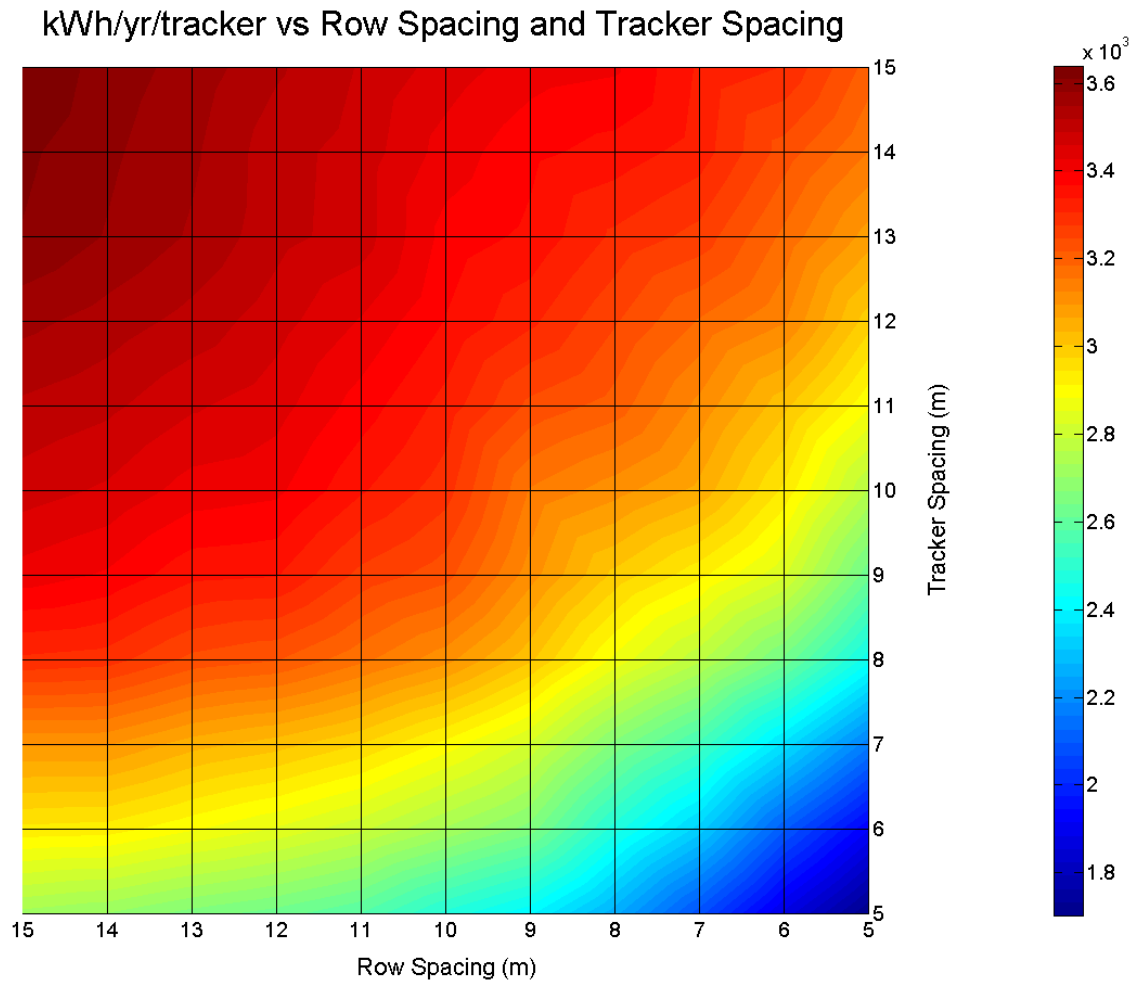


Figure 5.4 - Annual Tracker Output vs. Large Variations (1m) in Tracker and Row Spacing (Contours). Contours correspond to a change of 30.27 Wh/yr/tracker.

5.3 Small Variation in Spacing

To gain a better understanding of the relationship between tracker annual energy output and spacing, a more precise analysis was performed. Tracker and row spacing were increased from 5.0m and 6.0m in increments of 0.1m (again, a total of 121 annual simulations). This is the equivalent of zooming into the far bottom-right grid square of Figure 5.4. The results, shown in Figure 5.5, indicate that the non-linearity of shading losses as a function of tracker and row

spacing become much more pronounced on a smaller scale.

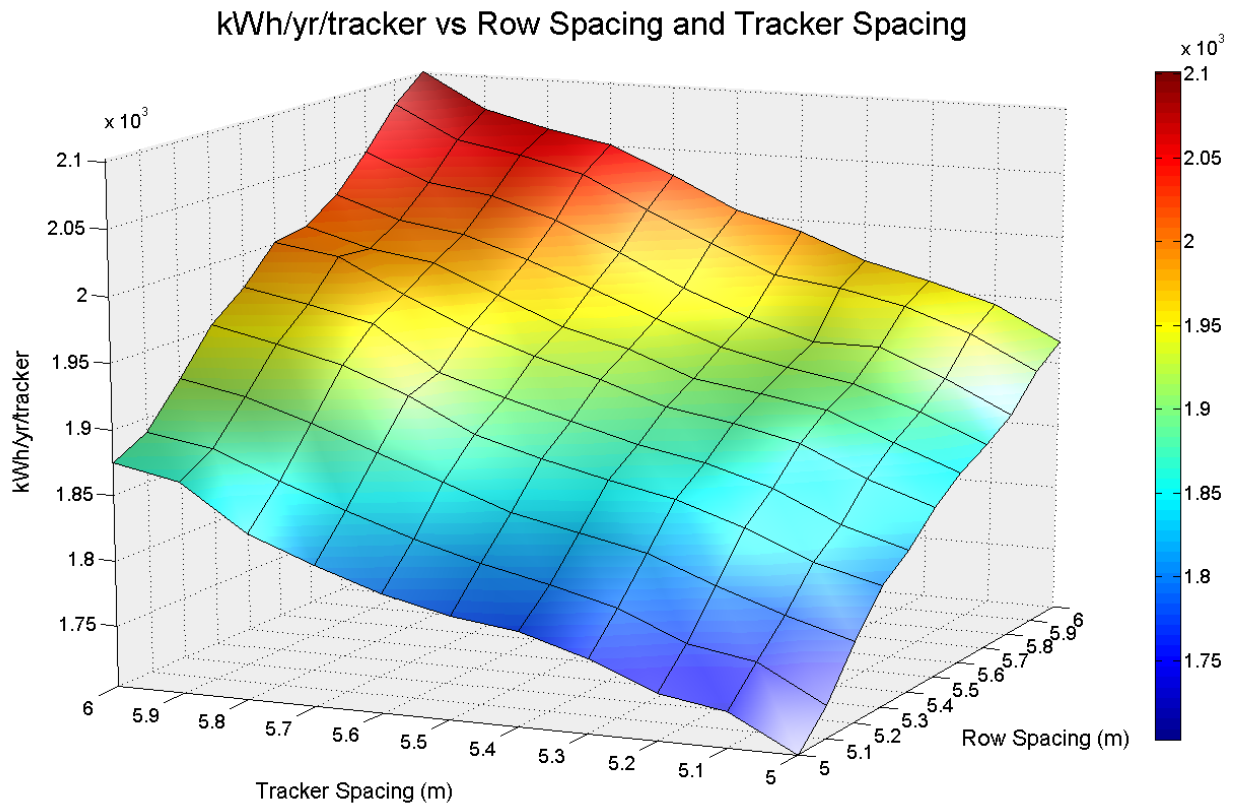


Figure 5.5 - Annual Tracker Output vs. Small Variations (0.1m) in Tracker and Row Spacing

To further analyze this relationship, a regression plane, which is the 3-D equivalent of a 2-D linear fit line, was fit to this data, as shown in Figure 5.6. A 3-D surface plot showing the excursions of the data from this regression plane is shown in Figure 5.7, and a contour plot of the same data is shown in Figure 5.8. In this range of tracker and row spacing, the simulated tracker output varies from the fitted plane by just over $\pm 1\%$. Due to the nature of this relationship, any form of optimization (such as to cost-optimize the spacing of trackers in a solar PV farm) which uses this data to find the local maxima and minima of a system must assume the data to be

uncertain; i.e. the maxima and minima cannot be found through predictive or deterministic numerical methods.

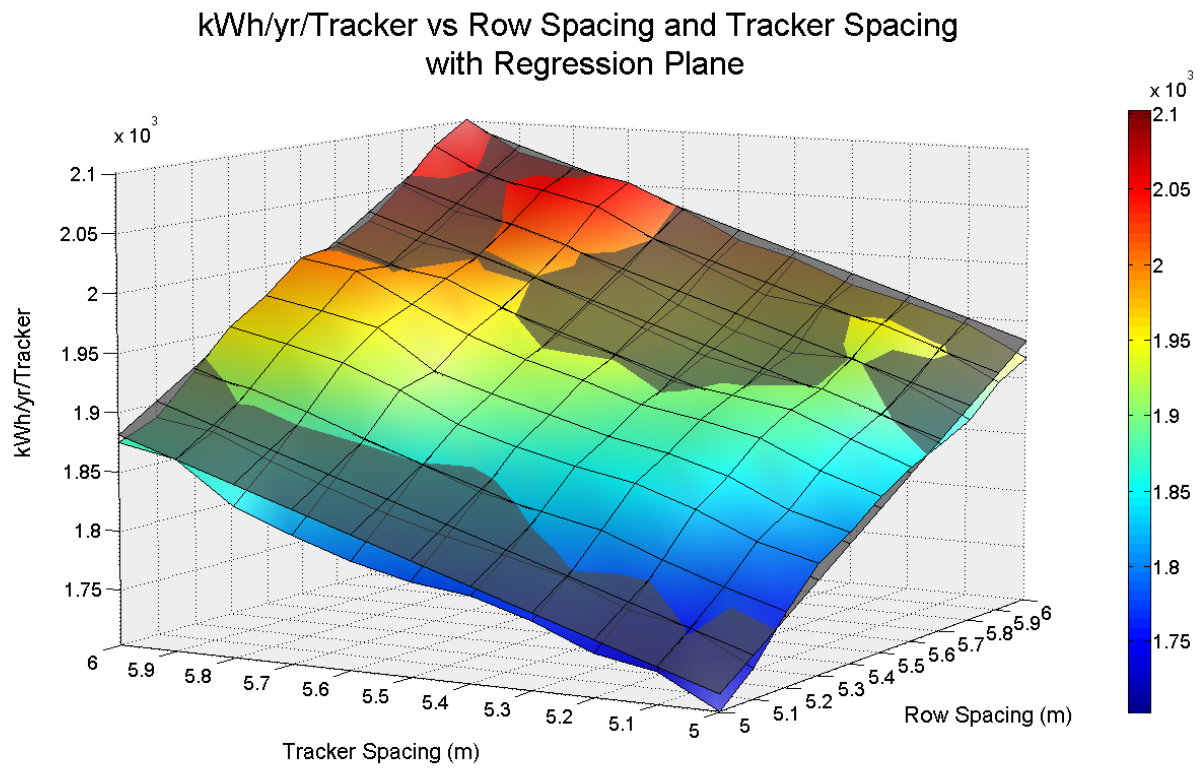


Figure 5.6 – Annual Tracker Output vs. Small Variations (0.1m) in Tracker and Row Spacing with Regression Plane

Delta from Regression Plane vs Row Spacing and Tracker Spacing

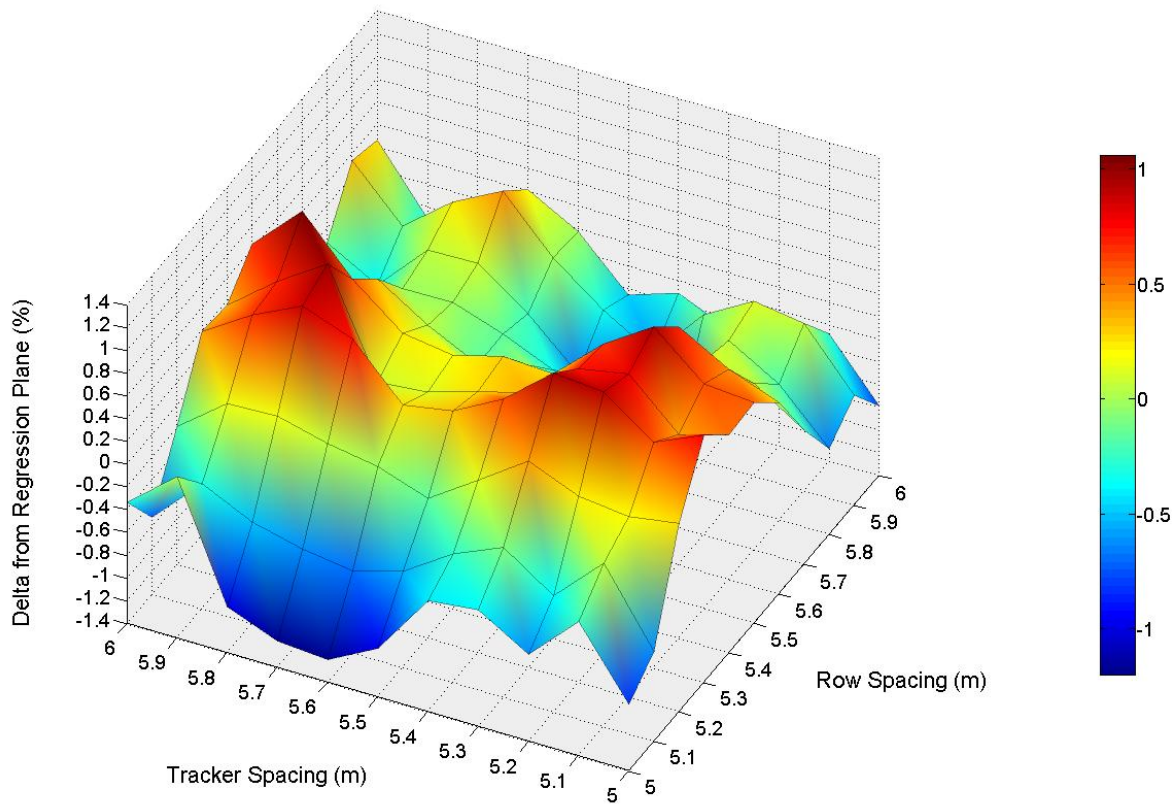


Figure 5.7 – Annual Tracker Output vs. Small Variations (0.1m) in Tracker and Row Spacing: Excursion of Data from Regression Plane

Delta from Regression Plane vs Row Spacing and Tracker Spacing

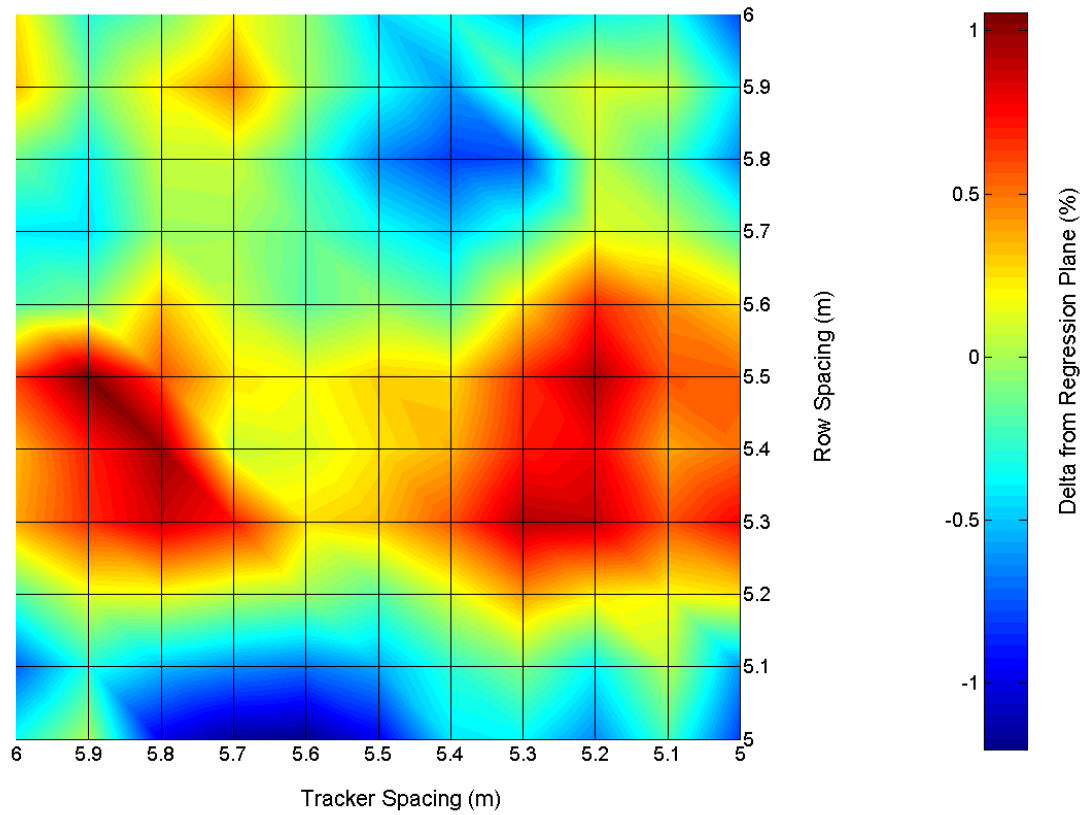


Figure 5.8 - Annual Tracker Output vs. Small Variations (0.1m) in Tracker and Row Spacing: Excursion of Data from Regression Plane (Contours). Contours correspond to a change of 0.0353%.

5.4 Optimization of Spacing for Cost of Energy

To show the potential value of the simulation data of this hypothetical system, a simple example of cost optimization follows. Arbitrary costs for land (\$5/m²) and trackers (\$5,500/unit) were chosen (maintenance costs were ignored for this analysis), and the first year energy output of the system based on the data of Figure 5.3 was extrapolated over a 25-year life assuming a 1% drop in output annually. The results of Figure 5.9, show the predicted cost of electricity generated by

the system over its lifetime (\$/kWh) as a function of tracker and row spacing. A contour plot of the same data is shown in Figure 5.10. The minimum of these plots represent the tracker and row spacing which would result in the lowest cost per unit energy generated based on the hypothetical costs assumed. In this example, this occurs when row spacing is 13m, and tracker spacing is 11m (which is only slightly better than a row spacing of 13m and a tracker spacing of 13m). The cost of electricity generated based on this spacing is \$0.080518/kWh. Re-running the simulation with 0.1m accuracy near the minimum would provide in an even more accurate result for optimal spacing.

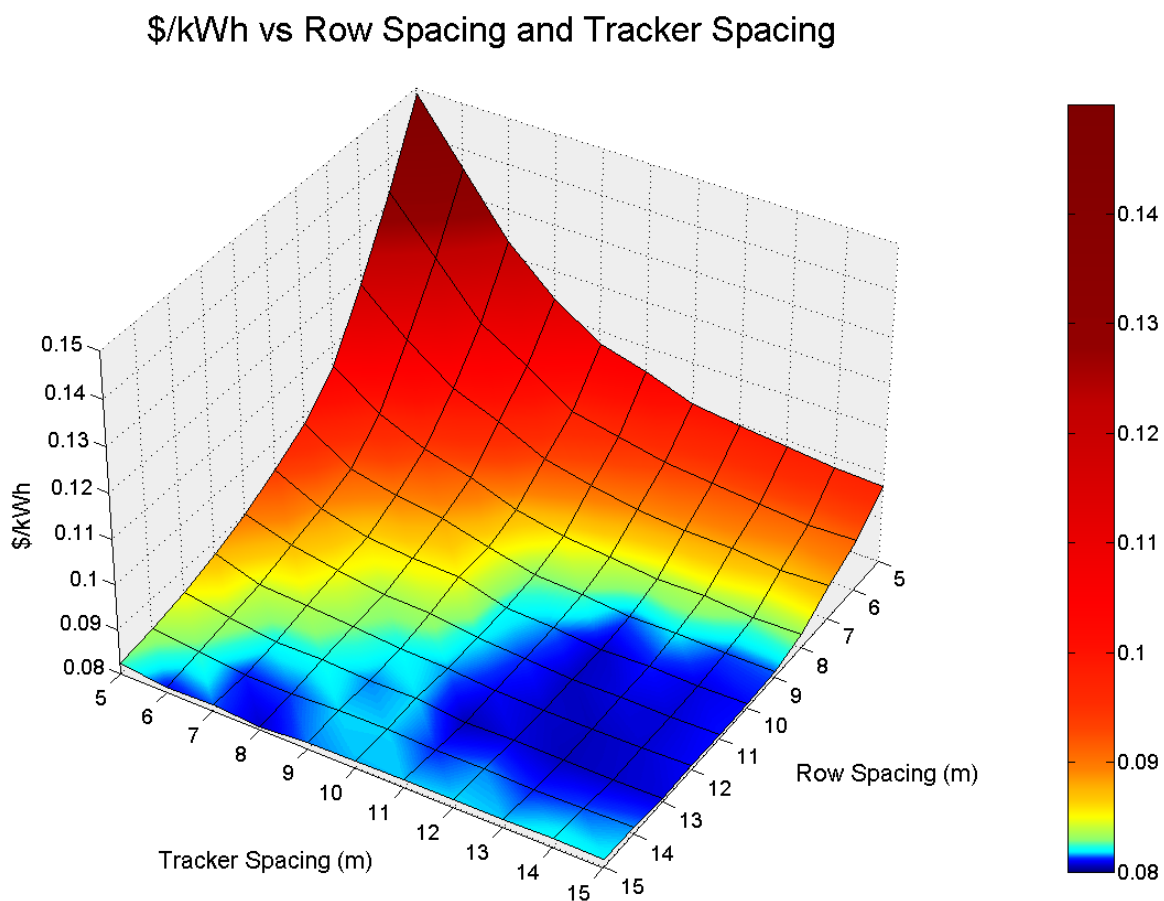
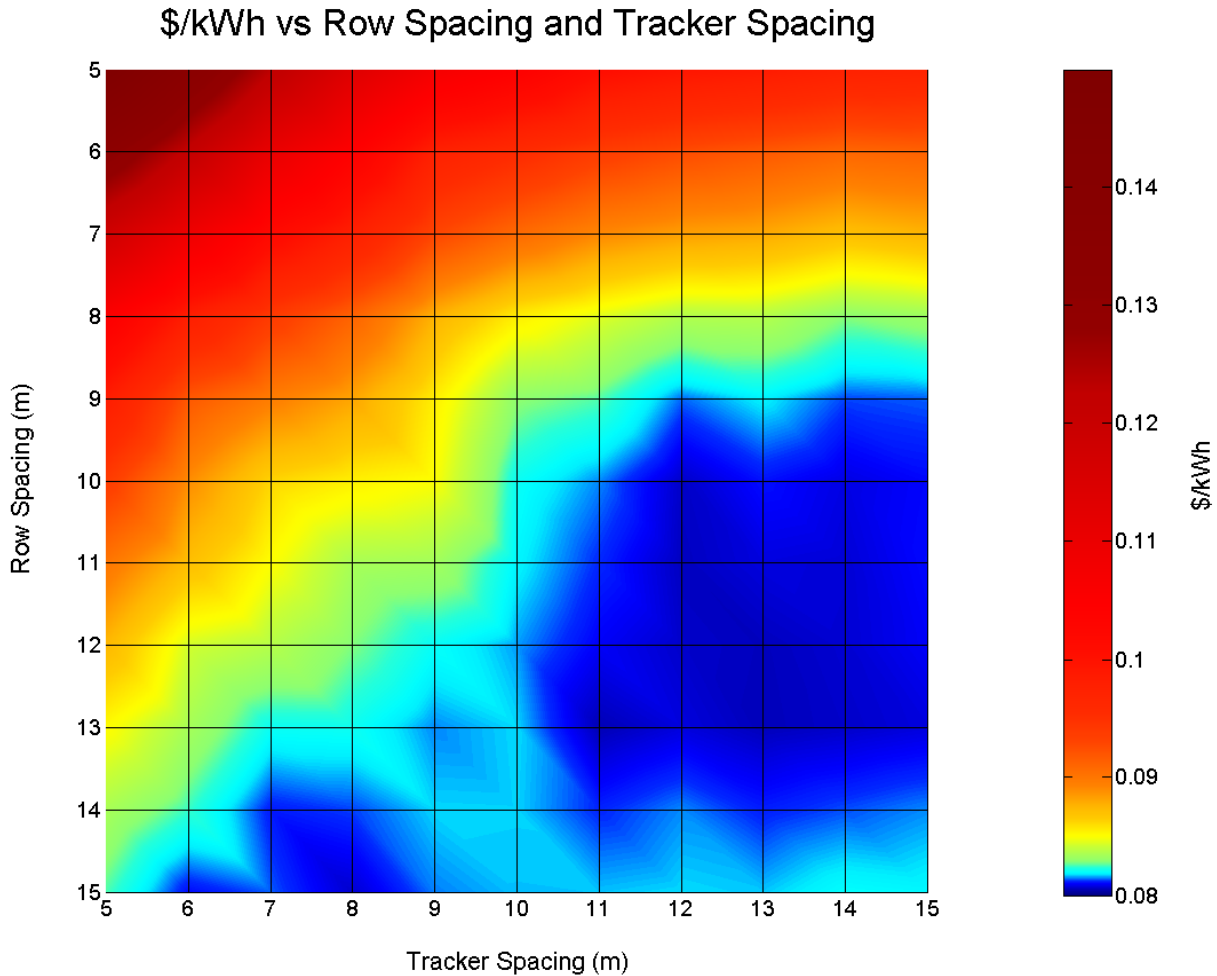


Figure 5.9 - Cost of Electricity (\$/kWh) as a Function of Tracker and Row Spacing



**Figure 5.10 - Cost of Electricity (\$/kWh) as a Function of Tracker and Row Spacing
(Contour).**

5.5 Comparison with Other Shading Loss Approximation Methods

In order to compare the shading loss predictions of the proposed PV simulation model with those of other less accurate shading loss approximation methods, modifications were made to the model in order to simulate these other methods. The simulation was run for each shading loss

calculation method using the settings shown in Table 5-1, a tracker spacing of 10m and a row spacing range of 5-15m. The results are shown in Figure 5.11. The first run (shown in green) did not factor in shading losses, and therefore the annual energy production did not change with increased row spacing. The second run (shown in dark blue) used the approximation that electrical shading losses are directly proportional to the fraction of the tracker shaded (as described in 2.3.2), which necessarily under-estimates actual shading losses (over-estimating annual energy production). The third run (shown in red) used the accurate PV-cell based shading model developed for this project. The fourth run (shown in purple) used the approximation that if any portion of a PV module is shaded, then that module is assumed to be completely shaded and therefore not producing any energy (which necessarily over-estimates shading losses). The final run (shown in light blue) used the assumption that if any portion of the tracker (which is composed of a single string of 12 PV modules) is shaded, then the entire tracker is assumed to be shaded and therefore not producing energy (as described in 2.3.1). As expected, the PV-cell based shading model predicts higher electrical shading losses than would be estimated based on the fraction of tracker shading alone, and lower electrical shading losses than would be estimated based on the assumption that a partially shaded module or string is completely non-productive. The results also show that as shading losses increase (as seen with closer row spacing), the error of the less-accurate shading loss approximation methods also increase. Over the range of tracker spacing shown, the average error in the approximation of annual energy output for the shade-area based approximation was +3.93%, for the module-level approximation, -3.82%, and for the string-level approximation, -18.05%. Note that these errors are specific to this hypothetical PV system only, at the installation site chosen, and would change with variations to any of the system design variables. If these rough shading loss approximation methods were used to

optimize the layout of a utility-scale PV farm, errors in the final optimization results would result.

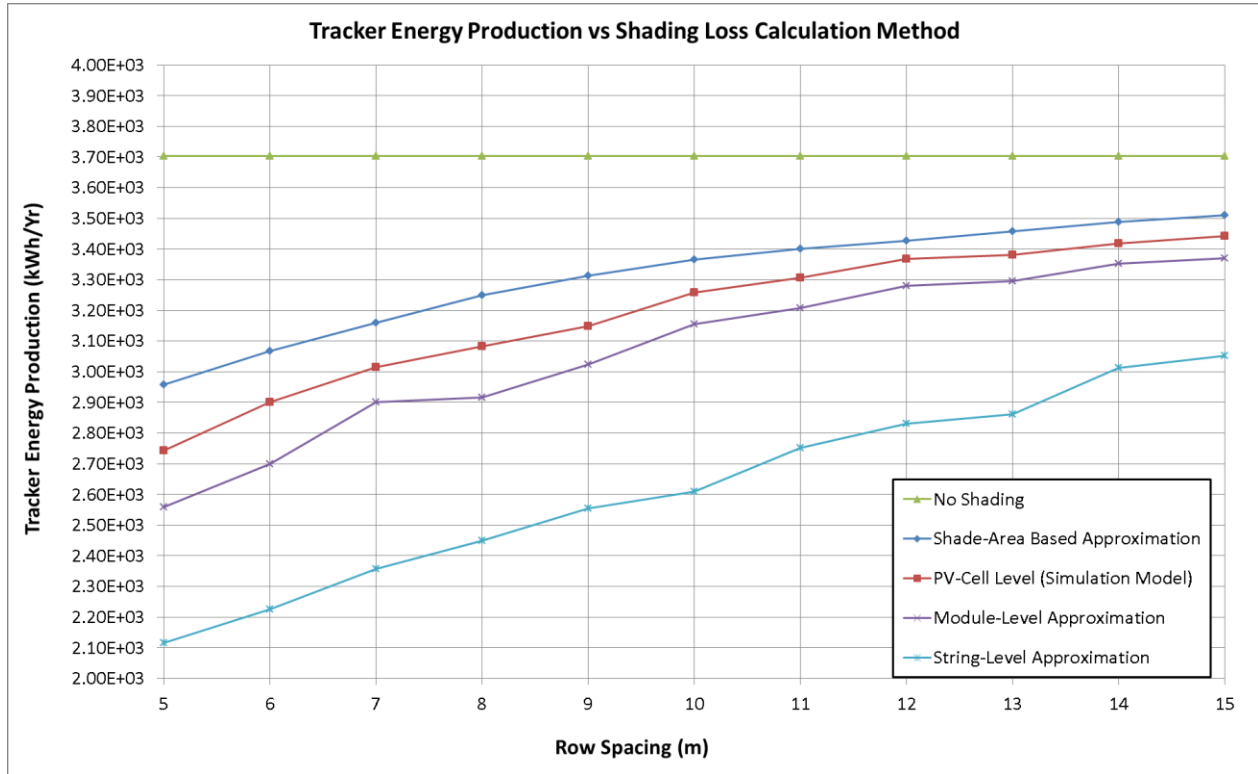


Figure 5.11 – Comparison of Simulation Model Shading Loss Estimates with Other Approximation Methods

5.6 Effect of Day-Intervals

The results thus far have been based on simulating every 10th day of the year (referred to as 10-day interval) for the purpose of reducing total simulation time. Though the significance of the simulation data lies in the *difference* in annual output as a function of the spacing, it is worthwhile to investigate the effect that day-intervals have on the simulated annual energy output. The simulation was run with the same settings as shown in Table 5-1, a tracker spacing of 5m, row spacing from 5-15m, and day interval set to 1, 2, 5, 10, and 30-days. The results are shown in Figure 5.12.

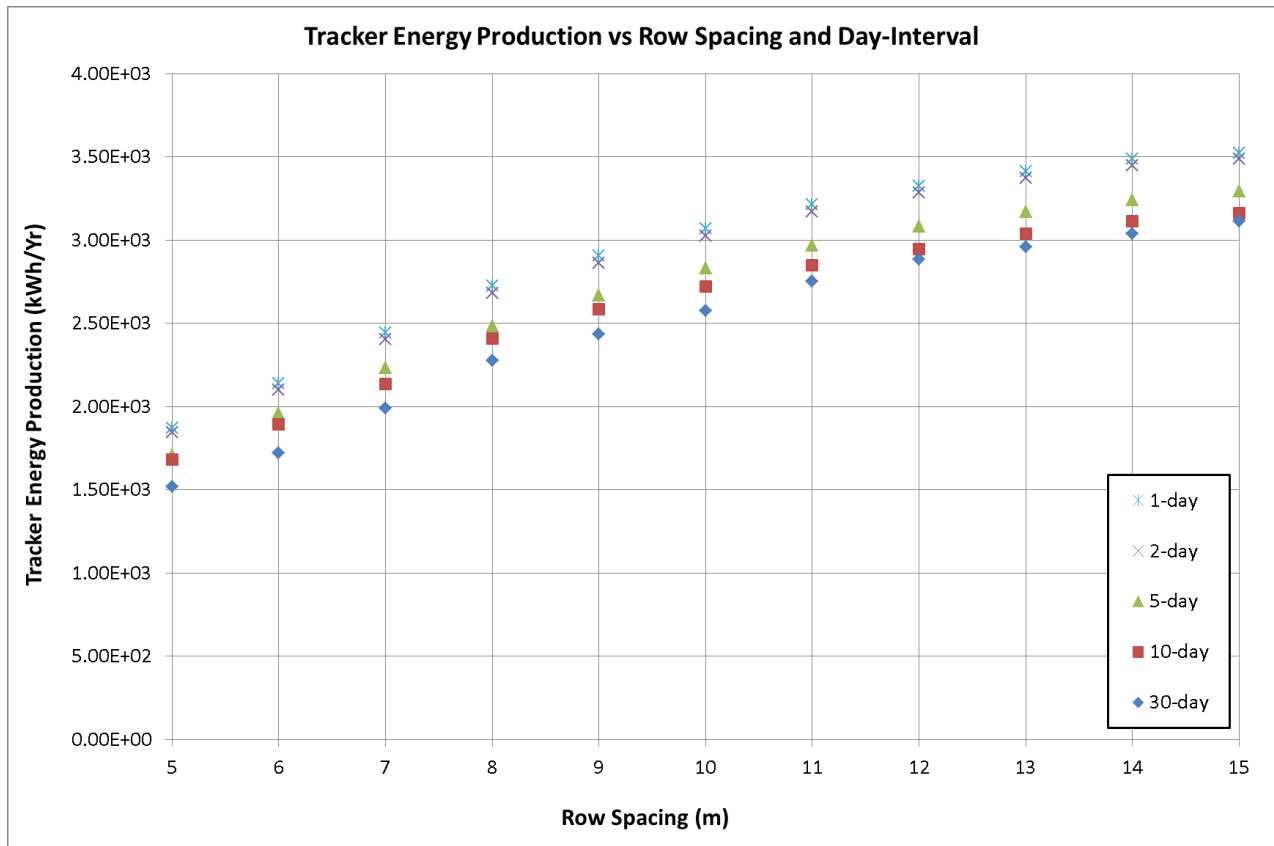


Figure 5.12 - Effect of Day-Intervals on Annual Energy Production

The results show that two-day intervals produce results which are very close to those produced by one-day intervals, and that increasing the day-interval results in a progressive loss in accuracy of annual energy production. It was surprising to observe that as the day-interval is increased, the estimated annual energy production dropped to successively lower levels, as opposed to a more randomized distribution higher and lower than the one-day baseline. An investigation into this phenomenon revealed that the main contributing factor to this trend is the fact that in each case, the first day of the year is included in the simulation. Since the first day of the year is very close to the winter solstice (December 22nd), the shortest day of the year, there is very little solar irradiation on this day, and this has an ever-more powerful effect on the extrapolated annual average energy production as the day-interval is increased. In the 30-day-interval case for

example, 13 days are simulated, including Jan 1st and Dec 27th, which are both very short days that are only five days apart in an annual cycle. If the simulation is changed such that the first day of the year is skipped in each case, this trend largely disappears, though the 30-day-interval is still markedly lower than the others.

Since most of the simulations presented in this chapter are based on a 10-day interval, it is noted that based on the data of Figure 5.12, using a 10-day interval can be expected to produce an annual energy production estimate 11.2% lower than if every day of the year were simulated. As mentioned previously however, the absolute accuracy of the simulation is of limited relevance since conclusions are drawn from the *difference* in results between successive simulations.

5.7 Code Execution Time Profile

One of the limiting factors for the simulation model is code efficiency, which to a large extent (along with CPU speed), determines the time taken to complete the simulation of the PV array. Though MATLAB is a powerful tool with many in-built functions, it is not regarded as a highly efficient programming language. MATLAB is optimized for operations involving matrices and vectors, as opposed to loops (for..., while...). Therefore in the interest of code efficiency, it is generally recommended to vectorize MATLAB code whenever possible, meaning that loops should be avoided. Due to the multitude of complex sequential operations required at each time-step of the simulation however (such as interpolations), vectorization proved impractical, meaning that the power of MATLAB could not be fully leveraged. Because loops are heavily used, the simulation can take a fair amount of time to execute depending on the system and user settings. In order to offer some control over code execution time, various parameters are

available in the simulation settings to vary simulation accuracy which has a direct effect on code execution time. Some of these settings include day-interval (for a n -day-interval, every n^{th} day of the year is simulated), angle step size (round to the nearest m -degrees for sun angles during shading calculation and hourly simulation) and the ability to turn off all graphical plots, which are normally being continually updated as the simulation runs. Note that turning off graphical plots does not affect the accuracy of the simulation, but significantly speeds it up. Some sample code execution time profiles, each with different simulation accuracy settings are shown in Figure 5.13. Each of the four time profiles represents a one-year PV array simulation, for one particular setting of tracker and row spacing (7m and 7m in this case). The bottom profile has the loosest accuracy settings (10-day interval and 2-degree rounding) and does not provide graphical plots, and therefore has the fastest execution time, at about 89s. With these settings, running 121 variations of tracker and row spacing on a typical home PC, as was done earlier in this chapter, takes approximately three hours. Looking at the second-to-bottom time profile, the only change was to increase the angle accuracy from 2-degree rounding to 1-degree rounding. This effectively doubled the time required to calculate PV tracker shading, and also increased the execution time of the main simulation loop. The total execution time for this profile was 142s. Next, the angle accuracy was returned to 2-degrees, but the day-interval was decreased from 10-day to 1-day, meaning that every day of the year were being simulated instead of every 10th day. The only notable change in execution time from the base case was an increase in the main loop execution time, which increased by almost a factor of ten. The total execution time for this profile was 198s. The final profile, shown at the top of the chart, is identical to the base case at the bottom of the chart with the exception that graphical plotting was enabled. The accuracy and results are identical, however the code execution time increased from 89s to 414s. Clearly, the

MATLAB visualizations are computationally intensive, and are therefore a luxury that should only be used as a check to verify that the simulation appears to be working as expected. It should be noted that there is significant room for improvement in the method of writing results to the Excel spreadsheet, which is shown in orange on the time profiles (a crude method is being employed currently).

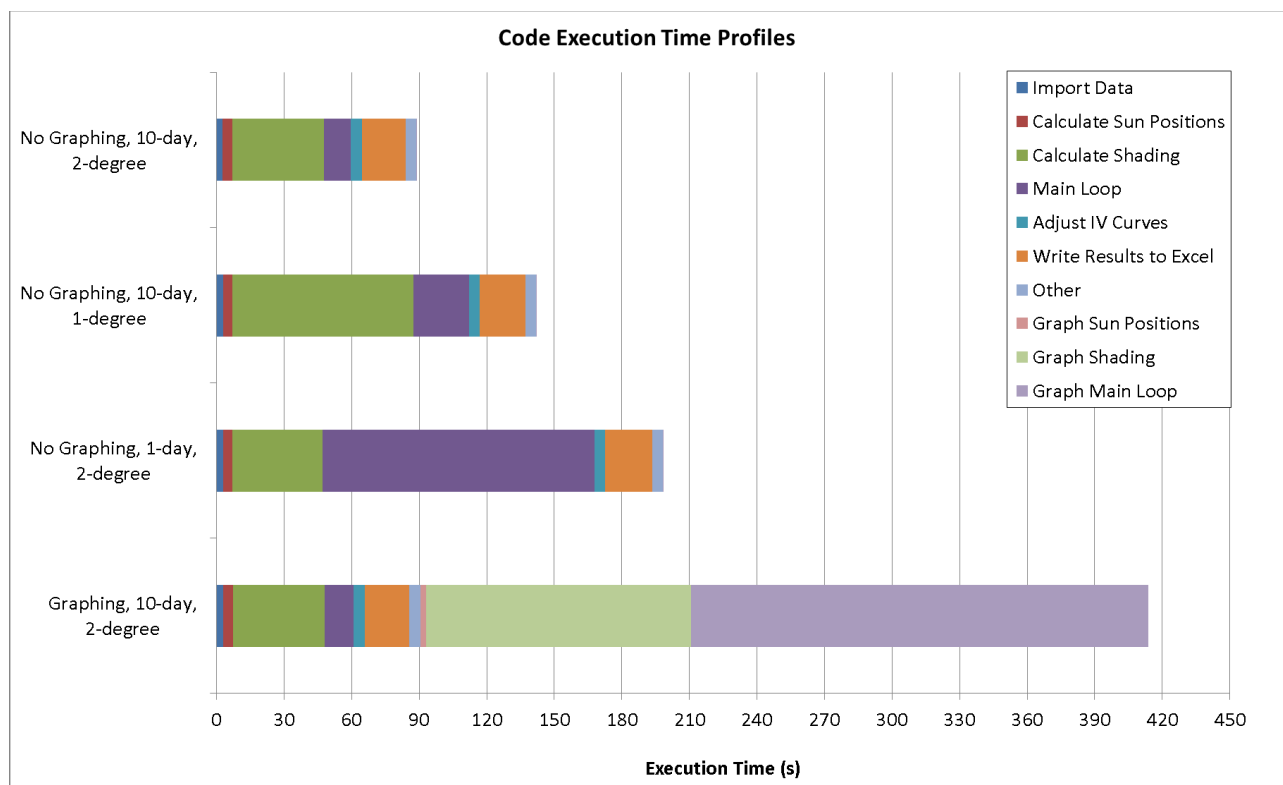


Figure 5.13 - Code Execution Time Profiles

Chapter Six: Discussion

In Chapter Four, the simulation model was verified for absolute accuracy (without shading) against a publically available tool, SAM, developed by NREL. In Chapter Five, a hypothetical PV system was defined, with sample costs, and run through the proposed simulation model for a one-year period with varying tracker and row spacing in order to determine the optimal spacing for the lowest cost of electricity (\$/kWh). Below, the opportunities for improvement to the simulation model are discussed, along with the potential to use the model for the optimization of solar PV farm design characteristics beyond tracker and row spacing.

6.1 Assumptions and Approximations

Though the following assumptions and approximations will result in errors in the prediction of the absolute annual energy produced by the modeled PV system, the primary purpose of the model is to observe the *change* in system output as one or several parameters of the design are varied. These assumptions and approximations will affect the simulation results of each incremental variation in the design roughly equally, and will have a negligible effect on the *differences* between the outputs of successive runs. Therefore the usefulness of the simulation model is not greatly affected by these inaccuracies.

6.1.1 Albedo

Albedo is a factor added to some PV simulation models in order to account for the additional irradiation directed to PV modules due to the reflection of direct solar irradiation from the surface of the ground. This factor depends on the reflectivity of the surrounding ground (e.g.

snow-covered ground has a much higher albedo than ground covered with vegetation). A common method of including albedo in a simulation model is to allow the user to enter the factor (e.g. 0.20) to be used for the entire year, or a different factor for each month. This factor is applied to the direct solar irradiation present for each time step, and added to the total irradiation incident on the PV modules. In the proposed simulation model, the albedo of the surrounding ground is assumed to be zero, which is an underestimation that will result in a slightly lower prediction of absolute annual energy production.

6.1.2 Sky Diffuse Model

The proposed PV simulation model assumes an isotropic sky, in which diffuse irradiation is uniform across the entire sky. There exist more complex models which more accurately predict the distribution of diffuse irradiation, resulting in an orientation-dependant diffuse component to irradiation incident on the PV modules. For example, Perez et. al. developed such a model based on a set of empirical coefficients [34], which is implemented in the PVSyst system simulator.

6.1.3 System Losses

Various system losses were not modeled in the proposed PV simulation model. Firstly, the efficiency of the inverter (which includes the efficiency of its MPPT algorithm) is assumed to be 100%. In reality, this efficiency depends on the specific inverter chosen, and the load factor profile the inverter is subjected to over the course of a year. Each inverter has a characteristic efficiency curve which provides its efficiency as a function of the inverter load factor (the inverter efficiency varies as the irradiation incident on the PV array varies over the course of each day). Though relatively simple to implement in the model, the use of an inverter efficiency

curve was left for future improvements. To provide a rough approximation, it would be reasonable to apply a loss of 5% to account for inverter MPPT and conversion losses.

Secondly, it was assumed that no soiling losses occur. In reality, soiling losses can vary between 1% and 5% [25], as surface contaminants such as dust and snow absorb and/or scatter incident irradiation, reducing the power generating potential of the PV module. The amount of soiling depends on whether, and how often the PV modules are cleaned, how much rain the area receives (rain naturally cleans the surfaces), the amount of snow accumulation, the amount of airborne contaminants in the area, and other factors. As a result this loss, which is difficult to approximate and is site-specific, is left as a future improvement to the model.

Thirdly, DC wiring losses were assumed to be zero. In reality, resistive wire losses depend on the system currents, wire gauges and wire lengths. Typical wiring power losses may total 1.5% to 2% of the PV system's total annual energy output [25].

Finally, the solar tracker was assumed to perfectly track the sun's position at all times. In reality, there is often an angle error associated with the tracking system, which depends on the specific tracker used. Future improvements to the model may include a loss factor for tracking error, which could be set by the user according to the specifications of the tracker to be used.

6.1.4 Edge Trackers

The PV farm is assumed to be sufficiently large that the reduced shading losses experienced by trackers positioned around the edge of the farm have a negligible effect on the average tracker output. All PV trackers are therefore assumed to be subject to the same shading patterns and therefore produce identical output.

6.1.5 Tracker Layout

A hexagonal layout of trackers was assumed in this model. A relatively simple future improvement would be to introduce an E-W skew between alternating tracker rows. When the skew reaches half of the E-W distance between trackers along a row, the layout would become rectangular. All that would be required is a modification to the geometry calculations which determine the position of shadows cast onto the tracker.

6.1.6 Time Interval

Currently, the simulation model time interval is fixed at one hour steps, to match the weather data used. If weather data were available with a shorter time interval, the model could easily be modified to use this new time interval, potentially offering higher accuracy in the results.

6.1.7 PV Cell Model

As mentioned in Chapter Four, there exist various mathematical models for a c-Si PV cell. The single-diode model was used in this project due to its relative ease of implementation in a computer program as compared to the alternatives. The two-diode model, though perhaps a more accurate representation of PV cell's physical characteristics, would be significantly more difficult to solve and would require much more processing time. While the single-diode model has a system of non-linear equations with five unknowns, the two-diode model has a system with seven unknowns. At least one study has shown a negligible difference in accuracy between the two models as compared to the measured behavior of an actual PV cell [8]. Even more complex models exist, but they were not considered for this project. Note that both PVSyst and SAM (and likely most if not all other commercial products as well) use the single-diode model.

6.1.8 Reverse-Bias Characteristics of a PV Cell

An assumption was made in the simulation model that for any sub-module (cell-group) current above which a shaded PV cell becomes reverse-biased (by any amount), the bypass diode protecting this cell group will conduct, thereby bypassing the entire cell group. In reality the reverse-biased behavior of a PV cell is not strictly so simple, as it will continue to conduct beyond its short-circuit current (as dictated by incident irradiation) in a reverse-biased state up to a certain point as dictated by cell parameters. Above this current, the cell becomes so reverse-biased so as to overcome the positive bias of all the other cells in the cell-group, resulting in an overall negative terminal voltage at the output of the cell-group. This produces a forward-bias across the anti-parallel bypass diode, which begins to conduct, causing all current to bypass the cell-group. This PV cell reverse-bias behavior, which can be approximated using Bishop's model [35], does somewhat affect the shape of the I - V curves of modules with shaded cells, but often has little effect on the maximum power point of the module. The modeling of PV cell reverse-bias behavior is an added element of realism which is left for future improvements to the model.

6.1.9 PV Cell Operating Temperature

Firstly, a rough approximation was made to determine a PV cell's operating temperature based on the ambient dry-bulb temperature and the irradiation incident upon it using a simple empirical formula as shown in Chapter Four. A more accurate model of the temperature of PV cell would increase the accuracy of the simulation. Furthermore, an assumption was made that the operating temperatures of cells within a sub-module are always equal, and taken to be that of the most-shaded cell in the sub-module. In reality, cells within a sub-module that un-shaded will operate at a higher temperature than those which are shaded. In situations where a sub-module contains

cells of differing shading factors, the output voltage of the sub-module will be over-estimated. In many cases, however, a sub-module that is partially shaded is bypassed, in which case the outputs of its component cells will not contribute to the power output of the system, and will have no effect on the rest of the PV array.

6.2 Other Optimization Opportunities for the Proposed Simulation Model

In this thesis, the simulation model developed was used to optimize the spacing between dual-axis trackers in the N-S and E-W directions of a hexagonal layout. There are however, many other PV system design parameters that could be optimized in a similar manner using the proposed simulation model in its current form. For example as touched on in [23], the arrangement of cells into diode-groups (sub-modules) in a PV module could be optimized, since the existing user interface of the proposed simulation model allows the user to define specifically which cells are grouped together in antiparallel with a bypass diode. For example, it may be advantageous to group cells at the corners of the module as opposed to the industry standard of vertical/horizontal strips, due to the tracking of shadows across the module. Indeed, it was found in [23] that for wider inverter MPPT ranges, diagonal groupings were more productive than the other schemes tested. Of course, there can be no generalizations made about which arrangement is superior, since this will depend on the multitude of other design factors in the system (including installation site latitude and weather), and therefore each project must be analyzed on a case-by-case basis.

Another obvious candidate for optimization is the physical arrangement of PV modules on a tracker. There are many different ways to arrange the same number of PV modules onto a tracker; not just in placement, but also in orientation (portrait vs. landscape). An internet search

of photos of existing PV farm installations revealed that designs in this regard are quite varied, with no obvious industry standard. The proposed simulation model allows the user to select the physical location and orientation of each PV module on the tracker. Furthermore, the electrical interconnection of PV modules (into series and parallel combinations) may also be defined, which offers another opportunity for optimization.

Other optimization opportunities exist with the simulation model in its current form, including the optimization of inverter type by comparing the outputs of micro-inverters, string inverters and a central inverter. Experimentation is also possible with the number of bypass diodes in each PV module, and the sorting and grouping individual PV modules based on their unique manufacturer-tested parameters (each PV module has its own row for unique parameters in the PV module data entry spreadsheet).

6.3 Other Optimization Methods

In order to determine the optimal N-S and E-W spacing of dual-axis trackers in this thesis, a brute-force method was used in which each combination of N-S and E-W spacing in a grid-search pattern was tested with pre-defined step sizes. Of course, there are more efficient methods of discovering the optimal solution by using alternative optimization algorithms, such as those based on a genetic algorithm. Pertinent design variables could be chosen, and the goal set to minimize the cost of electricity generated. Due to the nature of shading losses however, which were shown in Chapter Five to have a complex relationship with tracker spacing, care must be taken to ensure that the global minimum or maximum is found as opposed to a local minima or maxima. This is left for future improvements to the simulation model.

Chapter Seven: Conclusions and Future Work

7.1 Summary of Work

A search of the literature on the calculation of shading losses for dual-axis tracking PV systems revealed that though there have been various experimental models developed to simulate these effects, the vast majority use one of two broad approximations for shading losses. The first is to approximate a partially-shaded PV module as completely shaded from the standpoint of electrical energy production, which necessarily over-estimates shading losses. The second is to approximate the electrical energy production losses to be equal to the physical shading ratio of the PV modules, which necessarily under-estimates shading losses in almost all circumstances. Commercial and government-funded PV simulation tools also have poor treatment of shading losses in tracking systems. Some perform no shading analysis at all, and instead rely on the user to manually enter shading loss factors. The most thorough treatment of shading losses in tracking systems was found in PVSyst, which approximates shading losses by allowing the user to pick some combination of each of the broad approximations listed above.

The most likely reason why shading losses are not calculated accurately is that it is a very computationally intensive process. It is proposed in this thesis that the analysis should begin at a PV-cell level, with shading ratios determined for each individual PV cell on the tracker for every time-step of the time-sequenced model. The PV-cells can then be combined into sub-modules, each protected by an anti-parallel bypass diode, and the I - V curves of each sub-module determined based on the shading ratios of its component cells, their cell parameters and the current weather conditions (temperature and irradiance). Sub-module I - V curves can then be combined to form PV module I - V curves according to the layout of sub-modules within the PV

modules. Finally, PV module curves can be combined to form string I - V curves (for groups of modules connected in series) and an array I - V curve (for groups of strings connected in parallel) according to the series/parallel connection of the modules as chosen by the user. Depending on the type of inverter chosen for analysis (micro-inverter, string inverter or central inverter), the appropriate I - V curve can be converted into a P - V curve and the maximum power point found within the constraints of the MPPT input voltage range of the inverter. Due to the nature of the process of combining series and parallel combinations of I - V curves, which requires interpolation between data points (for which there are no simple shortcuts), the processing time is significant. Nevertheless, a simulation model was built to calculate shading losses originating from a PV-cell level, and techniques were used to speed up the processing time where possible. Instead of re-calculating I - V curves from the single-diode equation for each time-step, baseline curves were calculated once, stored and then adjusted at each time-step based on the ambient temperature and incident irradiation. A user-interface was developed to allow the user to define the parameters of the PV system, and graphical outputs were created which display shading and I - V curve data while the simulation model executes. Parts of the model were verified against commercial PV simulation tools where possible. Execution time profiling was performed on the simulation model in order to identify where processor time was being used. Finally, the impact on simulation time of varying the accuracy of various simulation parameters was investigated.

7.2 Summary of Results and Contributions

Once the proposed simulation model was complete, a hypothetical dual-axis PV tracking system was defined and run for a range of tracker spacing in the N-S and E-W directions (from 5m to 15m in 1m increments). The annual energy production was plotted relative to tracker spacing in

the N-S and E-W directions, and revealed that in general there are diminishing returns from increased spacing in terms of reducing shading losses. When the spacing step-size was decreased to 0.1m increments in the range of 5m to 6m in each direction, the plotted results showed a complex, uncertain relationship between tracker and row spacing, and shading losses. Due to the nature of this relationship, the annual energy output can vary by up to about $\pm 1\%$ over as little as 0.1m from what might be predicted based on a best-fit regression plane.

Finally, the energy prediction results were combined with hypothetical component and land cost data, and the optimal tracker spacing was determined based on the minimum cost of electricity generated over the system's life (lowest \$/kWh).

The contributions of this thesis were:

1. A review of published work on the analysis and calculation of dual-axis shading losses, and the testing of existing commercial and public (government-funded) PV simulation tools. This research revealed that very little work had been done on analysing shading losses accurately (electrically, down to a PV-cell level) for dual-axis tracking systems over an annual period. Instead, basic approximations are universally applied in existing simulators of tracking PV systems.
2. A model developed in MATLAB Simulink which iteratively calculates the equivalent series resistance (R_s) and shunt resistance (R_{sh}) of a solar cell based on known parameters provided from the manufacturer's data sheet (I_{sc} , V_{oc} , I_{mp} and V_{mp}) and an assumption for diode ideality (n). These parameters are required for the single-diode model of a PV cell.
3. A user interface built in Microsoft Excel which allows the user to input many different design and simulation parameters for a tracking PV array.

4. A PV simulation model developed in MATLAB which reads settings from the user-interface and weather data from a standardized EPW file, calculates solar angles and the positions of physical shadows cast by trackers onto one another for each solar angle, determines the shading ratio of every PV cell on a tracker array for every valid sun angle, calculates the I - V and P - V curves of each sub-module, module, string and array using the single-diode model of a PV cell and based on the weather conditions for each hour of the year, and finally determines the power generated by various inverter schemes by applying inverter maximum power point (MPP) limits to the PV curve data over an annual period.
5. A simulation model which is able to reveal for dual-axis PV tracking systems, the relationship between shading losses and any number of different system design variables, however in this thesis, only the relationship between shading losses and tracker spacing is studied.
6. The results of a simulation of a hypothetical PV system which was run through the simulation model, which revealed a non-linear, complex relationship between tracker spacing and shading losses.
7. The results when hypothetical system component costs are combined with the predicted annual energy outputs of the system over a range of spacing, with the goal of determining the optimal spacing of trackers and trackers rows (in this case, optimal spacing meaning the spacing which results in the lowest cost of electricity generated).
8. A roadmap for future model development, including suggestions for additional features to be added in future versions of the simulation model. The roadmap details feature sets

to be added to reach successive phases of the project. This project represents phase I of a proposed three-phase roadmap.

7.3 Recommendations for Future Work

There are various aspects of the PV simulation model which could be improved or expanded upon in order to increase the usefulness of the proposed model.

1. Add an optimization algorithm which is able to quickly optimize various parameters in the design and layout of a tracking PV system based on the results of repeated runs of the simulation.
2. Where possible, vectorize code in MATLAB to decrease the execution time of the simulation.
3. Add the suggested simulation features of phases II and III as outlined in Chapter Four.
4. Of particular note, and as already suggested as a phase II improvement, add the ability to skew alternating rows of trackers. This will allow the testing of any tracker layout between hexagonal and rectangular.
5. Improve the absolute and relative accuracy of the model by reducing the errors introduced by the approximations and assumptions listed in Chapter Six.
6. Since many CPV systems employ dual-axis tracking, make modifications to the model to allow the testing of CPV systems.
7. Add a thin-film PV cell model to enable the testing of this technology.

References

- [1] N. Darghouth, R. Wiser G. Barbose, "Tracking the Sun V: An Historical Summary of the Installed Price of Photovoltaics in the United States from 1998 to 2011," Lawrence Berkeley National Laboratory, Technical Report November 2012.
- [2] N. Darghouth, R. Wiser, J. Seel G. Barbose, "Tracking the Sun IV: An Historical Summary of the Installed Cost of Photovoltaics in the United States from 1998 to 2010," Lawrence Berkeley National Laboratory, Technical Report September 2011.
- [3] PVSyst. (Last Accessed: 2013, August) PVSyst Photovoltaic Software. [Online].
<http://www.pvsyst.com/en/>
- [4] National Renewable Energy Laboratory. (Last Accessed: 2013, August) System Advisor Model. [Online]. <https://sam.nrel.gov/>
- [5] HOMER Energy LLC. (Last Accessed: 2013, August) HOMER Energy. [Online].
<http://homerenergy.com/>
- [6] Valentin Software. (Last Accessed: 2013, August) PV*SOL. [Online].
<http://www.solardesign.co.uk/pv.php>
- [7] RETScreen International. (Last Accessed: 2013, August) RETScreen. [Online].
<http://www.etscreen.net/>
- [8] G. Farahani, K. Rahmani M. Taherbaneh, "Evaluation the Accuracy of One-Diode and Two-Diode Models for a Solar Panel Based Open-Air Climate Measurements," in *Solar Cells - Silicon Wafer-Based Technologies*.: InTech, November 2011, ch. 10, pp. 201-228.
- [9] J.R. Gazoli, E.R. Filho M.G. Villalva, "Modeling and Circuit-Based Simulation of

- Photovoltaic Arrays," in *2009 Brazilian Power Electronics Conference. COBEP 2009*, Univ. of Campinas (UNICAMP), Campinas, Brazil, 2009, pp. 1244-54.
- [10] A. Suarez-Garcia, C. Carrillo, J. Cidras E. Diaz-Dorado, "Influence of the shadows in photovoltaic systems with different configurations of bypass diodes," in *SPEEDAM 2010 - International Symposium on Power Electronics, Electrical Drives, Automation and Motion*, 2010, pp. 134-139.
- [11] S. Jing, B. Haihong, K. Yukita, K. Ichiyanagi X. Qingshan, "Analysis of Photovoltaic Array Performance Under Shaded Conditions," in *2010 Asia-Pacific Power and Energy Engineering Conference*, 2010.
- [12] H. Patel, "MATLAB-based modeling to study the effects of partial shading on PV array characteristics," *IEEE Transactions on Energy Conversion*, vol. 23, no. 1, pp. 302-310, March 2008.
- [13] J. Appelbaum D. Weinstock, "Optimization of solar photovoltaic fields," *Journal of Solar Energy Engineering, Transactions of the ASME*, vol. 131, no. 3, pp. 0310031-0310039, August 2009.
- [14] A. Suarez-Garcia, C.J. Carrillo, J. Cidras E. Diaz-Dorado, "Optimal distribution for photovoltaic solar trackers to minimize power losses caused by shadows," *Renewable Energy*, vol. 36, no. 6, pp. 1826-35, June 2011.
- [15] H.J. Wenger J.M. Gordon, "Central-station solar photovoltaic systems: field layout, tracker, and array geometry sensitivity studies," *Solar Energy*, vol. 46, no. 4, pp. 211-217, 1991.

- [16] R. Winston Y.S. Kim, "Optimal Spacing of Dual-axis Trackers for Concentrating Photovoltaic Systems," in *AIP Conference Proceedings*, v 1407, 2011, pp. 370-3.
- [17] F. Dobon, A. Lugo, P.Valera, R.Osuna, L. Acosta, G.N. Marichal J. Monedero, "Minimizing energy shadow losses for large PV plants," in *Proceedings of 3rd World Conference on Photovoltaic Energy Conversion (IEEE Cat. No.03CH37497)*, 2003, pp. 2043-5.
- [18] S. Kang, R. Winston Y.S. Kim, "Modeling of a concentrating photovoltaic system for optimum land use," *Progress in Photovoltaics: Research and Applications*, vol. 21, no. 2, pp. 240-249, March 2013.
- [19] O. Perpinan, "Cost of energy and mutual shadows in a two-axis tracking PV system," *Renewable Energy*, vol. 43, pp. 331-342, July 2012.
- [20] M.C. Pereira T.O. Fartaria, "Simulation and computation of shadow losses of direct normal, diffuse solar radiation and albedo in a photovoltaic field with multiple 2-axis trackers using ray tracing methods," *Solar Energy*, vol. 91, pp. 93-101, May 2013.
- [21] J.R.P. Angel K. Stephens, "Comparison of collection and land use efficiency for various solar concentrating field geometries," in *Proceedings of the SPIE - The International Society for Optical Engineering*, v 4868, 2012, pp. 846804-846812.
- [22] E. Lorenzo L. Narvarte, "Tracking and ground cover ratio," *Progress in Photovoltaics: Research and Applications*, vol. 16, no. 8, pp. 703-714, December 2008.
- [23] S. Jensen, M. McDonald J. Bowman, "Inverter modeling for accurate energy predictions of tracking HCPV installations," in *AIP Conference Proceedings*, 2010, pp. 320-323.

- [24] J. Muñoz, E. Lorenzo F. Martinez-Moreno, "Experimental model to estimate shading losses on PV arrays," *Solar Energy Materials and Solar Cells*, vol. 94, no. 12, pp. 2298-2303, December 2010.
- [25] B. Bourne, O. Koehler, L. Rangel M. Shields, "Simulators: Basic explanation and PVSyst default edit instructions," SunPower Corporation, Web Release:
<http://www.physics.arizona.edu/~cronin/Solar/References/PV%20system%20modeling/SP%20model%20guide.pdf> 2009.
- [26] National Renewable Energy Laboratory. (Last Accessed: 2013, August) National Solar Radiation Data Base. [Online]. http://rredc.nrel.gov/solar/old_data/nsrdb/1991-2005/tmy3/
- [27] US Department of Energy. (Last Accessed: 2013, August) EnergyPlus Energy Simulation Software. [Online].
http://apps1.eere.energy.gov/buildings/energyplus/weatherdata_sources.cfm
- [28] Numerical Logistics Inc. (Last Accessed: 2013, August) Numerical Logistics Inc. [Online]. <http://www.numlog.ca/cwecformat.html>
- [29] B.H. Khan, *Non-Conventional Energy Resources*. New Delhi, India: Tata McGraw-Hill, 2006.
- [30] R. Gottschalg, D.G. Infield A. Johansson, "Modelling shading on amorphous silicon single and double junction modules," in *Proceedings of 3rd World Conference on Photovoltaic Energy Conversion (IEEE Cat. No.03CH37497)*, 2003, pp. 1934-1937 Vol.2.
- [31] K. Ishaque, H. Taheri Z. Salam, "An improved two-diode photovoltaic (PV) model for PV system," in *2010 Joint International Conference on Power Electronics , Drives and*

Energy Systems (PEDES) & 2010 Power India, 2010, p. 5.

[32] J. Venture R.A. Messenger, *Photovoltaic Systems Engineering*, 3rd ed.: CRC Press, Feb 2010.

[33] M. Walker. (Last Accessed: 2013, August) HOMER Energy Support. [Online].

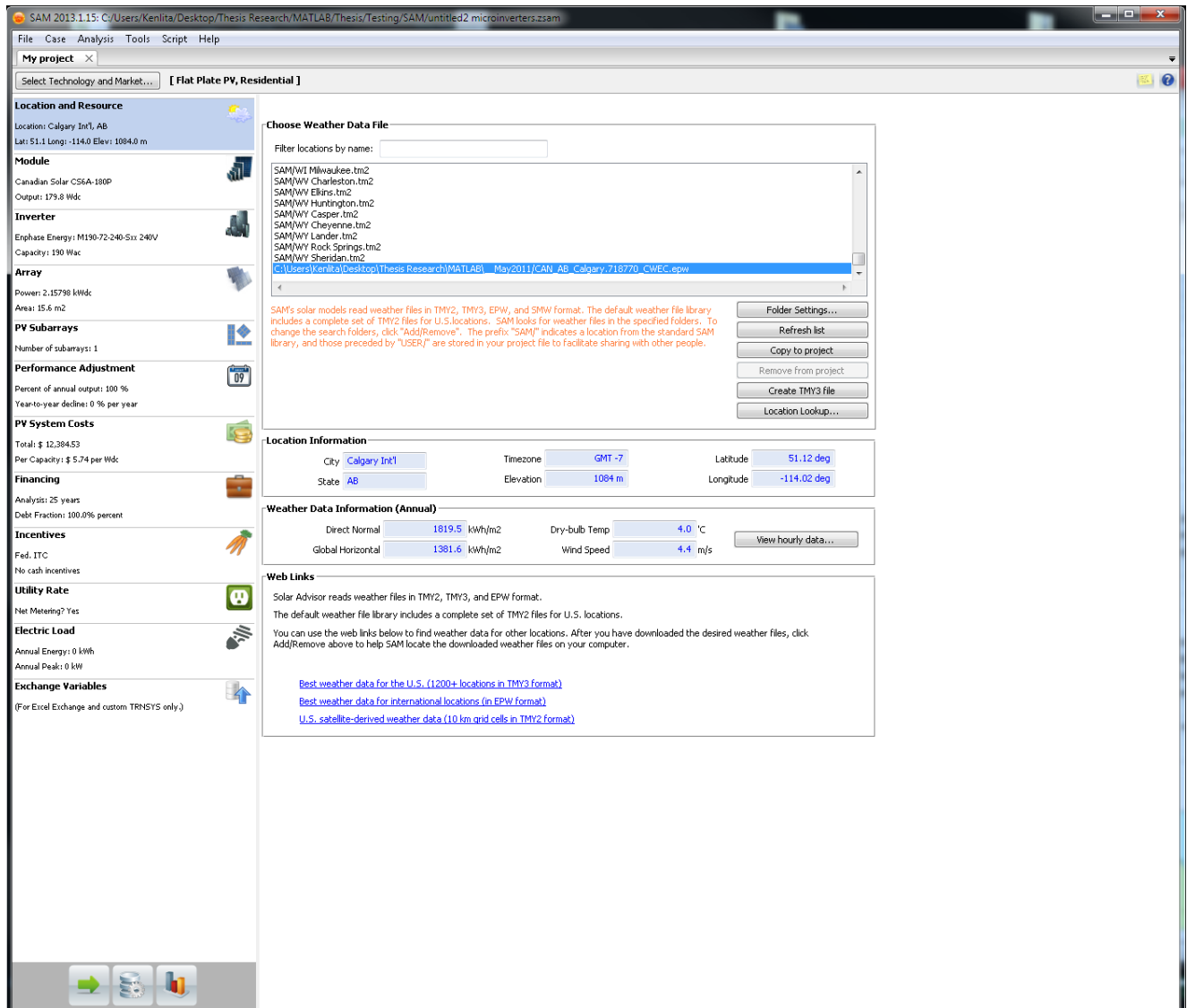
<http://support.homerenergy.com/index.php?Knowledgebase/Article/View/489/0/10487---how-homer-calculates-the-pv-cell-temperature>

[34] P. Ineichen, R. Seals, J. Michalsky, R. Steward R. Perez, "Modeling daylight availability and irradiance components from direct and global irradiance," *Solar energy*, vol. 44, no. 5, pp. 271-289, 1990.

[35] J.M. Ruiz, W. Herrmann M.C. Alonso-Garcia, "Computer simulation of shading effects in photovoltaic arrays," *Renewable Energy*, vol. 31, no. 12, pp. 1986-1993, October 2006.

APPENDIX A: SAM MODEL VERIFICATION - TEST SETUP AND RESULTS

The following images show the setup and simulation output of the SAM model used to verify the proposed PV simulation model:



SAM 2013.1.15: C:\Users\Kenlita\Desktop\Thesis Research\MATLAB\Thesis\Testing\SAM\untitled2 microinverters.zsam

File Case Analysis Tools Script Help

My project x

Select Technology and Market... [Flat Plate PV, Residential]

Location and Resource

Location: Calgary Int'l, AB
Lat: 51.1 Long: -114.0 Elev: 1084.0 m

Module

Canadian Solar CS6A-180P
Output: 179.8 Wdc

Inverter

Enphase Energy: M190-72-240-Sin 240V
Capacity: 190 Wac

Array

Power: 2.15798 kWdc
Area: 15.4 m2

PV Subarrays

Number of subarrays: 1

Performance Adjustment

Percent of annual output: 100 %
Year-to-year decline: 0 % per year

PV System Costs

Total: \$ 12,384.53
Per Capacity: \$ 5.74 per Wdc

Financing

Analysis: 25 years
Debt Fraction: 100.0% percent

Incentives

Fed. ITC
No cash incentives

Utility Rate

Net Metering? Yes

Electric Load

Annual Energy: 0 kWh
Annual Peak: 0 kW

Exchange Variables

(For Excel Exchange and custom TRNSYS only.)

CEC Performance Model with Module Database

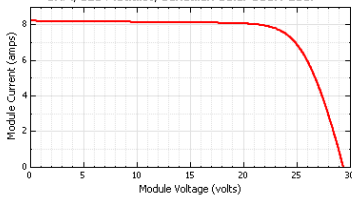
Search for modules by manufacturer or model name:

SAM/CEC Modules/Canadian Solar CS6P-165PE
SAM/CEC Modules/Canadian Solar CS5A-170M
SAM/CEC Modules/Canadian Solar CS5A-170MX
SAM/CEC Modules/Canadian Solar CS6A-170P
SAM/CEC Modules/Canadian Solar CS6P-170PE
SAM/CEC Modules/Canadian Solar CS5A-175M
SAM/CEC Modules/Canadian Solar CS5A-175MX
SAM/CEC Modules/Canadian Solar CS6A-175P
SAM/CEC Modules/Canadian Solar CS6P-175PE
SAM/CEC Modules/Canadian Solar CS5A-180M
SAM/CEC Modules/Canadian Solar CS5A-180MX
SAM/CEC Modules/Canadian Solar CS6A-180P
SAM/CEC Modules/Canadian Solar CS6P-180P

Module Characteristics at Reference Conditions

Reference conditions: Total Irradiance = 1000 W/m2, Cell temp = 25 C

SAM/CEC Modules/Canadian Solar CS6A-180P



Efficiency: 13.83 %
Maximum Power (Pmp): 179.832 Wdc
Max Power Voltage (Vmp): 23.6 Vdc
Max Power Current (Imp): 7.62 Adc
Open Circuit Voltage (Voc): 29.4 Vdc
Short Circuit Current (Isc): 8.2 Adc

Temperature Coefficients
-4.750e-001 %/C
-8.542e-001 W/C
-3.565e-001 %/C
-1.048e-001 V/C
4.500e-002 %/C
3.690e-003 A/C

Temperature Correction

☒ NOCT cell temp model
☐ Mounting specific cell temp model

Refer to Help for more information about CEC cell temperature models.

Nominal operating cell temperature (NOCT) parameters
Mounting standoff: Ground or rack mounted
Array height: One story building height or lower

Mounting configuration heat transfer cell temperature model
Mounting Configuration: Rack
Heat Transfer Dimensions: Module Dimensions
Mounting Structure Orientation: Structures do not impede flow underneath module
Module Width: 1 m
Module Length: 1.3 m

Rows of modules in array: 1
Columns of modules in array: 10
Temperature behind the module: 20 C
Gap Spacing: 0.05 m

Physical Characteristics

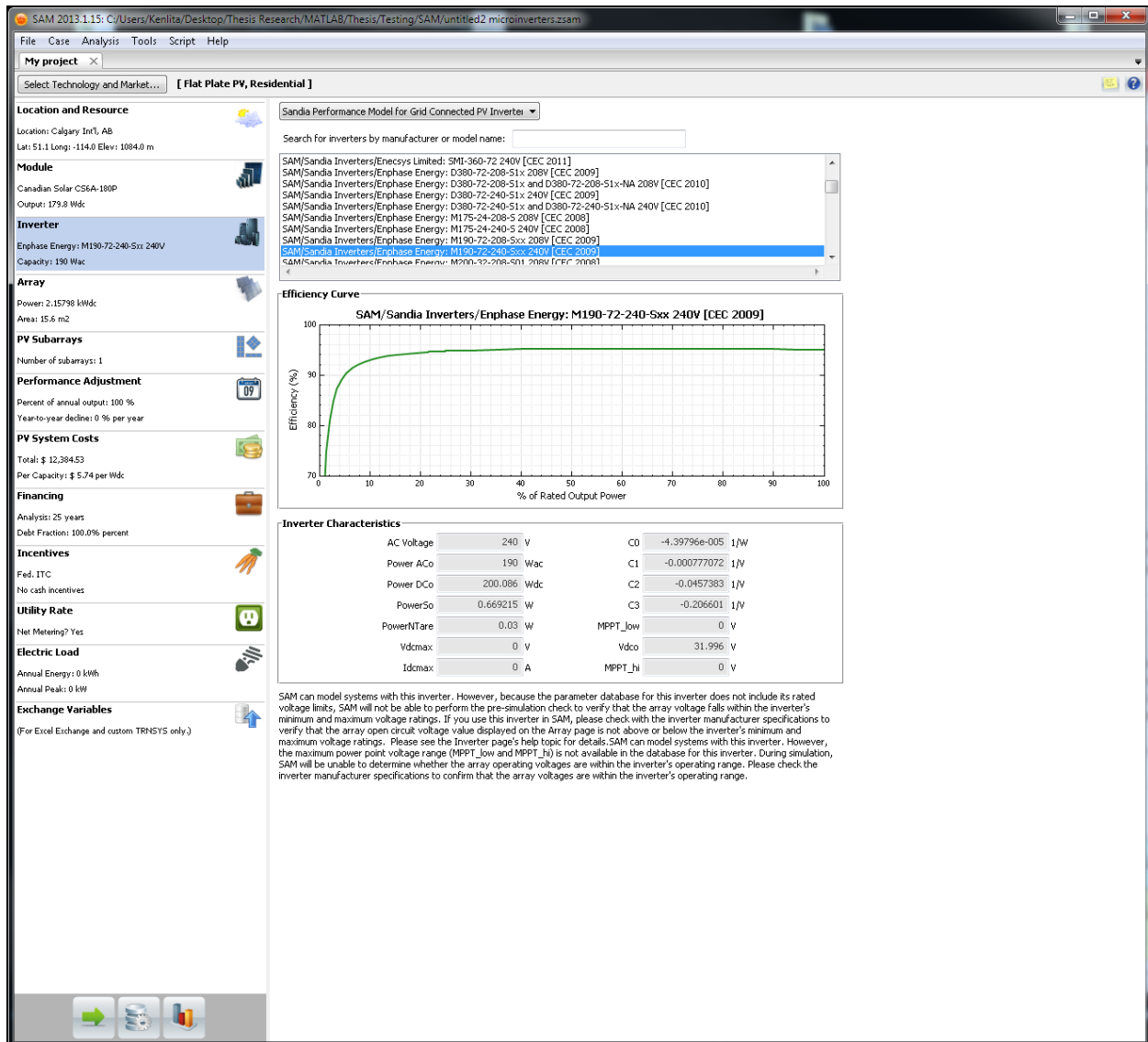
Material: Multi-j-c-Si
Module Area: 1.3 m2
Number of Cells: 48

Additional Parameters

T_noct: 49.5 C
A_ref: 1.2552 V
I_L_ref: 8.214 A
I_o_ref: 5.405e-010 A
R_s: 0.282 Ohm
R_sh_ref: 165.38 Ohm

References

For more information about the CEC model, see Help. For a detailed description of the model, see
[De Soto, W., 2004. Improvement and Validation of a Model for Photovoltaic Array Performance](#)
[Neises, T., 2011. Development and Validation of a Model to Predict the Temperature of a Photovoltaic Cell](#)



SAM 2013.1.15: C:\Users\Kenlita\Desktop\Thesis Research\MATLAB\Thesis\Testing\SAM\untitled2 microinverters.sam

File Case Analysis Tools Script Help

My project x

Select Technology and Market... [Flat Plate PV, Residential]

Location and Resource

Location: Calgary Int'l, AB
 Lat: 51.1 Long: -114.0 Elev: 1084.0 m

Module

Canadian Solar CS6A-180P
 Output: 179.8 Wdc

Inverter

Enphase Energy: M190-72-240-S12 240V
 Capacity: 190 Wac

Array

Power: 2.15798 kWdc
 Area: 15.6 m²

PV Subarrays

Number of subarrays: 1

Performance Adjustment

Percent of annual output: 100 %
 Year-to-year decline: 0 % per year

PV System Costs

Total: \$ 12,384.53
 Per Capacity: \$ 5.74 per Wdc

Financing

Analysis: 25 years
 Debt Fraction: 100.0% percent

Incentives

Fed. ITC
 No cash incentives

Utility Rate

Net Metering? Yes

Electric Load

Annual Energy: 0 kWh
 Annual Peak: 0 kW

Exchange Variables

(For Excel Exchange and custom TRNSYS only.)

Layout

Specify System Size

☐ Specify desired array size
☒ Specify numbers of modules and inverters

Desired Array Size: 4 kWdc
 Modules per String: 1
 Strings in Parallel: 12
 Number of Inverters: 12

Messages:
 Array DC capacity is 90% of inverter DC capacity. Check for more sizing messages after running simulations. See Help for details.

Actual Layout

Modules		Inverters	
Nameplate Capacity	2.15798 kWdc	Total Capacity	2.28 kWac
Number of Modules	12	Number of Inverters	12
Modules per String	1	Vdcmax (dc-inverter)	0 V
Strings in Parallel	12	MPPT_low	0 V
Total Module Area	15.6 m ²	MPPT_hi	0 V
Voc (String)	29.4 V	Nameplate capacity and Vmp are at module reference conditions. Voc is at 1000 W/m ² irradiance and 25 °C cell temperature.	
Vmp (String)	23.6 V		

Interconnection Derates (AC)

AC wiring losses: 1 (0..1)
 Step-up transformer losses: 1 (0..1)
 Total interconnection derate: 1 (0..1)

Land Area

Packing Factor: 2.5
 Total Land Area: 0.0096369 acres

Ground Reflectance

☐ Use albedo in weather file if it is specified
 Ground Reflectance (albedo): 0.2

Tilted Surface Radiation Model (Advanced)

☒ Isotropic
☐ HDKR
☐ Perez

-Radiation Components-
☒ Beam and Diffuse
☐ Total and Beam

Self Shading Calculator for Fixed Tilt Arrays

☐ Enable Self-Shading Calculator

Module

Orientation: Landscape
 Length: 1.932 m
 Width: 0.673 m
 Number of Cells along Length: 8
 Number of Cells along Width: 6
 Number of Bypass Diodes: 3

Characteristics from Module Page

Area: 1.3 m² Number of cells: 48

Array

String Wiring: Vertical
 Number of Strings along Bottom: 1
 Number of Modules along Bottom: 12
 Number of Modules along Side: 3
 Side Length: 2.019 m
 Row Spacing: 5 m
 Number of Rows: 0

Layout from Array Page

Modules per String: 1
 Strings in Parallel: 12

Enable the Self Shading option to model self shading of modules within the array.
 The self shading model only works when you chose the CEC or Sandia model option on the Module page, and when you choose fixed tracking on the Array page.
 The self-shading parameters must be consistent with the parameters you specify on the Module and Array pages. See Help for details.
 The number of cells along the bottom must be an integer multiple of the number of diodes, or the number of diodes must be an integer multiple of the number

SAM 2013.1.15: C:\Users\Kenlita\Desktop\Thesis Research\MATLAB\Thesis\Testing\SAM\untitled2 microinverters.zsam

File Case Analysis Tools Script Help

My project X

Select Technology and Market... [Flat Plate PV, Residential]

Location and Resource

Location: Calgary Int'l, AB
Lat: 51.1 Long: -114.0 Elev: 1084.0 m

Module

Canadian Solar CS6A-180P
Output: 179.0 Wdc

Inverter

Enphase Energy: M190-72-240-S11 240V
Capacity: 190 Wac

Array

Power: 2.15798 kWdc
Area: 15.6 m2

PV Subarrays

Number of subarrays: 1

Performance Adjustment

Percent of annual output: 100 %
Year-to-year decline: 0 % per year

PV System Costs

Total: \$ 12,384.53
Per Capacity: \$ 5.74 per Wdc

Financing

Analyst: 25 years
Debt Fraction: 100.0% percent

Incentives

Fed. ITC
No cash incentives

Utility Rate

Net Metering? Yes

Electric Load

Annual Energy: 0 kWh
Annual Peak: 0 kW

Exchange Variables

(For Excel Exchange and custom TRNSYS only.)

Defining subarrays

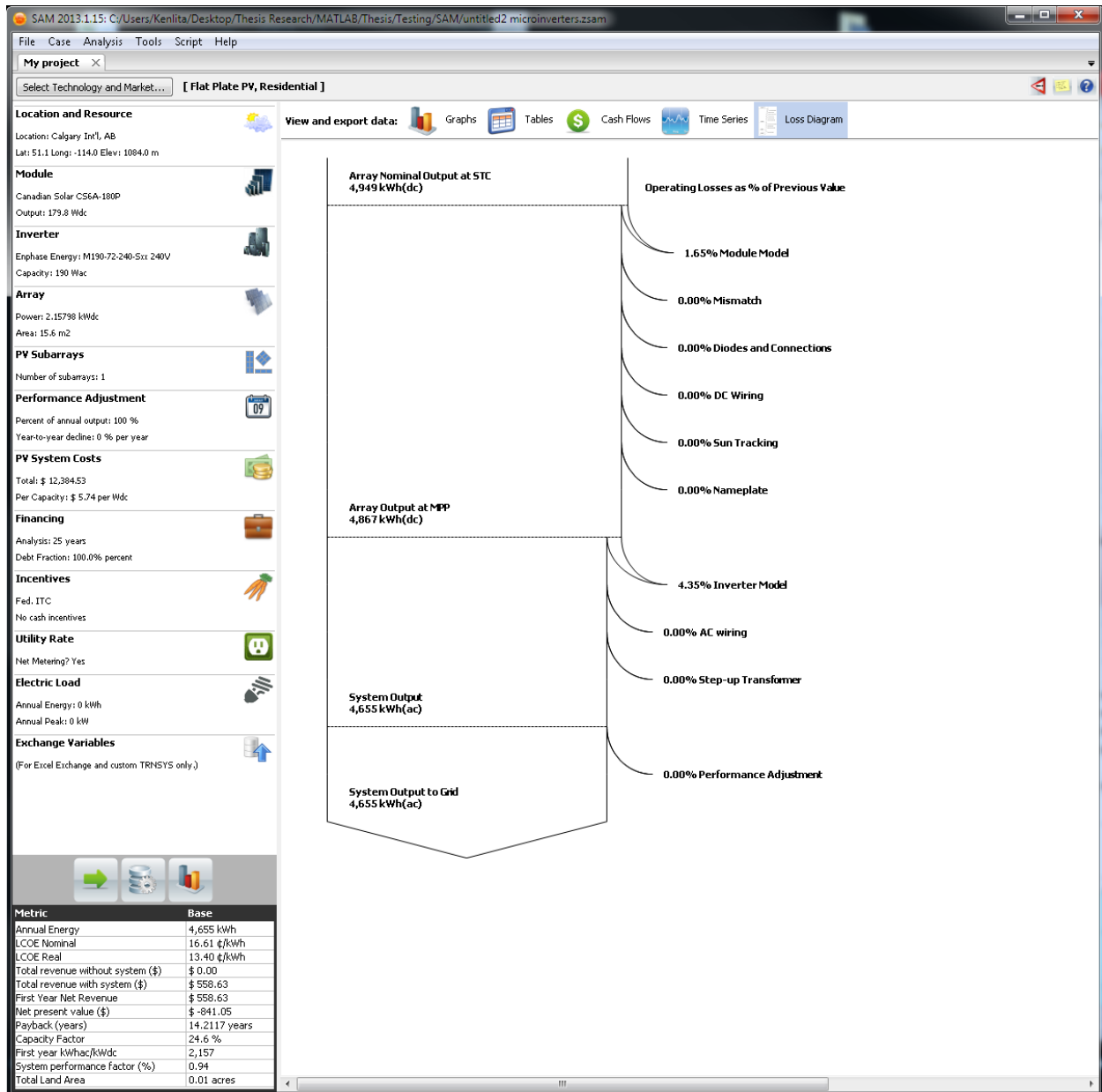
To model a system with one array, specify properties for Subarray 1 and disable Subarrays 2, 3, and 4.

To model a system with up to four subarrays connected in parallel to a single bank of inverters, for each subarray, check Enable and specify a number of strings and other properties.

Each subarray can have its own set of orientation, tracking, shading, and DC derate properties.

	Subarray 1	Subarray 2	Subarray 3	Subarray 4
String Configuration				
Strings in array	12	(always enabled)		
Strings allocated to subarray	12			
Tracking & Orientation				
	<input checked="" type="radio"/> Fixed <input type="radio"/> 1 Axis <input checked="" type="radio"/> 2 Axis <input type="radio"/> Azimuth Axis <input type="checkbox"/> Tilt=latitude Tilt (deg) 0 Azimuth (deg) 180 Tracker rotation limit (deg) 45 <input type="checkbox"/> Backtracking Row width (m) 2 Space between edges of adjacent rows (m) 1	<input checked="" type="radio"/> Fixed <input type="radio"/> 1 Axis <input type="radio"/> 2 Axis <input type="radio"/> Azimuth Axis <input type="checkbox"/> Tilt=latitude Tilt (deg) 20 Azimuth (deg) 180 Tracker rotation limit (deg) 45 <input type="checkbox"/> Backtracking Row width (m) 2 Space between edges of adjacent rows (m) 1	<input checked="" type="radio"/> Fixed <input type="radio"/> 1 Axis <input type="radio"/> 2 Axis <input type="radio"/> Azimuth Axis <input type="checkbox"/> Tilt=latitude Tilt (deg) 20 Azimuth (deg) 180 Tracker rotation limit (deg) 45 <input type="checkbox"/> Backtracking Row width (m) 2 Space between edges of adjacent rows (m) 1	<input checked="" type="radio"/> Fixed <input type="radio"/> 1 Axis <input type="radio"/> 2 Axis <input type="radio"/> Azimuth Axis <input type="checkbox"/> Tilt=latitude Tilt (deg) 20 Azimuth (deg) 180 Tracker rotation limit (deg) 45 <input type="checkbox"/> Backtracking Row width (m) 2 Space between edges of adjacent rows (m) 1
Shading & Soiling	Configure shading scene Edit shading... Monthly soiling factors Edit soiling... Annual average soiling (0..1) 1	Edit shading... Edit soiling... 0.95	Edit shading... Edit soiling... 0.95	Edit shading... Edit soiling... 0.95
Pre-inverter Derates	Mismatch (0..1) 1 Diodes and connections (0..1) 1 DC wiring loss (0..1) 1 Tracking error (0..1) 1 Nameplate (0..1) 1 Estimated DC power derate (0..1) 1	0.98 0.995 0.98 1 1 0.955598	0.98 0.995 0.98 1 1 0.955598	0.98 0.995 0.98 1 1 0.955598
Subarray Mismatch	<p>When subarrays have different orientations, modules in each subarray are exposed to different levels of solar radiation and wind speed, which results in different subarray cell temperatures and maximum power point voltages (Vmp). The voltage mismatch causes electrical losses and an inverter input voltage less than Vmp. By default, SAM estimates the inverter input voltage by averaging the subarray Vmp values.</p> <p>If you are using the CEC module model option, SAM can more accurately estimate the inverter input voltage. This option requires longer simulation times to calculate mismatch losses. This more accurate method generally results in lower system output than the default method. See Help for details.</p> <p><input type="checkbox"/> Calculate maximum power voltage for array and associated losses due to subarray mismatch (CEC module model only)</p>			





APPENDIX B: PV MODULE PARAMETERS

Isc	Voc	Impp	Vmpp	Rs	Rp	NomTemp	NomIrr
8.213	29.484	7.659	23.871	0.259	186	23.3	992.009
8.137	29.388	7.619	23.268	0.531	156.364	23.3	996.008
8.312	29.644	7.81	23.758	0.47	197.579	23.2	986.811
8.115	29.286	7.697	23.279	0.478	238.619	23	987.61
8.125	29.288	7.647	23.427	0.473	271.153	23	1000.007
8.09	29.255	7.599	23.448	0.481	366.662	23	981.612
7.982	29.02	7.423	23.171	0.512	112.622	23.1	993.209
8	29.259	7.496	23.377	0.494	483.984	22.9	991.609
7.964	29.303	7.578	23.148	0.502	371.31	22.6	995.209
7.886	29.138	7.421	23.074	0.513	208.939	22.3	991.21
8.006	29.197	7.433	23.232	0.505	108.468	23.6	990.81
7.997	29.298	7.555	23.229	0.502	431.761	24	996.408